Copyright Warning & Restrictions

The copyright law of the United States (Title 17, United States Code) governs the making of photocopies or other reproductions of copyrighted material.

Under certain conditions specified in the law, libraries and archives are authorized to furnish a photocopy or other reproduction. One of these specified conditions is that the photocopy or reproduction is not to be "used for any purpose other than private study, scholarship, or research." If a, user makes a request for, or later uses, a photocopy or reproduction for purposes in excess of "fair use" that user may be liable for copyright infringement,

This institution reserves the right to refuse to accept a copying order if, in its judgment, fulfillment of the order would involve violation of copyright law.

Please Note: The author retains the copyright while the New Jersey Institute of Technology reserves the right to distribute this thesis or dissertation

Printing note: If you do not wish to print this page, then select "Pages from: first page # to: last page #" on the print dialog screen

ABSTRACT

EXPERIMENTAL INVESTIGATION OF THE EFFECT OF SONICATION ON THE PRECIPITATION OF GRISEOFULVIN BY IMPINGING JETS

by
Ankit H. Patel

Almost 80% of drugs on the market are manufactured as solid dosage forms, such as tablets. Drug bioavailability increases as the particle size decreases and the surface area per unit volume of drug increases. Therefore, there is a keen interest by the pharmaceutical industry to develop techniques that can be used to manufacture particles of active pharmaceutical ingredients (API) in the nano/micro particle range. Impinging jets is one of the most promising techniques to do so.

In this work, a submerged impinging jet system coupled with an ultrasonic probe (sonicator) was used to precipitate Griseofulvin, a common, poorly water-soluble antifungal drug. The drug was initially dissolved in acetone and then precipitated using water as the antisolvent. Experiments were carried out for different values of the sonication power, impinging jet velocity, and reactor volume. Their effect on the size and morphology of the precipitated crystals was quantified. The crystals were analyzed using a laser diffraction method (for particle size distribution), electron microscopy (for crystal morphology), and X-ray diffraction (for crystallinity). The results obtained here indicate that increasing the sonication power, and, to a much more limited extent, the impinging jet velocity decreases the crystal size, but that eventually an asymptotic value of the mean particle size is achieved. The reactor volume does not appear to play a major role, at least in the system examined here. The results obtained in this work could have important implications for the manufacturing of drug particles for solid dosage form use.

EXPERIMENTAL INVESTIGATION OF THE EFFECT OF SONICATION ON THE PRECIPITATION OF GRISEOFULVIN BY IMPINGING JETS

By
Ankit H. Patel

A Thesis
Submitted to the Faculty of
New Jersey Institute of Technology
in Partial Fulfillment of the Requirements for the Degree of
Master of Science in Pharmaceutical Engineering

Otto H. York Department of Chemical Engineering

August 2008

APPROVAL PAGE

EXPERIMENTAL INVESTIGATION OF THE EFFECT OF SONICATION ON THE PRECIPITATION OF GRISEOFULVIN BY IMPINGING JETS

Ankit H. Patel

Dr. Piero M. Armenante, Thesis Advisor — Date
Distinguished Professor of Chemical Engineering, NJIT

Dr. Robert B. Barat, Committee Member — Date
Professor of Chemical Engineering, NJIT

Dr. Somenath Mitra, Committee Member — Date
Professor of Chemistry and Environmental Science, NJIT

BIOGRAPHICAL SKETCH

Author: Ankit H. Patel

Degree: Master of Science

Date: August 2008

Undergraduate and Graduate Education:

- Master of Science in Pharmaceutical Engineering,
  New Jersey Institute of Technology, Newark, NJ, 2008

- Bachelor of Science in Pharmacy,
  Gujarat University, Ahmedabad, India, 2004

Major: Pharmaceutical Engineering

To my Family, who offered me unconditional love and support in all the way since the beginning of my life

ACKNOWLEDGMENT

First and foremost I like to thank my parents and family members for their endless support, encouragement and providing loving environment throughout my life.

From the formative stage of this thesis, so as the final draft, I owe an immense debt of gratitude to my advisor Dr. Piero M. Armenante, who not only served as my research advisor, providing valuable and countless resources, insight, and intuition, but also constantly gave me support, encouragement, and reassurance throughout my academic program. This thesis could not have been completed without him. Special thanks are given to Dr. Robert B. Barat and Dr. Somenath Mitra for actively participating in my committee.

For his efforts and assistance, a special thanks as well to Giuseppe L. Di Benedetto. His continuous support throughout my project helped me to finish my thesis in short time. I would be remiss without mentioning my other fellow graduate students in mixing lab, Deepak Madhrani and Micaela Caramellino, for their continuous support and encouragement.

To each of the above, I extend my deepest appreciation.

TABLE OF CONTENTS

TABLE OF CONTENTS
(Continued)

LIST OF FIGURES

Figure **Page**

CHAPTER 1

INTRODUCTION

1.1 Background

About two thirds of the products used in, and manufactured by, the pharmaceutical industry are in the form of particulate solids, typically formulated as solid dosage forms such as tablets. High bioavailability, short dissolution time, purity and product consistency are some of the desired properties of this type of pharmaceutical compounds. Particle size can considerably affect the bioavailability and dissolution time of solid dosage forms and eventually affect the efficacy of the dosage form, especially for active pharmaceutical ingredients (API's) that are poorly soluble. Typically, the smaller the particle size, the faster the dissolution rate and higher the bioavailability will be. Therefore, there is a keen interest by the industry to develop robust methods that can be used to manufacture small API particles in the range of nano/micro-meters in order to achieve these objectives. A significant amount of research is taking place in pharmaceutical industry to generate smaller sized particles. Crystallization is one of the processes through which the desired particle size with the required purity and consistency can be achieved.

It has been common practice in the pharmaceutical industry to mill powders to a final desired size in order to reduce the particle size, increase surface area and eventually improve the drug's bioavailability. However, this method has numerous disadvantages. Excessive local temperature and stresses can cause degradation of costly pharmaceutical ingredients. The introduction of impurity during milling is another concern. Noise and

unwanted personal exposure to highly potent pharmaceutical compounds are other disadvantages. For these reasons, the development of crystallization methods that can produce fine crystals of controlled size is an area of active research.

Crystallization is the most important separation and purification process used in the production of a wide range of materials ranging from bulk commodity chemicals and pharmaceuticals. It is also considered a chemical separation technique in which mass transfer of a solute from the liquid solution occurs to produce pure crystalline solid. A crystallization process consists of two separate but coexisting processes, namely nucleation and crystal growth. Nucleation is the step where the solute molecules dispersed in the solvent start to gather into clusters that becomes stable under the operating conditions. If the clusters are not stable, they redissolve. Therefore, the clusters need to reach critical size in order to become stable nuclei. This depends on operating conditions such as temperature, supersaturation level, agitation, impurities, and others. Crystal growth consists in the subsequent growth of the nuclei that have already reached a critical size. Nucleation and crystal growth occurs simultaneously under supersaturation conditions. Supersaturation is the driving force for crystallization. Depending on the operating conditions, either nucleation or crystal growth may be predominant over the other. Control of crystal size and shape is one of the challenges often encountered in pharmaceutical development.

Crystallization can be accomplished by reducing the temperature (cooling crystallization), removing the solvent (evaporation crystallization), chemical reaction (precipitation crystallization), or the addition of second solvent to reduce the solubility (anti-solvent or drown-out crystallization). The last of these methods involves contacting

a saturated solution of the compound to be crystallized with an appropriate anti-solvent in a vessel (anti-solvent crystallization). Mixing can affect the crystallization operation including nucleation, crystal growth, and the maintenance of a crystal slurry. The pharmaceutical industry typically uses stirred tank reactors for these processes, although other more novel approaches could also be used.

Crystallization using impinging jet technique is a relative new anti-solvent crystallization technique to produce micro/nano size crystals, where the solute solution and the antisolvent solution are contacted by making them impact against each other in the form of liquid jets. High mixing intensities can be achieved with this approach. The mixing intensity can change the induction time for nucleation. Induction time has reported to decrease with increased mixing up to a critical speed, after which it remains unchanged.

Impinging jets have been mainly used to increase the contact areas between two fluids (e.g., to improve heat or mass transfer in gas-liquid-solid applications), or to produce a spray of fuel droplets that can be combusted easily. One typical impinging jet mixers is shown in the Figure 1.1. Impinging jet mixers are typically made up of two high velocity jets facing each other. Fluids are passed through these jets at very high linear velocities so the impingement of fluids can create a region of high turbulence (impinging plane). This helps to reduce the induction time and enhance the nucleation step.

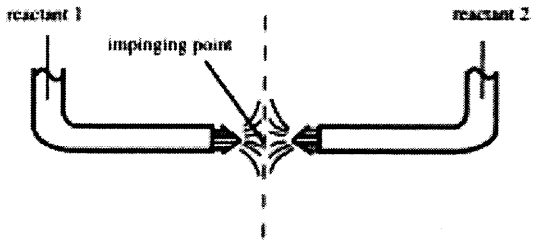

Figure 1.1. Schematic of impinging jets aligned each other with impinging point.

The use of impinging jets for precipitation or crystallization is a relatively new approach to crystallization. Midler et al. (1994) were the first to apply impinging jets to the precipitation of the pharmaceutical products. They used the anti-solvent crystallization process also to form nano particles.

Midler et al. (1994) patented the use of impinging jets to achieve high intensity micro mixing in a continuous crystallization process to provide high surface area particles of high purity and stability. In this invention, two or more jets were used to micromix two or more fluids prior to nucleation in the crystallization process. The two fluids had different composition. The fluid passed through one of the jets was a solution of the compound to be crystallized in a suitable solvent or a combination of solvents, while the other jet was a suitable antisolvent capable of initiating precipitation of the compound from the solution (Figure 1.2).

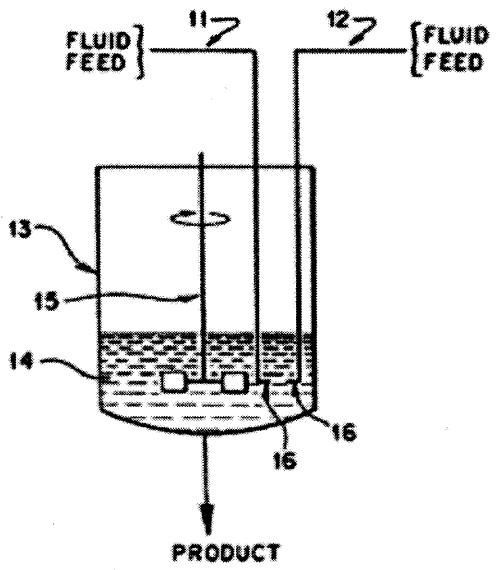

Figure 1.2. Schematic of submerged impinging jet mixer (Midler, Jr. et al, 1994) Specification of numerical numbers can be found in original reference.

Research into the influence of ultrasound on crystallization processes has been conducted over the last 70 years. This work has revealed that the nucleation of solid crystals from a number of liquids ranging from organic fluids to metal is affected by presence of ultrasonic waves. Abbas et al. (2007) have shown the importance of sonication on the crystallization procedure, which is referred to as sonocrystallization. The effects of temperature, ultrasonic power input and salt concentration have been investigated to determine their impact on the size and morphological characteristic of the crystals. They concluded that ultrasounds had a significant effect on the crystals. Sonication helps to reduce the crystal size and narrow the size distribution.

Lindrud et al. (2001) modified the impinging jet crystallization apparatus by adding a sonication probe at the point of impingement to achieve the micromixing of fluids to form a homogenous composition prior to the start of nucleation in continuous

crystallization process. They placed the sonication probe in the gap between the jets on plane of the jets (Figures 1.3 and 1.4). Their sonication probe had a power output in the range 30-150 W.

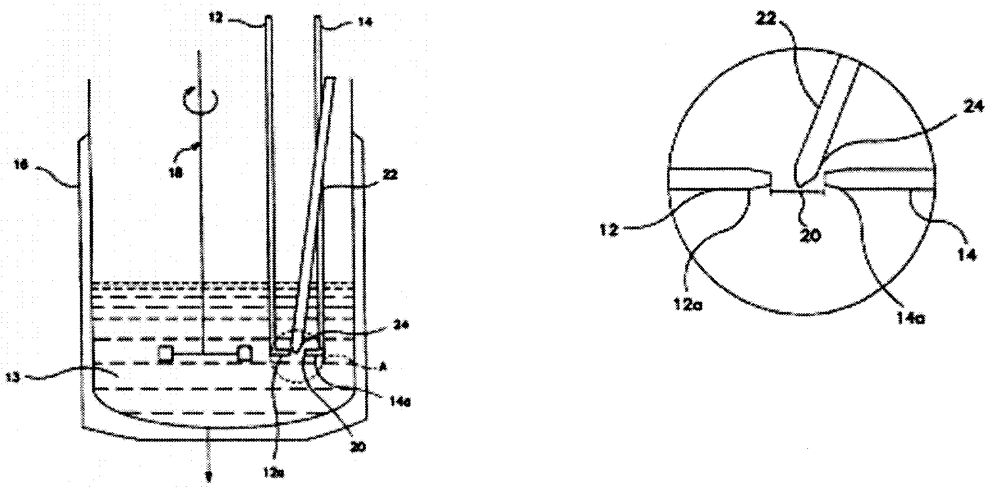

Figure 1.3. Schematic of submerged impinging jet with sonication and positioning of the Impinging jet and sonication probe tips (Lindrud et al, 2001) Specification of numerical numbers can be found in original reference.

The sonocrystallization approach appears to be very promising for the developments of robust processes that can be used manufacture API's with appropriate particle size distribution and properties. This approach was used here to precipitate a commonly used API compound.

1.2 Objective of this Work

As already mentioned, there is growing interest in the pharmaceutical industry to develop techniques that can be used to generate uniform micro/nano size crystals. Impinging jet crystallization is one of the most promising of these methods especially if coupled with

additional methods to increase the power delivered in the precipitation zone, such through local sonicaton. Therefore, the objective of this work was to investigate the influence of sonication power and impinging jet velocity on the final particle size in a continuous impinging jet crystallization process. In order to make this approach more relevant to pharmaceutical processing, an existing, poorly soluble API was selected, i.e., Griseofulvin. Griseofulvin ($C_{17}H_{17}ClO_6$; Figure 1.4) is an orally administered, anti-fungal drug that is currently produced by different companies. The drug is used to treat ringworm infections of the skin and nails in both animals and humans.

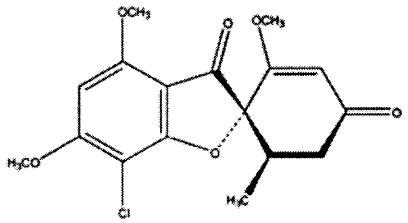

Figure 1.4. Chemical structure of Griseofulvin.

Griseofulvin is a highly hydrophobic drug (water solubility less than 1 mg/mL at 70 °F), and has a highly variable bioavailability (25% to 70%) when microsized. It has a molar mass of 352.766 g/mol, and a density of 1.440 g/cm^3. The melting point is 220.0 °C (428.0 °F). Griseofulvin is slightly soluble in various organic solvents, including acetone, which was used here as the solvent. Water was used here as the main anti-solvent.

In this work, experiments were conducted in a continuous impinging jet system in the presence or absence of a sonicator, which was used here to enhance the process. Experiments with two different impinging jet velocities and five different sonication intensities were performed in order to determine the effect of these variables on the particle size of the precipitated Griseofulvin.

CHAPTER 2

EXPERIMENTAL SYSTEM AND METHOD

In this work, a submerged impinging jet system combined with an ultrasonic probe (sonicator) was used to precipitate an active pharmaceutical ingredient (API), namely Griseofulvin. This is a widely used antifungal drug, available as a tablet, capsule and liquid to taken by oral route. The system consisted of two smaller nozzles facing each other at 180° and placed in a stirred tank. The nozzles were fed, respectively, with a solution of Griseofulvin in acetone (Solution A) and with a solution of water, a stabilizer, i.e., Hydroxypropyl Methylcellulose (HPMC) and a surfactant, i.e., Sodium Dodecyl Sulfate (SDS) or Tween 80 (Solution B). Experiments were conducted at two different impinging jet velocities and in the presence and the absence of sonication. The intensity of the sonication power delivered by the ultrasonic probe was varied according to the experiment. Volume inside the stirred tank is also changed. The effect of these variables on crystal size and crystal structure was quantified. The particle size distribution of the resulting crystals was analyzed using laser diffraction method and structure of the crystals was determined using Scanning Electron Microscopy (SEM). Crystallinity was compared by X-Ray Diffraction method (XRD). Most experiments were conducted in replicates in order to quantify the reproducibility. Details about the experimental materials, equipment and procedures are provided in the following sections.

2.1 Materials

Griseofulvin, the model drug used in the experiment, is appreciably soluble in Acetone but poorly soluble in water. Therefore Acetone (technical grade, purity: 99+%, Acros Organics, Somerville, New Jersey) was used as solvent for Griseofulvin in Solution A, while distilled/de-ionized water was used as the as anti-solvent in this case. To increase the stability of the resulting suspension, HPMC (HY124, Hypromellose 2208, HPMC USP, Spectrum Chemical Mfg. Corp., New Brunswick, New Jersey) and SDS (ultrapure, Biomedicals LLC, Solon, Ohio) for higher velocity experiments while Polyethylenesorbitan Monooleate (Tween 80, P-8074, Sigma Ultra, St. Louis, Missouri) for lower jet velocity experiments were used in the preparation of the anti-solvent solution (Solution B). All the ingredients were used as such, without any further purification or processing. The preparation methods for the drug solution and anti-solvent solution are described in the Experimental Procedure section below.

2.2 Equipment

Two different experimental sets up were used for lower jet velocity (0.722 m/s) and higher jet velocity (15 m/s) experiments.

2.2.1 Experimental Set- up for Higher Jet Velocity Experiment

The experimental setup for higher jet velocity is shown in Figure 2.1. Two jacketed 1-liter reservoirs contained the drug solution (Griseofulvin in acetone) and the anti-solvent solution (water plus HPMC and SDS) separately. The reservoir with the anti-solvent solution was jacketed and cooled by circulating cold water through jacket using an

external water bath provided with a pump (endocal RTE-110, Neslab Instruments Inc., Newington, New Hampshire). The drug solution did not have to be heated or cooled so the corresponding reservoir was not connected to any water bath.

Each reservoir was connected to a gear pump through recirculation loop; made of stainless steel piping; using ½ inch diameter tubing (HDPE), which then fed the impinging jet assembly downstream. These pumps were a Lobee 2LOE-S (Lobee Pump & Machinery Company, Gasport, New York) for the anti-solvent solution, and a Shertech GPST2 (Hypro Industrial Products Group, New Brightan, Minnesota) for the drug solution. The flow rates of each solution passing through the gear pumps were controlled by adjusting the recirculation flow around the gear pumps through respective globe valves (CF8M, ½ inch diameter, Sharpe Valves, Northlake, Illinois), as shown in Figure 2.1.

The impinging jet assembly consisted of two separate vertical stainless steel tubes (ID: 3.175 mm (1/8 inch); OD: 6.35 mm (1/4 inch)) connected at the top end to the pumps through ½ inch HDPE tubing and at the bottom end to the impinging jet nozzles via 90° elbows (Figure 2.3). The tubes were kept in place by metal braces. The nozzles were made of small tubes with 1.016 mm ID (1/25 inch) for the anti-solvent solution and 0.506 mm ID (1/50 inch) for the solvent solution. The OD of both nozzles was 1.59 mm, i.e., 1/16 inch). The distance between two nozzles was 7 mm.

The nozzle assembly was mounted inside a jacketed receiving tank. Two different receiving tanks, 5 inch diameter (2 liter) and 8 inch diameter (5 liter) were used depending on the experiment. The receiving tank was cooled by circulating coolant through its jacket using circulatory pump (Cole-Parmer, 12108-20). The 8-inch diameter

receiving tank was stirred by a 3-blade, retreat-blade impeller, 89 mm in diameter driven by a 1/8 HP motor (455479, G K Heller Corp., Floral Park, New York). The impeller clearance off the tank bottom was 35 mm. External stirring was not possible in case of smaller diameter tank due to insufficient space. The nozzles were facing each other at 180° and were place at about the same height as of impeller (i.e., closer to bottom of the tank).

A sonication probe was placed between two nozzles, as shown in the figure 2.3. The probe was connected to a 250 W sonicator (Omni-Ruptor 250, Omni International Inc., Marietta, Georgia). Two different sonication probes having diameter of 3.8 mm and 12.7 mm were used in different experiments in order to cover a wide range of sonication powers.

2.2.2 Experimental Set-up for Lower Jet Velocity Experiment

Experimental set up for the lower jet velocity (0.772 m/s) experiment is described in Figure 2.2. Reservoirs described in previous section were connected directly with two centrifugal pumps (KL3404, Baldor Industrial Motor, Sonoma, California, for anti-solvent solution and VL3507, Baldor Industrial Motor, Sonoma, California, for drug solution) using ¼ inch diameter HDPE pipes (recirculation loop was not used to control the flow rate) and outlets of the pumps were connected to the impinging jet assembly using same ¼ inch diameter HDPE tubing. Size of both the nozzles in the impinging jet assembly was same (0.506 mm ID (1/50 inch) and 1.59 mm OD (1/16 inch). All other specifications were same as described in the previous section.

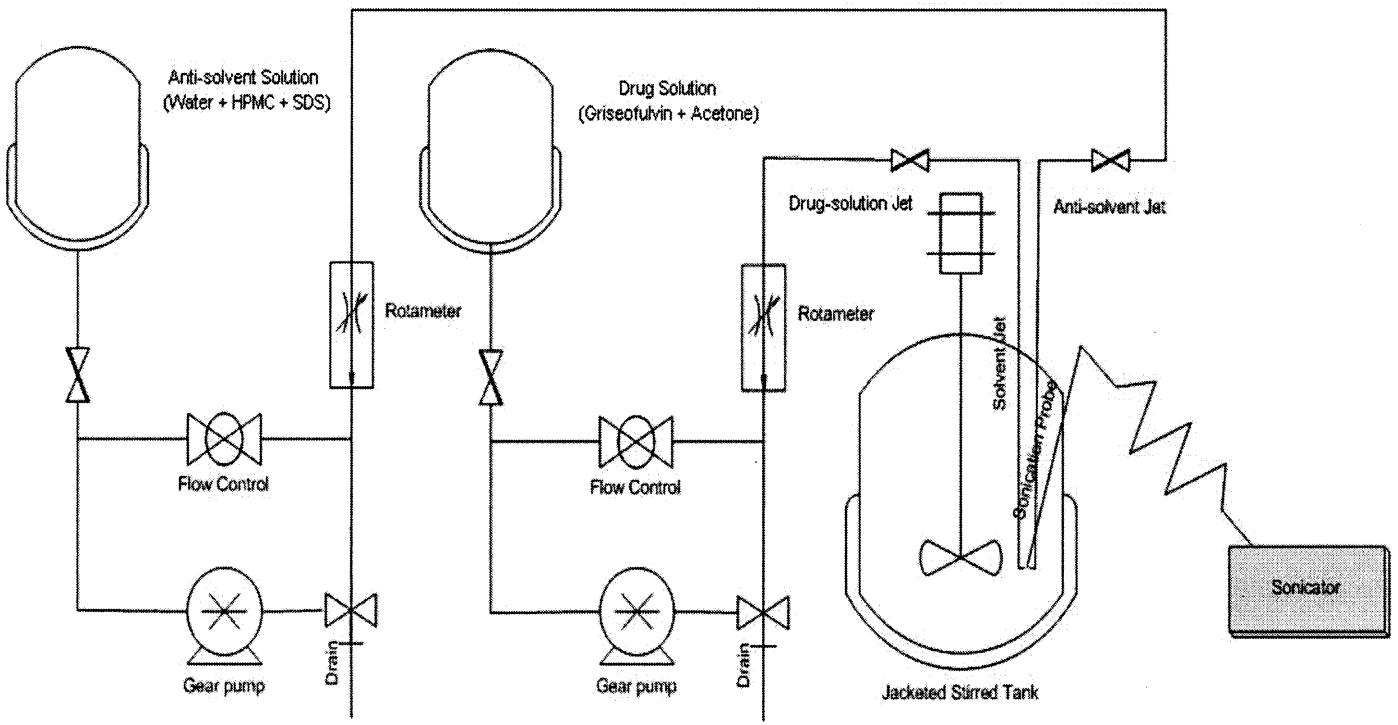

Figure 2.1. Schematic of the impinging Jet technique for the micro/ nano particle formation with higher jet velocity (15 m/s)

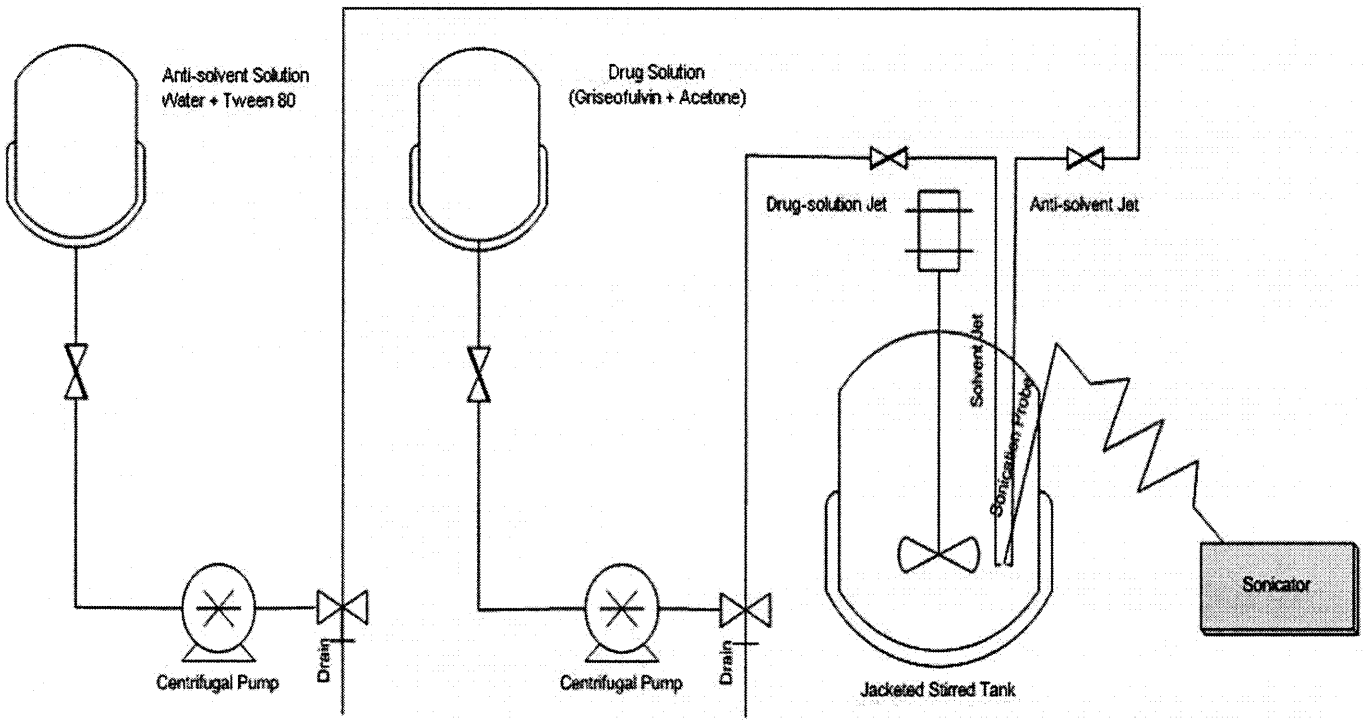

Figure 2.2. Schematic of the impinging Jet technique for the micro/ nano particle formation for lower jet velocity (0.722 m/s)

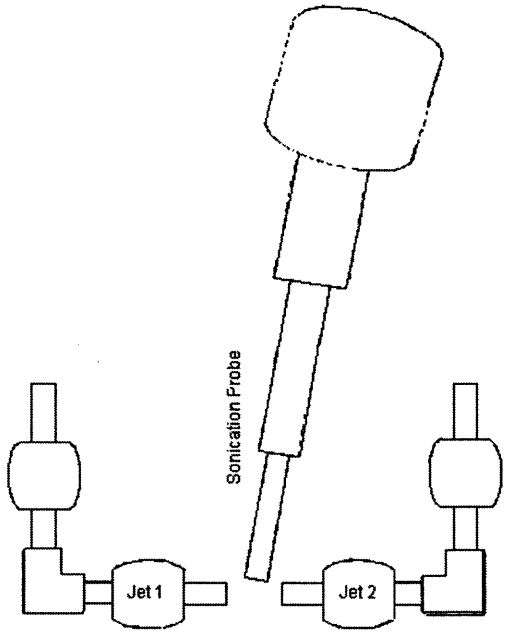

Figure 2.3. Schematics of the impinging jets coupled with sonication probe.

2.3 Experimental Procedure

2.3.1 Preparation of Drug Solution (Solution A)

A weighed amount of Griseofulvin (usually 8.4 g of drug for 200 mL of acetone or 10.5 g of drug for 250 mL of acetone) was transferred to a volumetric flask and the required volume of acetone was added to it. The flask was then placed in a sonication bath to dissolve the drug in acetone (typically 1 hour). The drug solution was stored at room temperature. The resulting concentration of Griseofulvin in acetone was 42 g/L. This solution was used as a feed solution in all experiments.

2.3.2 Preparation of Anti-solvent Solution (Solution B)

2.3.2.1 Anti-solvent for Higher Jet Velocity Experiments

A stock solution was prepared by transferring 700 mL of distilled/de-ionized water to a 2-L Erlenmeyer flask, and then heating and stirring the flask with a magnetic stirrer on a hotplate (Jenway 1000, Essex, UK) until the temperature reached 75°C. Then, 1.5 g of HPMC was added while stirring. After 5 minutes, heating was stopped and 700 mL of distilled/de-ionized water was added. When the solution was sufficiently cooled (50°C), 1.5 g of SDS was added. Stirring was continued for 5 minutes, and then 600 mL of distilled/de-ionized water was added to make 2 Liter of a stock solution. The concentrations of HPMC and SDS in the final solution were both 0.075%W/V. The solution was capped and stored in the same Erlenmeyer flask at room temperature until needed.

2.3.2.2 Anti-solvent for Lower Jet Velocity Experiments

4000 mL of distilled water was taken in a 4-L volumetric cylinder. Measured amount of Tween 80 (18.8 mL) was added and solution was stirred using magnetic stirrer for 15 minutes. This solution was used as stock solution and stored in the same volumetric cylinder by closing its mouth. Final concentration of Tween 80 in the solution was 0.47 % V/V.

2.3.3 Impinging Jet Crystallization Process

The anti-solvent reservoir was filled with 1 L of the anti-solvent solution. The water bath for the anti-solvent reservoir was switched on and run for at least 1 hour before the

experiments started so that the anti-solvent temperature was low enough (4°C) for the experiment.

After checking the alignment of the jets (visually) so that they would point to each other at 180°, the jet assembly was placed in the receiving tank, which had been previously cooled to 4°C by passing the coolant through the jacket. The flow rate of both jets had been adjusted prior to the experiment by passing acetone or water through the jets so that the desired impinging jet velocity was obtained (this is also a method to check alignments of impinging jet). During this operation, a barrier was placed between the jets so that they would not be contaminated with the other jet's solvent. The impinging velocity was the same (0.722 m/s or 15 m/s) for both jets, but their flow rate was different since the ID of the anti-solvent jet was twice as big as that of the drug solution jet. The sonication probe was placed in between the jets, as shown in figure 2.3. Depending on the experiment, the receiving tank was initially partially filled with a measured amount of cooled anti-solvent solution so that the jets would not be submerged before experiments started in order to reduce the possibility of jet clogging. In this case, the anti-solvent solution was placed 1 liter beaker and kept in the circulatory bath and cooled down around 4°C.

When the anti-solvent solution was sufficiently cooled, the drug solution was placed in its reservoir tank (150 mL of drug solution when the larger tank was used, and 100 mL when the smaller tank was used) and both the drug solution and the anti-solvent solution were forced to pass through the jets by turning on the gear pumps simultaneously. Measured amount of anti-solvent solution was added to submerge the jets and at this time the sonicator and the main impeller (in the larger tank only) were

switched on at specific rate as soon as jets were submerged (impeller speed was kept constant at 300 RPM in all the experiments). This is usually an instantaneous process, which only takes few seconds from turning on pump to the impeller and sonicator. Jets were stopped as soon as drug solution ran out.

2.3.4 Analytical Methods

2.3.4.1 Particle Size Distribution Determination via Light Scattering

Samples were collected at the end of each experiment by opening the bottom valve of the larger tank and incase of smaller tank samples were collected from the top. The samples were collected in multiple centrifugal vials (50 mL) to check for homogenous distribution as well as error in the analytical method and their particle size distribution was determined immediately by using a Beckman Coulter LS230 particle size analyzer apparatus (Beckman Coulter LS230, Beckman Coulter, Inc., Fullerton, California). These samples were used as such, without any dilution. The LS230 apparatus measures particle volume distribution using both Fraunhofer and Mie light scattering. It can measure particle sizes ranging from 0.04 μm to 2000 μm. A sample was circulated through a sample cell at constant speed, and as a beam of laser light passed through the sample it was diffracted by the particles within the sample and the scattered light was collected by series of detectors. A 17% acetone/ 83% water solution was used as reference fluid to match the refractive index of the sample solution. Each sample was analyzed at least 2 times to check for any error. These multiple data are averaged and used for further investigation.

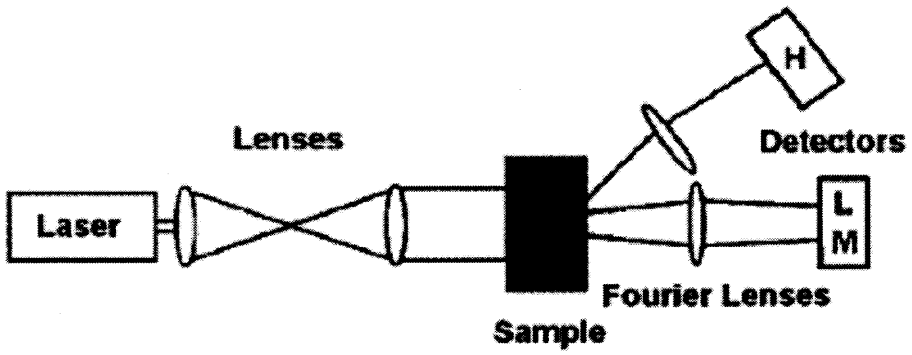

Figure 2.4. Schematic drawing of the LS230 Laser Diffractometer (from Schoofs [1990])

2.3.4.2 Structural Analysis by Scanning Electron Microscopy (SEM)

A scanning electron microscope (LEO 1520 VP FESEM, Zyvex Instruments, Richardson, Texas) was used to perform the detailed structural analysis of the samples. Particle size and morphology were studied. SEM stubs were prepared by adding few drops of the suspension from the centrifugal vials collected for LS analysis. At least two stubs were prepared for the each experiment performed. Each stub was placed under vacuum in desiccators to dry the sample. Micrographs of different regions of the stub were taken and analyzed. Other group member of this project, Giuseppe Di Benedetto, carried out SEM analysis primarily.

2.3.4.3 Determination of Crystallinity by X-Ray Diffraction (XRD)

XRD (Philips PW3040 X-Ray Diffractometer) was used to reveal details about the crystallographic structure of the Griseofulvin. XRD is powerful and versatile nondestructive analytical techniques for the identification and quantitative determination of the crystalline solid phases. XRD sample was prepared by filtering the resulting

suspension using filter paper (Glass Fiber Filter, 61631, Pall Life Sciences, Ann Arbor, Michigan) and subsequent drying in the desecrator. Other group member of this project, Giuseppe Di Beneddetto, carried out XRD analysis primarily.

CHAPTER 3

RESULTS AND DISCUSSION

3.1 Results of Experiments at Lower Jet Velocity (0.722 m/s)

A total of five experiments at five different sonication powers were conducted at the lower jet velocity (0.722 m/s) using the equipment previously described and shown in Figure 2.2. The five sonication power values were as follows: 0 W (no sonication), 75 W, 125 W, 200 W and 250 W. No replicate experiments were conducted. However, for each experiment, the particle size distribution was determined multiple times with the LS 230 apparatus, and the results averaged accordingly. The most significant results for this series are presented in this section, and the complete set of data and figures are given in Appendix A.

Figure 3.1 shows the crystal size distribution for the experiment conducted at the lower jet velocity (0.722 m/s) without sonication (Experiment 23/2). A broad particle size distribution can be observed, with particles ranging from 4-5 μm to 130 μm. The mean particle size was found to be 43.09 μm using the LS 230 apparatus. A micrograph of the Griseofulvin particles obtained from the same experiment shows that the particles were crystalline, but that their sizes varied over a significant range (Figure 3.2). The crystals were typically elongated (needle shaped), and many crystals were agglomerates of smaller crystals, which resulted in an increase in the average size of the particles. The average mean particle size calculated from the 8 replicate LS 230 measurements for the same experiment was found to be 38.83 μm (Appendix A; Summary Table). The particle size distribution was similar in all measurements and the crystal structure also appeared

to be similar in all SEM scans. Additional experimental results for this case are presented in Appendix A1.

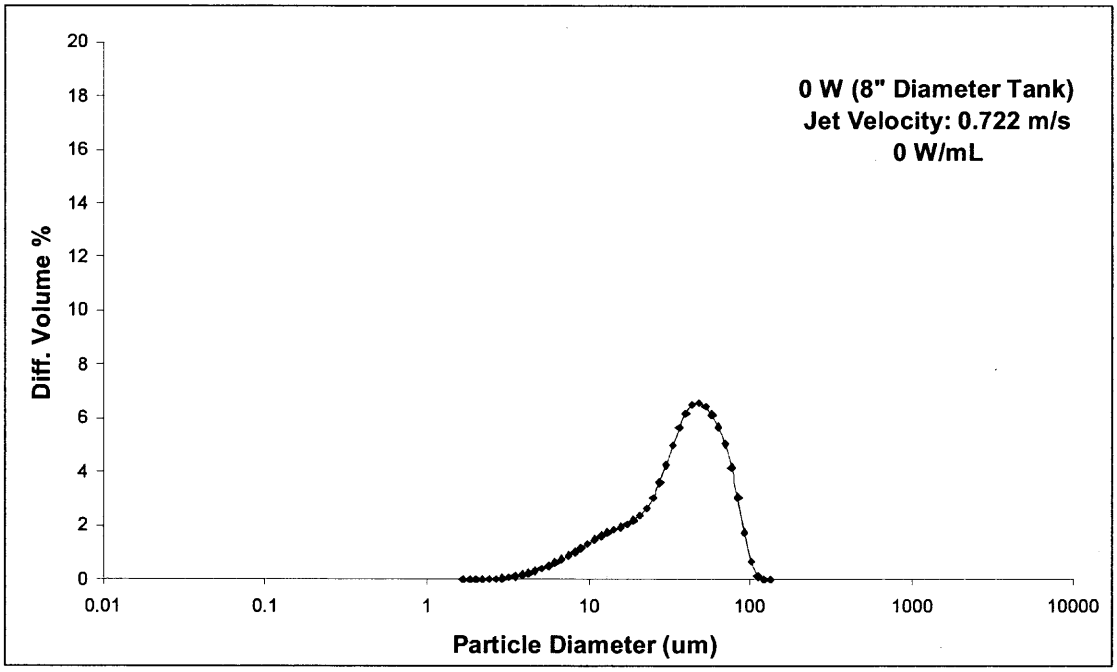

Figure 3.1. Particle size distribution of Griseofulvin crystals measured with the LS230 apparatus. Experiment 23 (10/27/07): jet velocity=0.722 m/s; no sonication. These data were obtained in collaboration with Giuseppe Di Benedetto.

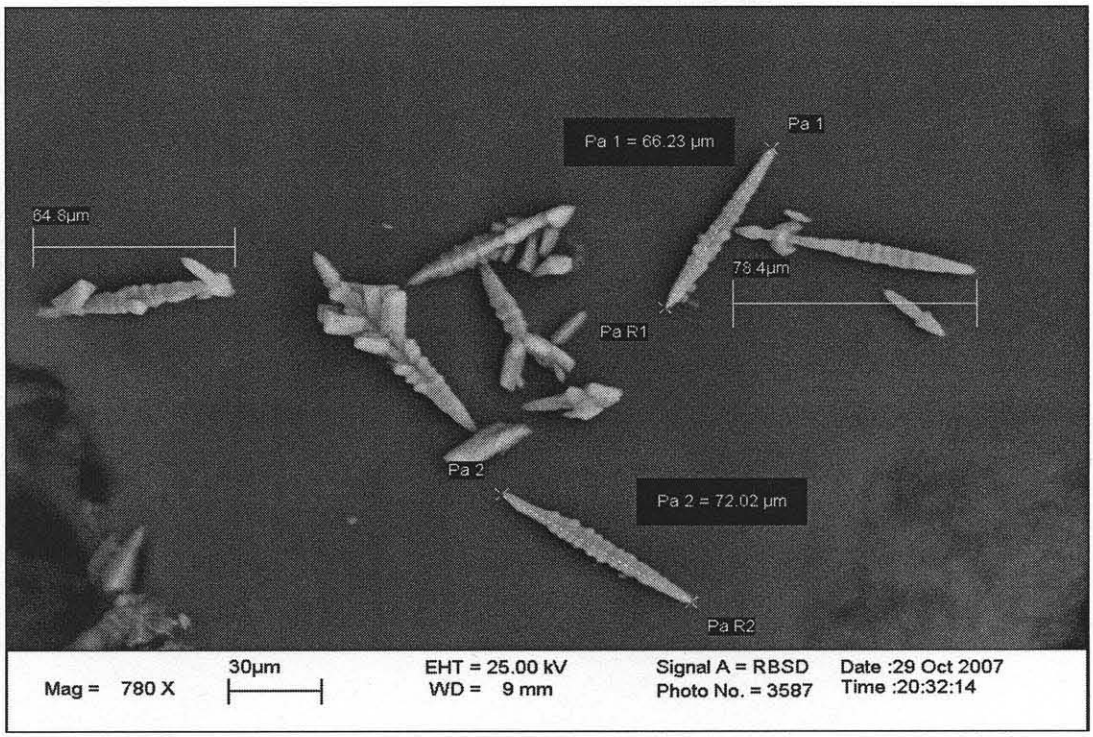

Figure 3.2. Electron micrographic picture of Griseofulvin crystals measured with the SEM apparatus. Experiment 23 (10/27/07): jet velocity=0.722 m/s; no sonication. These data were obtained in collaboration with Giuseppe Di Benedetto.

Figure 3.3 shows the particle size distribution for the experiment with the lower jet velocity (0.722 m/s) and 75 W of sonication power. The particle size distribution ranged from 1 µm to 30 µm. The mean particle size was found to be 8.146 µm. A micrograph for the same experiment is shown in Figure 3.4. The crystals still showed some agglomeration, but the agglomerates were not as many as when no sonication was applied. The crystals were still elongated in shape. The average mean particle size calculated from 6 replicate measurements was found to be 8.141 µm (Appendix A; Summary Table), i.e., appreciably smaller than in the case with no sonication. The particle size distribution was similar in all measurements. The crystal structure also appeared to be similar in all SEM scans. Additional experimental results for this case are presented in Appendix A2.

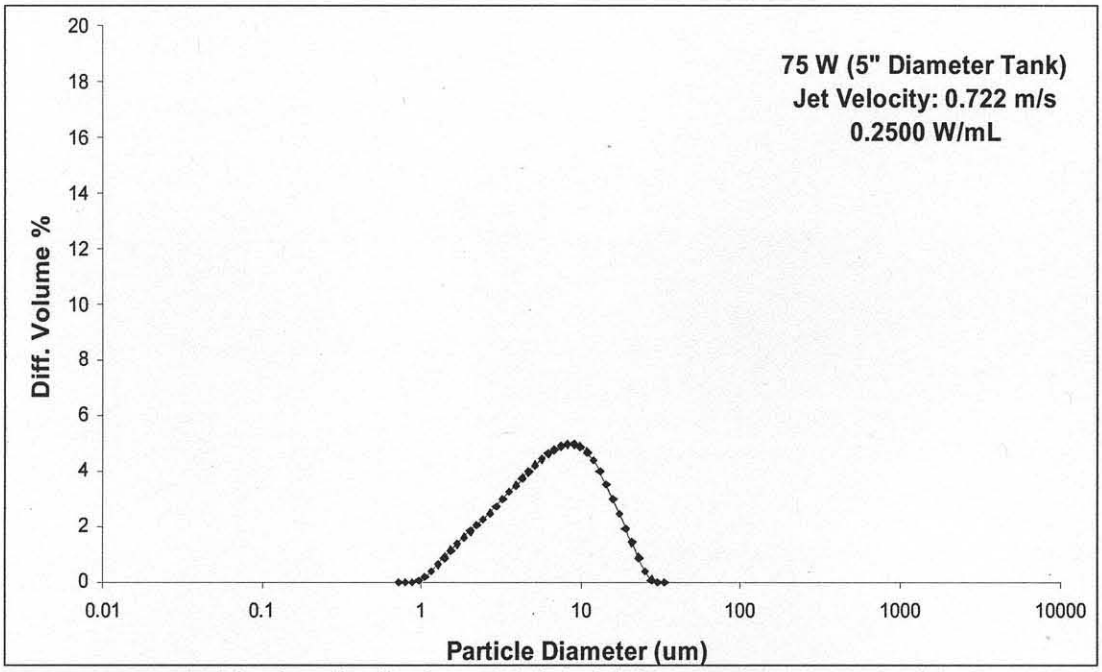

Figure 3.3. Particle size distribution of Griseofulvin crystals measured with the LS230 apparatus. Experiment 33 (02/07/08): jet velocity=0.722 m/s; sonication power=75 W.

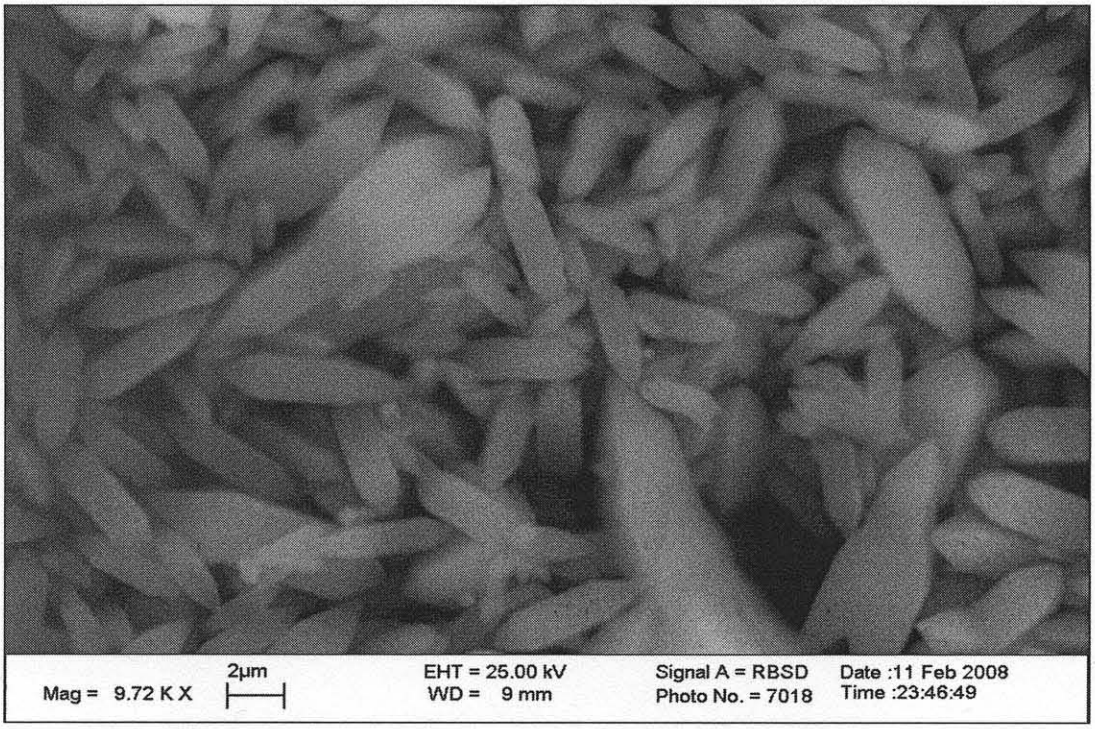

Figure 3.4. Electron micrographic picture of Griseofulvin crystals measured with the SEM apparatus. Experiment 33 (02/07/08): jet velocity=0.722 m/s; sonication power=75 W.

Figures 3.5 and 3.6 show, respectively, the particle size distribution and a micrograph picture of the crystals for the experiment with lower jet velocity (0.722 m/s) and 125 W of sonication power. The particle size distribution ranged from 1 μm to 21 μm, and the mean particle size was found to be 5.84 μm. The crystals did not appear to be agglomerated, and the particle size was significantly more uniform than in the previous cases. The average mean particle size calculated from the results of the 6 replicate LS 230 measurements was found to be 6.14 μm (Appendix A; Summary Table). Additional experimental results for this case are presented in Appendix A3.

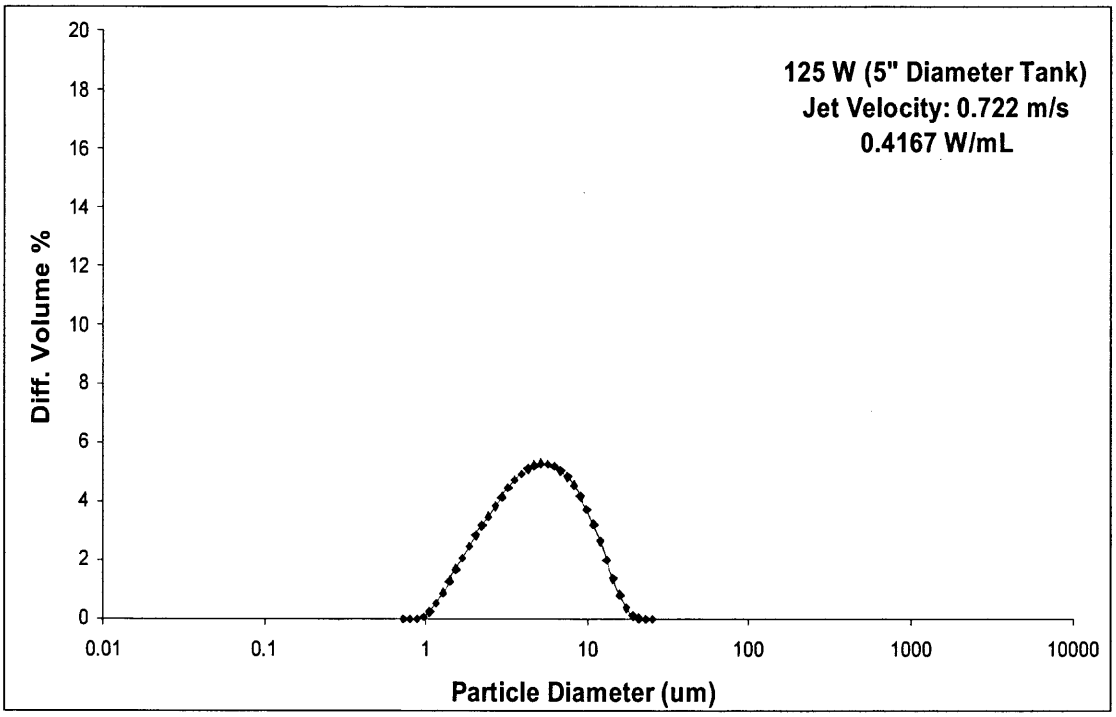

Figure 3.5. Particle size distribution of Griseofulvin crystals measured with the LS230 apparatus. Experiment 32 (02/06/08): jet velocity=0.722 m/s; sonication power=125 W.

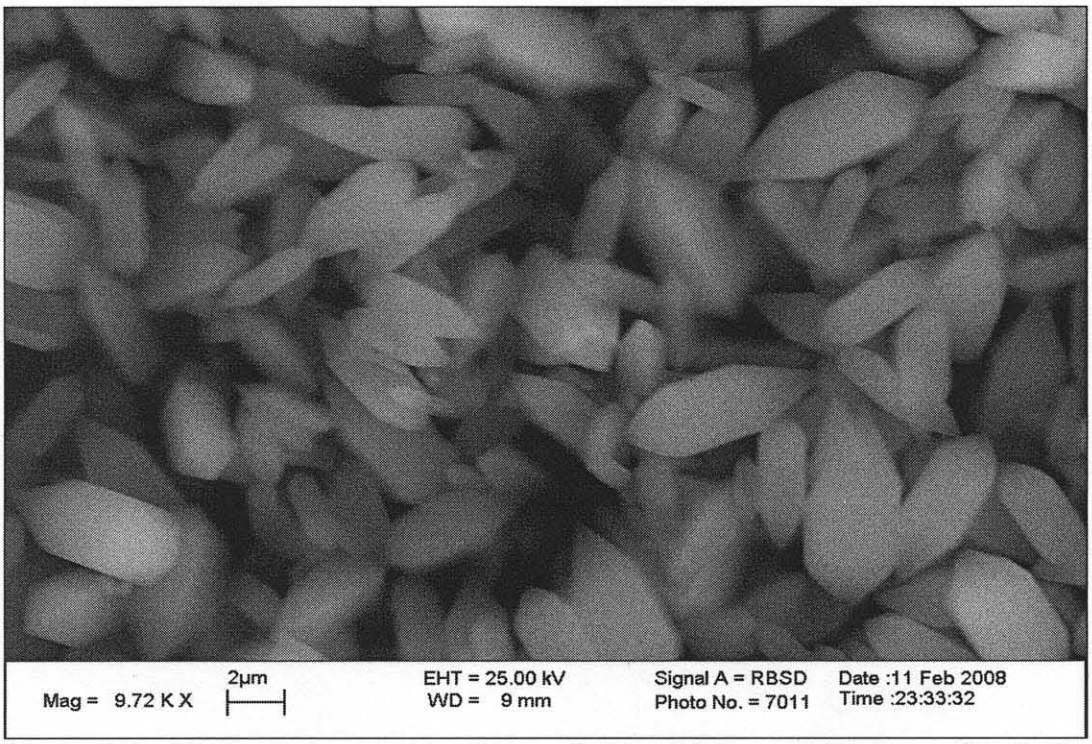

Figure 3.6. Electron micrographic picture of Griseofulvin crystals measured with the SEM apparatus. Experiment 32 (02/06/08): jet velocity=0.722 m/s; sonication power=125 W.

Finally, Figures 3.7 and 3.8 show, respectively, the particle size distribution and a micrograph of the crystals for the experiment with the lower jet velocity (0.722 m/s) and 200 W of sonication power, while Figures 3.9 and 3.10 are the corresponding figures for the 250 W case. In both cases, the particle size distribution ranged from 1 µm to 18 µm, and the mean particle sizes were found to be 6.63 µm for the 200 W case and 6.64 µm for the 250 W case. The average mean particle size calculated from the 8 replicate measurements were found to be, respectively, 7.33 µm and 6.66 µm (Appendix A; Summary Table). Additional experimental results are in Appendices A4 and A5.

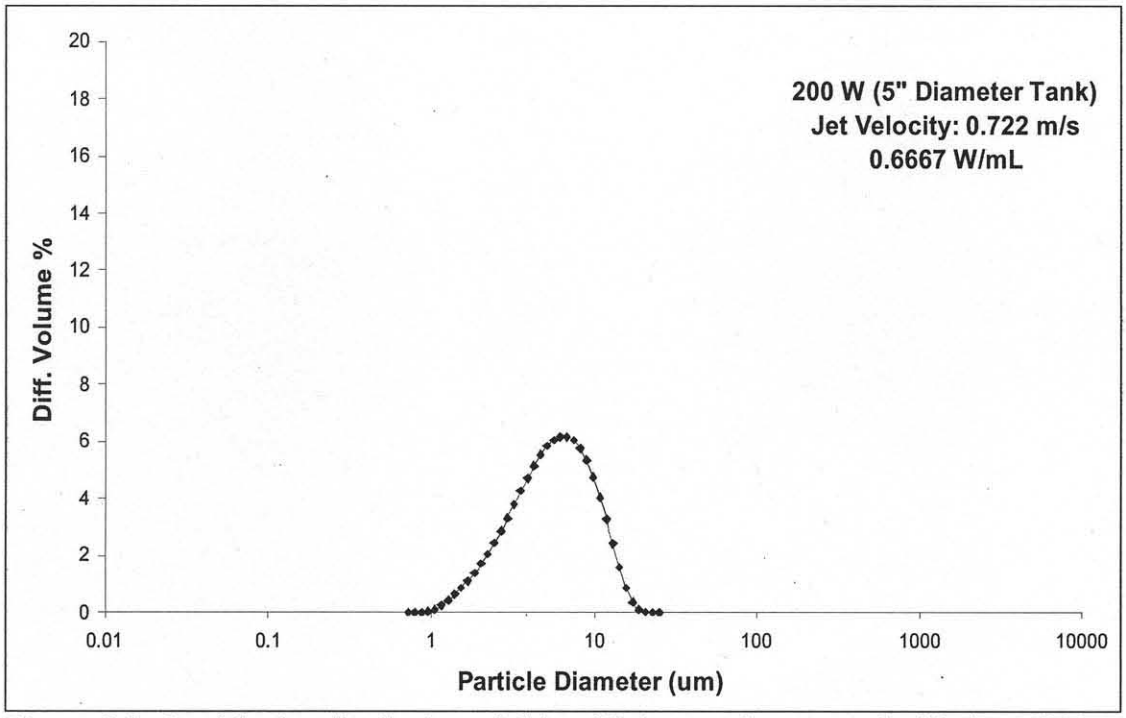

Figure 3.7. Particle size distribution of Griseofulvin crystals measured with the LS230 apparatus. Experiment 36 (02/12/08): jet velocity=0.722 m/s; sonication power=200 W.

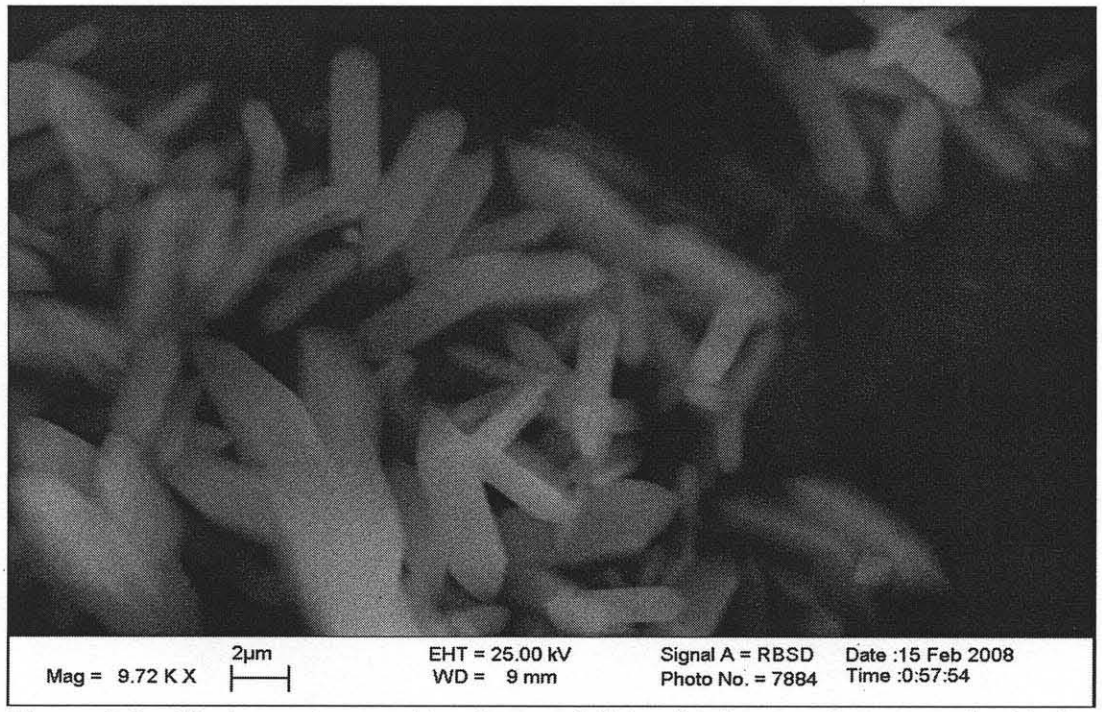

Figure 3.8. Electron micrographic picture of Griseofulvin crystals measured with the SEM apparatus. Experiment 36 (02/12/08): jet velocity=0.722 m/s; sonication power=200 W.

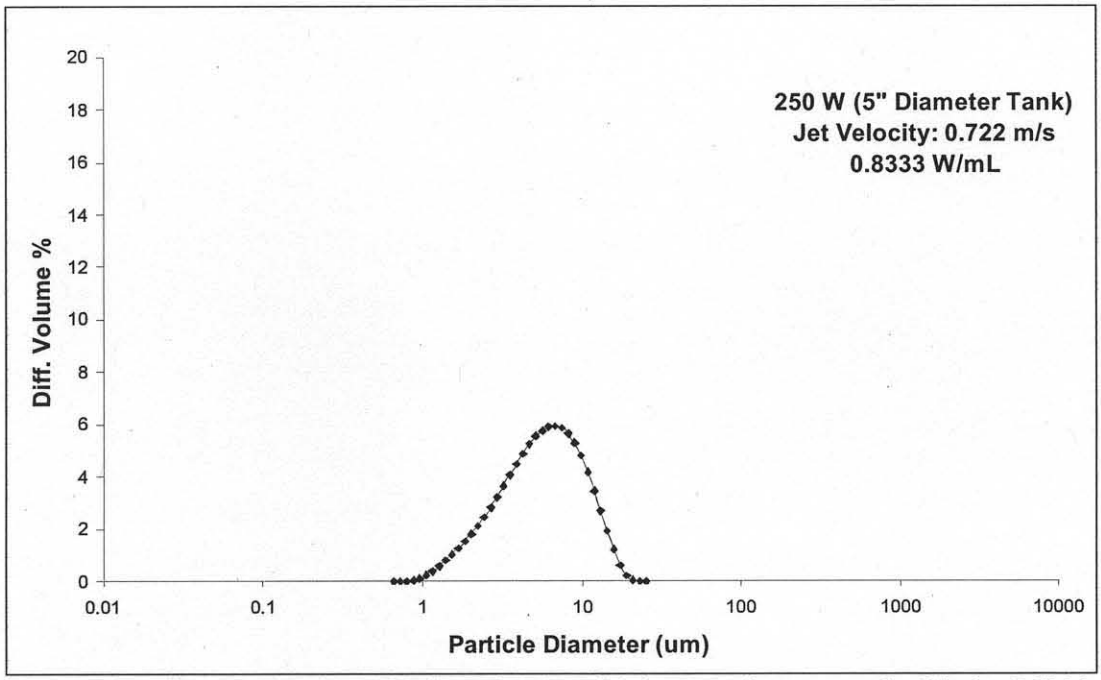

Figure 3.9. Particle size distribution of Griseofulvin crystals measured with the LS230 apparatus. Experiment 35 (02/11/08): jet velocity=0.722 m/s; sonication power=250 W.

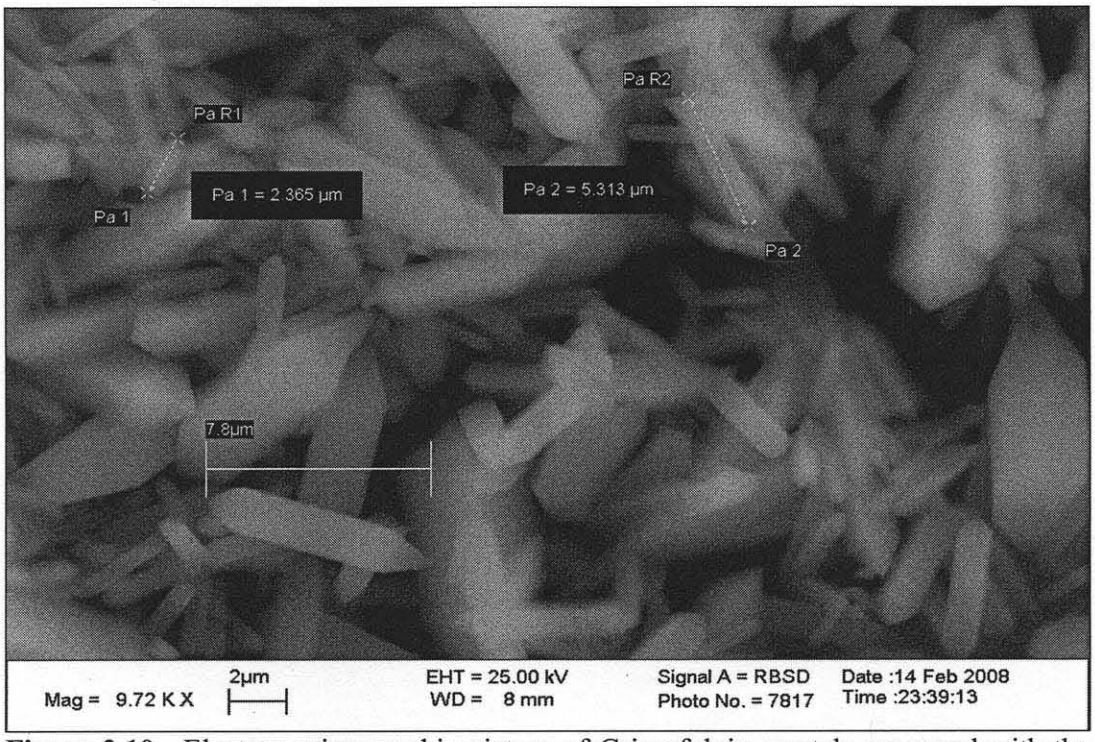

Figure 3.10. Electron micrographic picture of Griseofulvin crystals measured with the SEM apparatus. Experiment 35 (02/11/08): jet velocity=0.722 m/s; sonication power=250 W.

3.2 Results of Experiments at Higher Jet Velocity (15 m/s)

A total of 28 experiments at five different sonication powers were conducted at the higher jet velocity (15 m/s) using the equipment previously described and shown in Figure 2.1. As in the previous case with the lower jet velocity, the five sonication powers used here values were as follows: 0 W (no sonication), 75 W, 125 W, 200 W and 250 W. Each experiment was replicated between 3 and 5 times. The most significant results for this series of experiments are presented in this section. The complete set of data and figures are given in Appendix B.

Figures 3.11 and 3.12 show the crystal size distribution for two duplicate experiments conducted at the higher jet velocity (15 m/s) without sonication (Experiments 40/1 and 45/3). A broad particle size distribution can be observed, with particles ranging from 2-3 μm to 84 μm. The mean particle size was found to be 29 μm for Figure 3.11 and 28.2 μm for Figure 3.12. A micrograph of the Griseofulvin particles obtained from the same experiment shows that the particles were crystalline, but that the crystals were typically elongated (needle shaped), and tended to form agglomerate structures of smaller crystals, which resulted in an increase in the average size of the particles. The average mean particle size obtained from triplicate experiments (10 replicate LS 230 measurements were taken for the each experiment) was found to be 28.87 μm (Appendix B; Summary Table). The particle size distribution was similar in all replicate experiments and replicate measurements. The crystal structure also appeared to be similar in all SEM scans. Additional experimental results for this case are presented in Appendix B1.

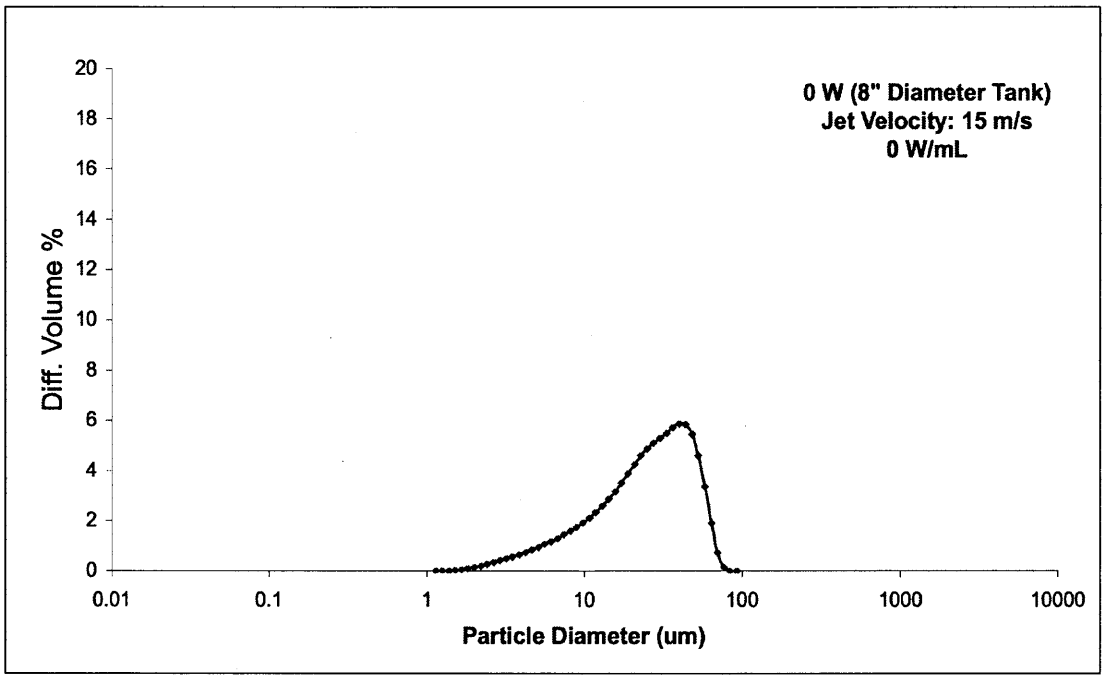

Figure 3.11. Particle size distribution of Griseofulvin crystals measured with the LS230 apparatus. Experiment 40 (04/10/08): jet velocity=15 m/s; no sonication.

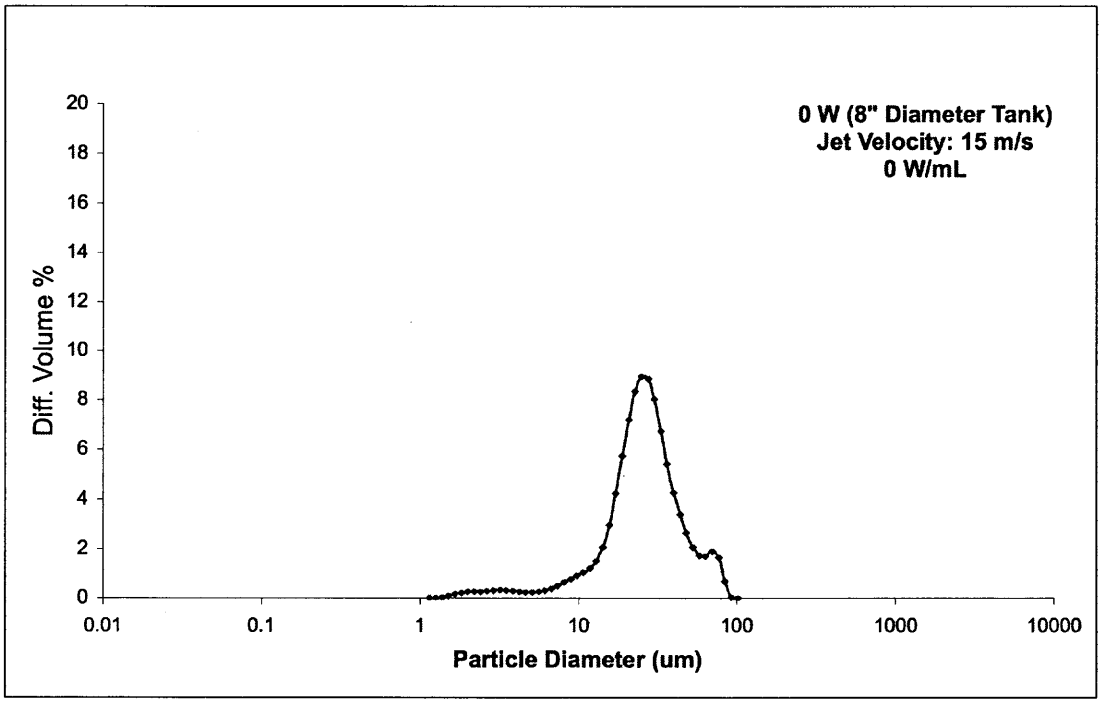

Figure 3.12. Particle size distribution of Griseofulvin crystals measured with the LS230 apparatus. Experiment 45 (04/15/08): jet velocity=15 m/s; no sonication.

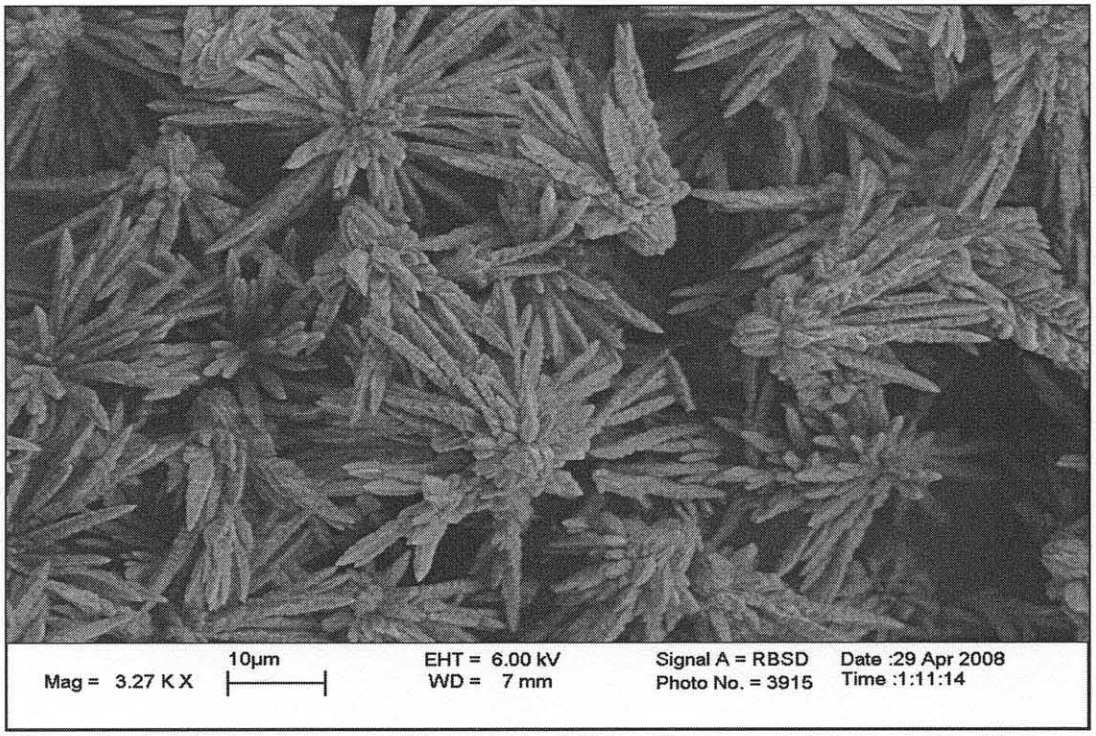

Figure 3.13. Electron micrographic picture of Griseofulvin crystals measured with the SEM apparatus. Experiment 42 (04/14/08): jet velocity=15 m/s; no sonication.

Figures 3.14 and 3.15 show the crystal size distribution for two duplicate experiments conducted at the higher jet velocity (15 m/s) and 75 W of sonication power. The particle size distribution ranged from 2-3 µm to 50 µm. The mean particle size was found to be 15.53 µm for Figure 3.14 and 9.92 µm for Figure 3.15. A micrograph for the same experiment is shown in Figure 3.16. The crystals still showed agglomeration. The crystals were still elongated in shape. The average mean particle size obtained from 6 replicate experiments (and multiple replicate LS 230 measurements taken for each experiment) was found to be 7.29 µm (Appendix B; Summary Table). The particle size distribution was comparable in all experiments. The crystal structure also appeared to be similar in all SEM scans. Additional experimental results for this case are presented in Appendix B2.

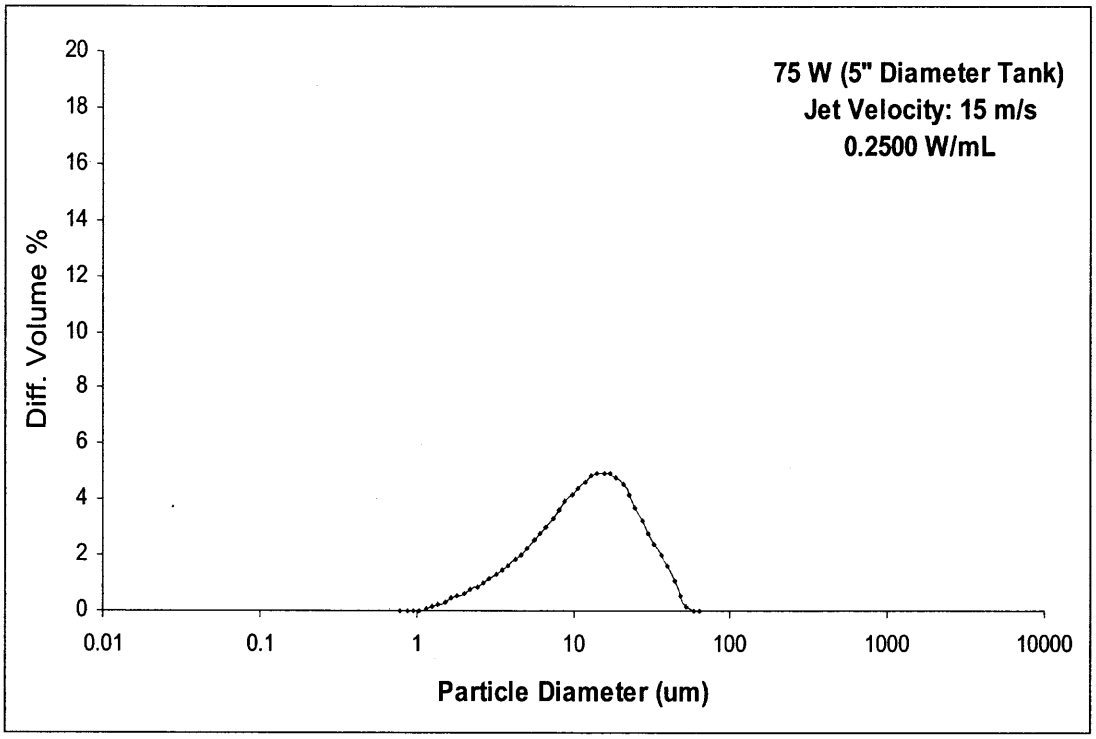

Figure 3.14. Particle size distribution of Griseofulvin crystals measured with the LS230 apparatus. Experiment 47 (04/16/08): jet velocity=15 m/s; 75 W sonication power.

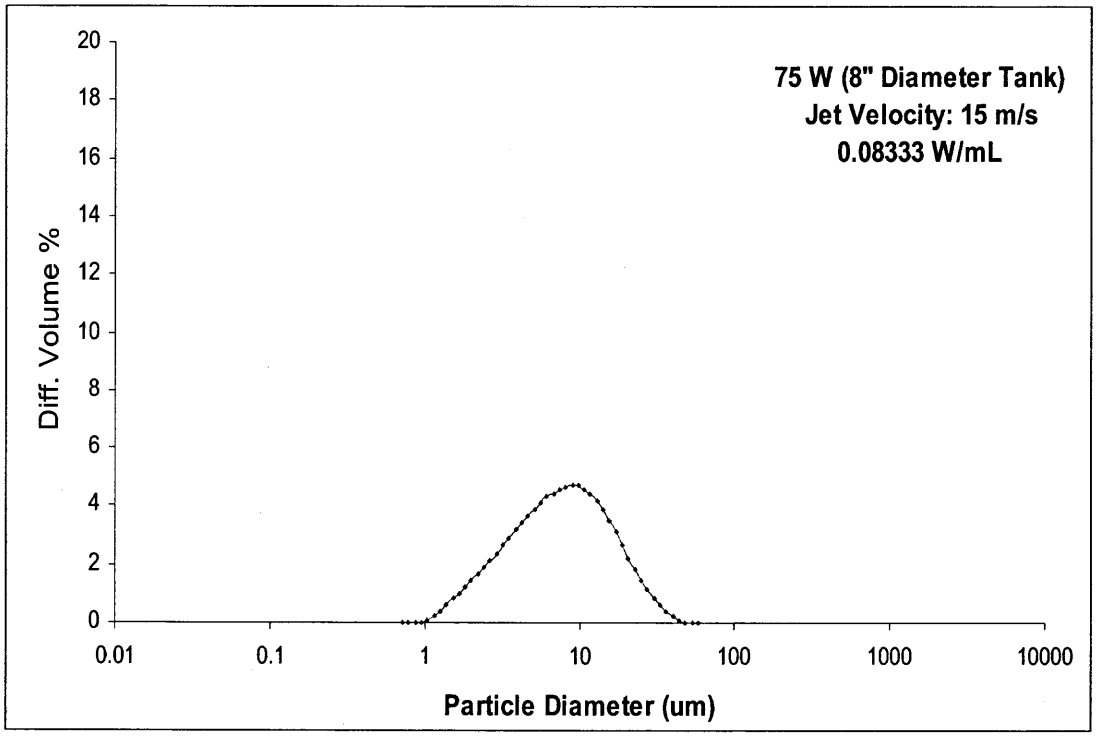

Figure 3.15. Particle size distribution of Griseofulvin crystals measured with the LS230 apparatus. Experiment 70 (04/30/08): jet velocity=15 m/s; 75 W sonication power.

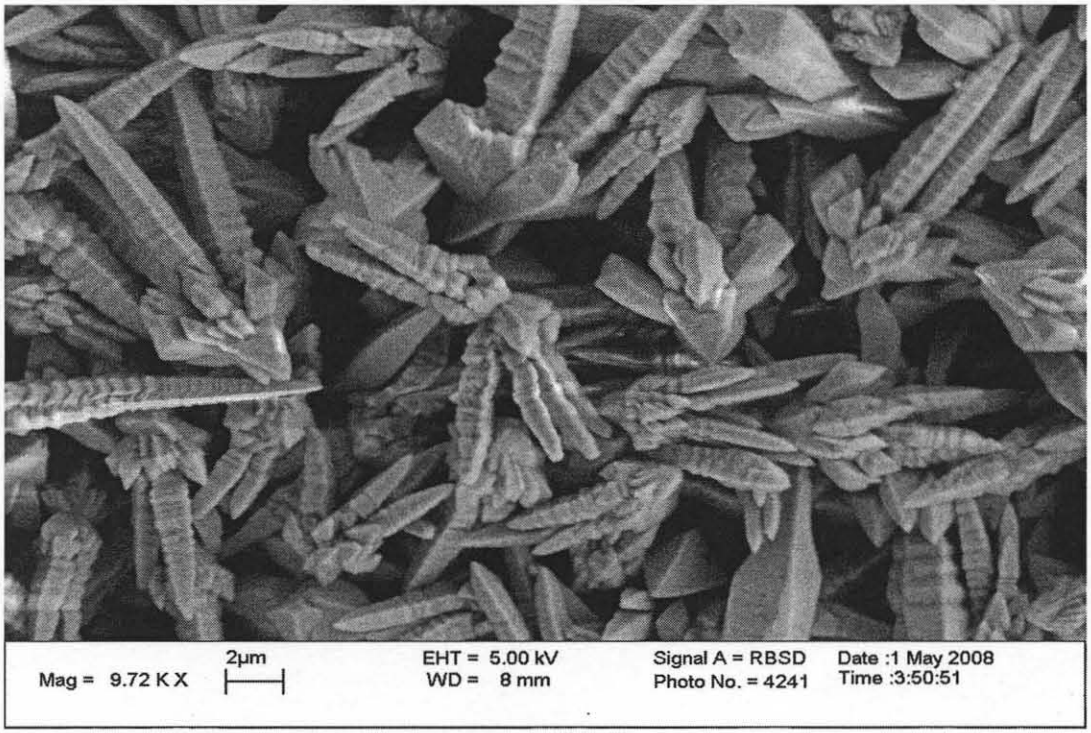

Figure 3.16. Electron micrographic picture of Griseofulvin crystals measured with the SEM apparatus. Experiment 46 (04/16/08): jet velocity=15 m/s; 75 W sonication power.

Figure 3.17 and 3.18 show the crystal size distribution for two duplicate experiments conducted at the higher jet velocity (15 m/s) and 125 W of sonication power. The particle size distribution ranged from 2µm to 15µm. The mean particle size was found to be 5.04 µm for Figure 3.14 and 5.72 µm for Figure 3.18. A micrograph for the same experiment is shown in Figure 3.19. The crystals still appear to be agglomerated, but the size of the agglomerates was smaller than in the previous cases, probably as a result of sonication. The average mean particle size obtained from 9 replicate experiments (and multiple (4-12) replicate LS 230 measurements taken for each experiment) was found to be 4.48 µm (Appendix B; Summary Table). The particle size distribution was comparable in all experiments. The crystal structure also appeared to be

similar in all SEM scans. Additional experimental results for this case are presented in Appendix B3.

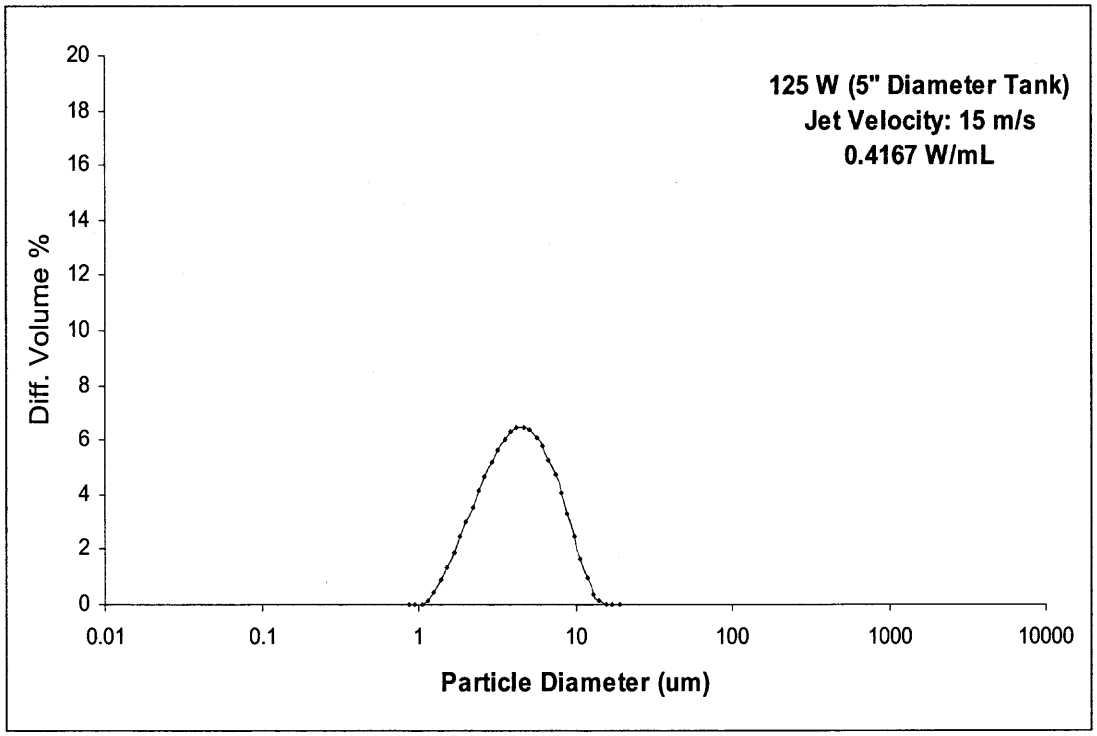

Figure 3.17. Particle size distribution of Griseofulvin crystals measured with the LS230 apparatus. Experiment 56 (04/22/08): jet velocity=15 m/s; 125 W sonication power.

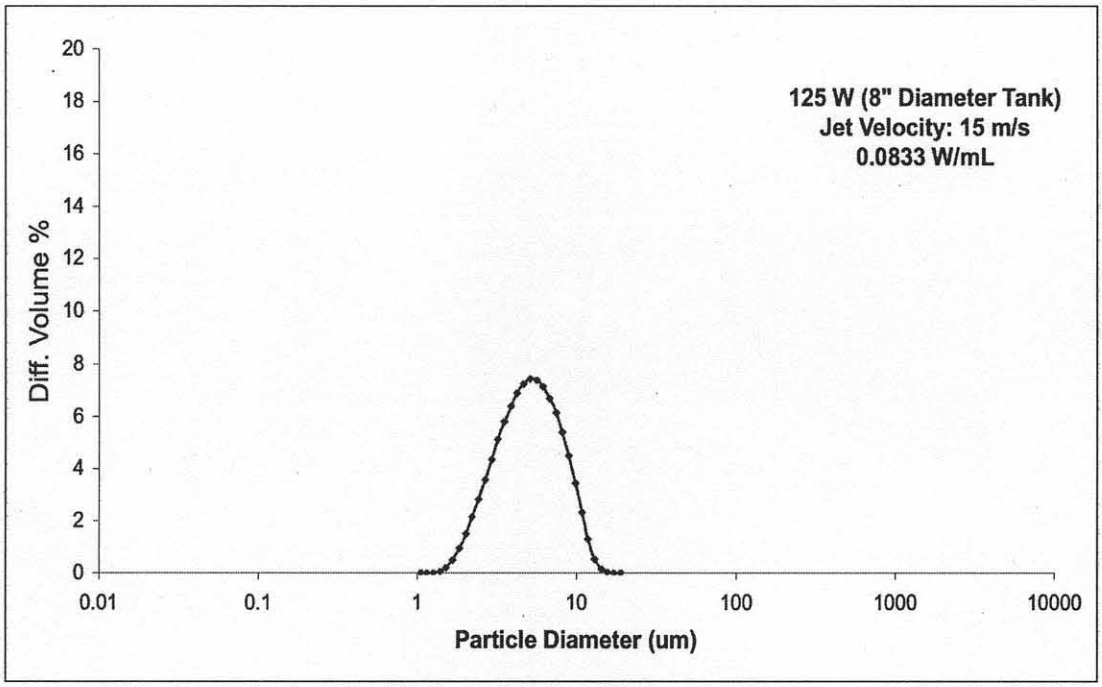

Figure 3.18. Particle size distribution of Griseofulvin crystals measured with the LS230 apparatus. Experiment 41 (04/11/08): jet velocity=15 m/s; 125 W sonication power.

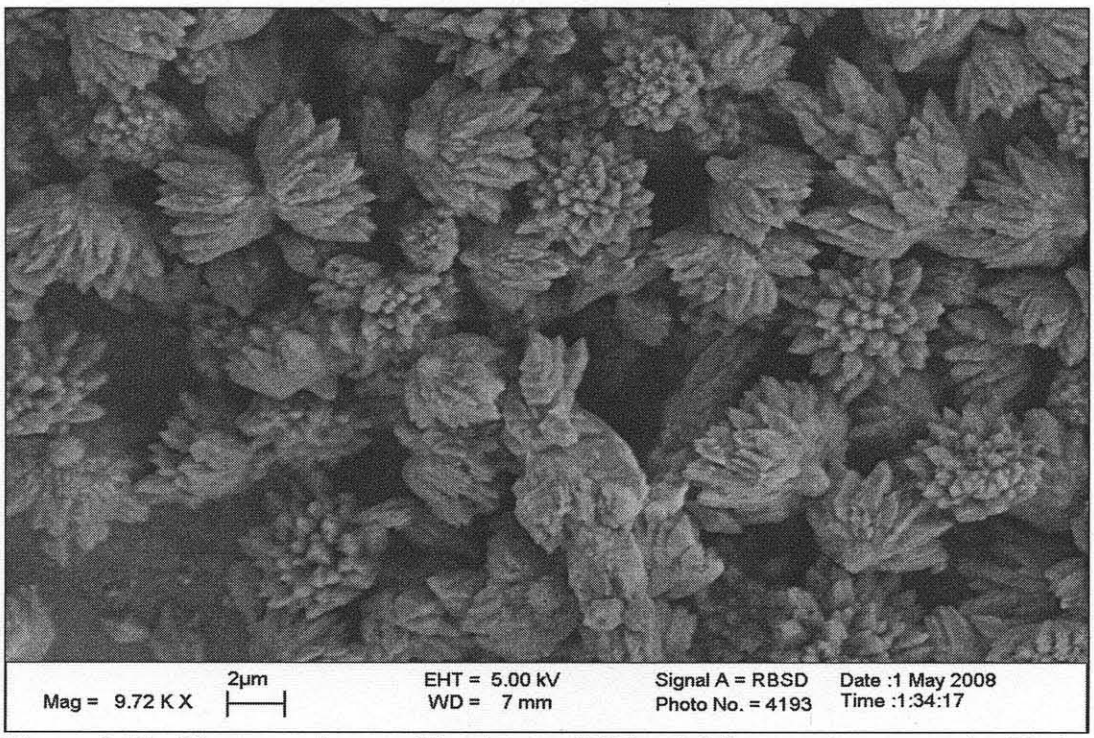

Figure 3.19. Electron micrographic picture of Griseofulvin crystals measured with the SEM apparatus. Experiment 44 (04/15/08): jet velocity=15 m/s; 125 W sonication power.

Finally, Figures 3.20 and 3.21 and Figure 3.22 show, respectively, the particle size distributions and a micrograph of the crystals for the experiment with the higher jet velocity (15 m/s) and 200 W of sonication power, while Figures 3.23 and 3.24 and Figure 3.25 are the corresponding figures for the 250 W case. In both cases, the particle size distribution ranged from 1 μm to 11 μm, and the mean particle sizes were found to be 3.40 μm and 4.42 μm for the 200 W case and 6.06 μm and 3.61 μm for the 250 W case. The average mean particle size obtained from 6 replicate experiments (and multiple (4-11) replicate LS 230 measurements taken for each experiment) was found to be 4.67 μm for the 200 W case (Appendix B; Summary Table). The average mean particle size obtained from 3 replicate experiments (and multiple (4-5) replicate LS 230 measurements taken for each experiment) was found to be 5.22 μm for the 250 W case (Appendix B; Summary Table). The particle size distribution was comparable in all experiments. The crystal structure also appeared to be similar in all SEM scans. However, it should be noticed that the crystal structures in these two cases was remarkably different from that obtained in the 125 W case and the other low sonication power cases. A comparison of the micrographs (Figure 3.19 vs. 3.22 and 3.25) shows that at 125 W the particles, although small and of sizes comparable to those obtained at 200 W and 250 W, were agglomerates of smaller crystals, whereas at 200 W and 250 W single well-defined crystals appeared. Additional experimental results for this case are presented in Appendices B4 and B5.

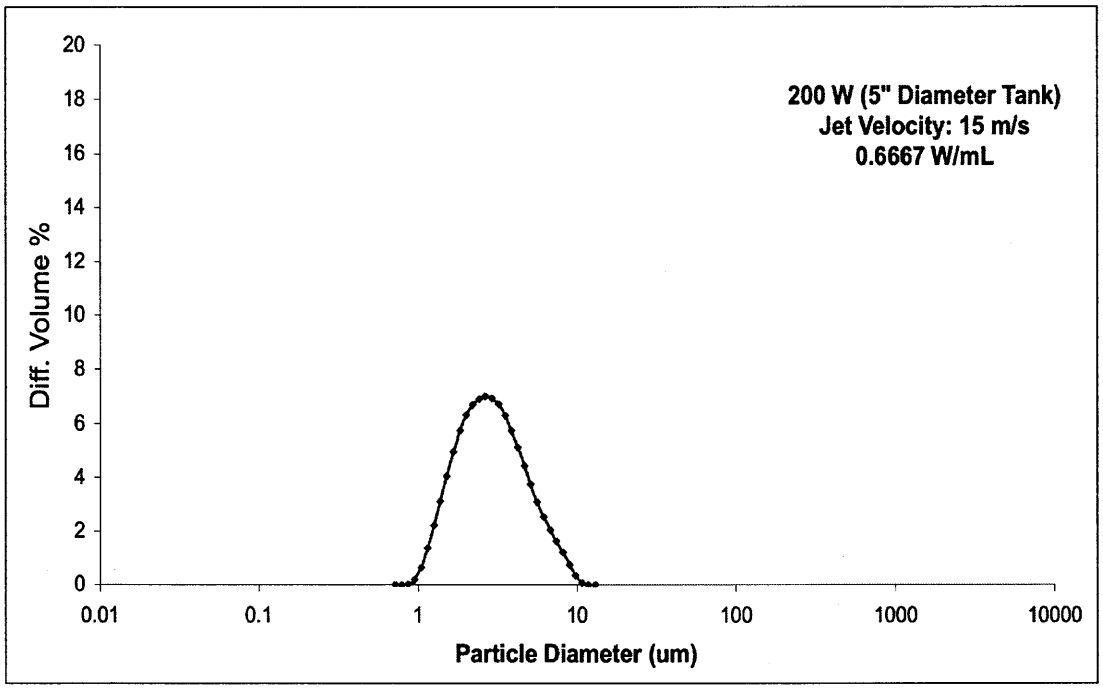

Figure 3.20. Particle size distribution of Griseofulvin crystals measured with the LS230 apparatus. Experiment 49 (04/17/08): jet velocity=15 m/s; 200 W sonication power.

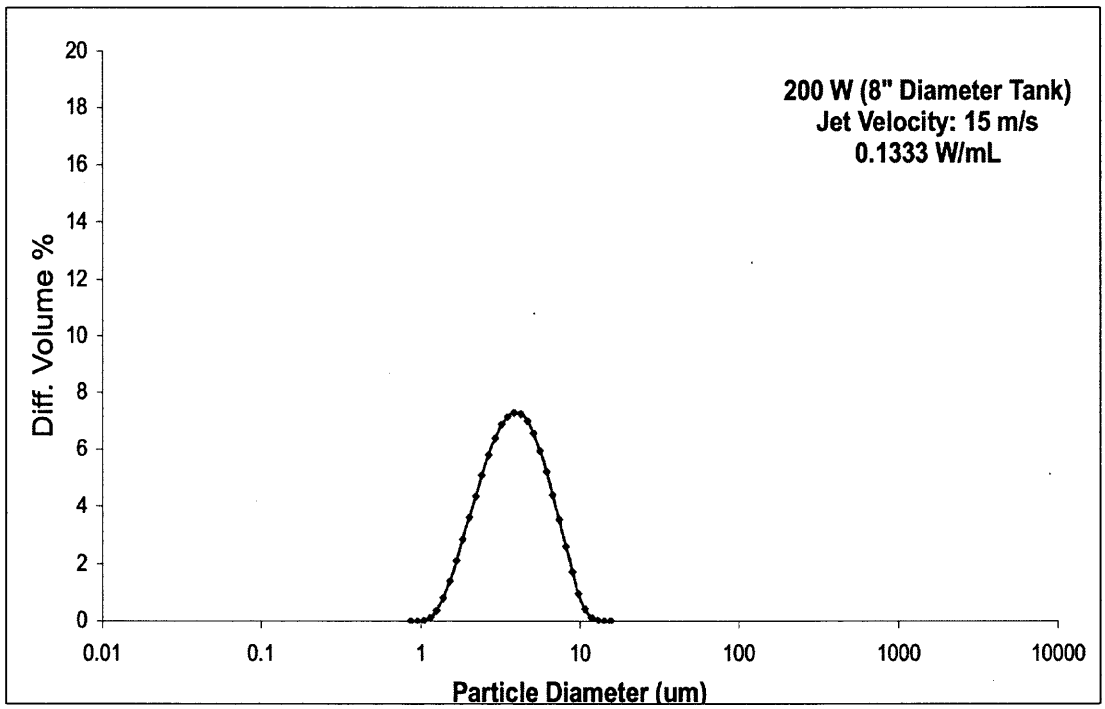

Figure 3.21. Particle size distribution of Griseofulvin crystals measured with the LS230 apparatus. Experiment 43 (04/14/08): jet velocity=15 m/s; 200 W sonication power.

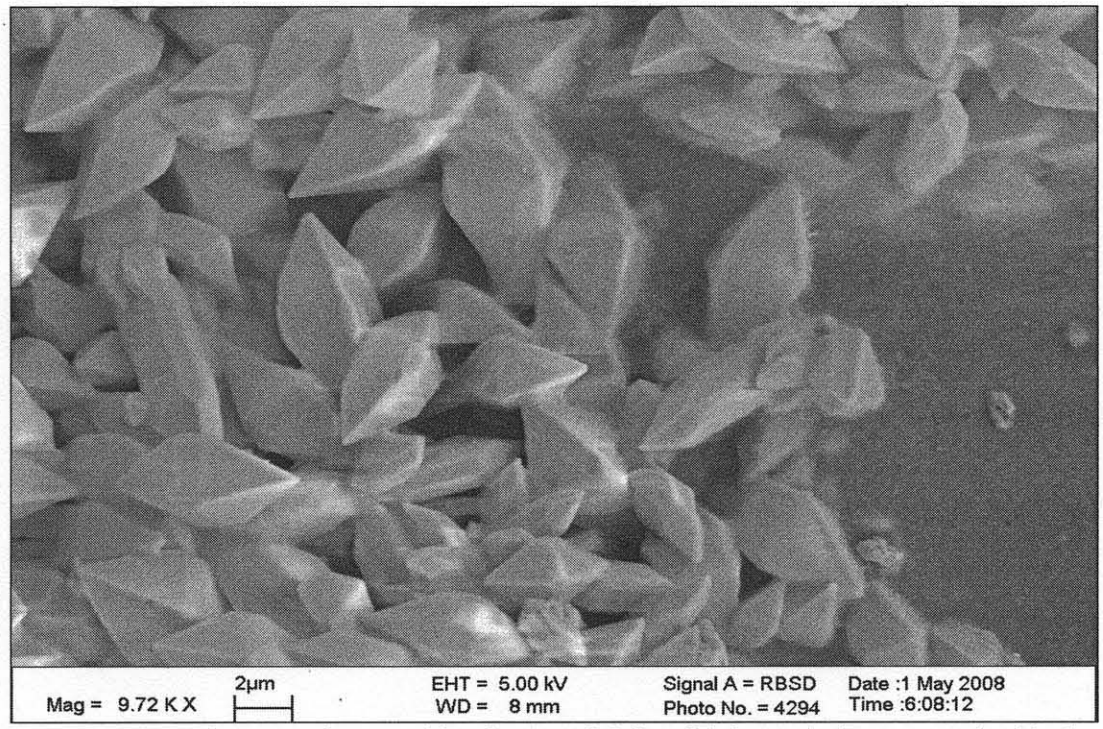

Figure 3.22. Electron micrographic picture of Griseofulvin crystals measured with the SEM apparatus. Experiment 49 (04/17/08): jet velocity=15 m/s; 200 W sonication power.

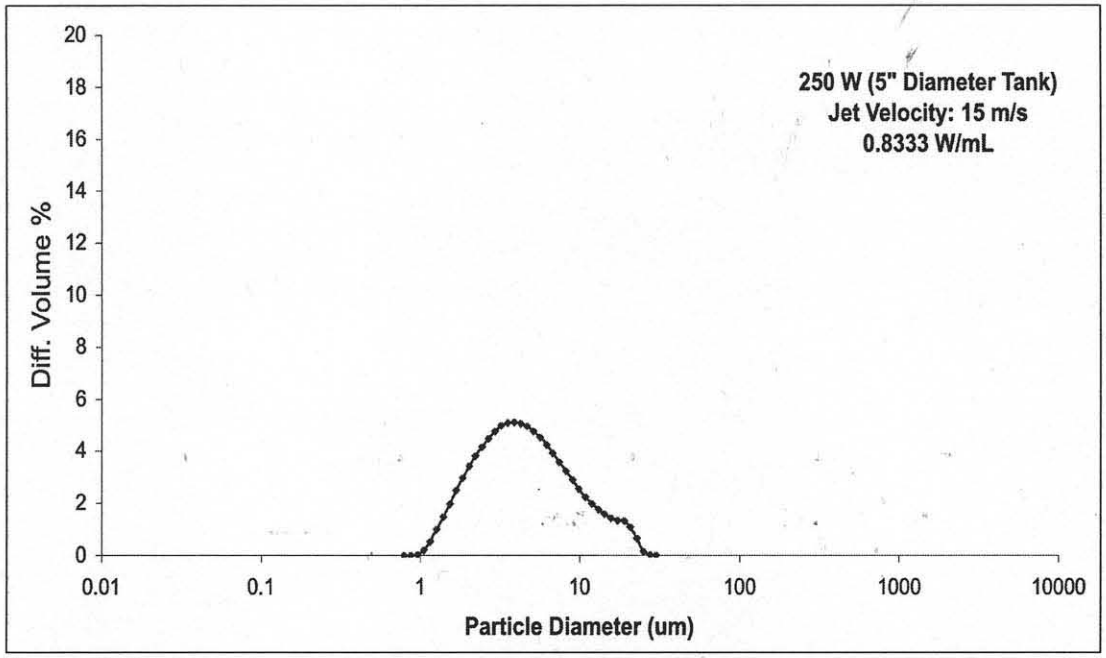

Figure 3.23. Particle size distribution of Griseofulvin crystals measured with the LS230 apparatus. Experiment 59 (04/22/08): jet velocity=15 m/s; 250 W sonication power.

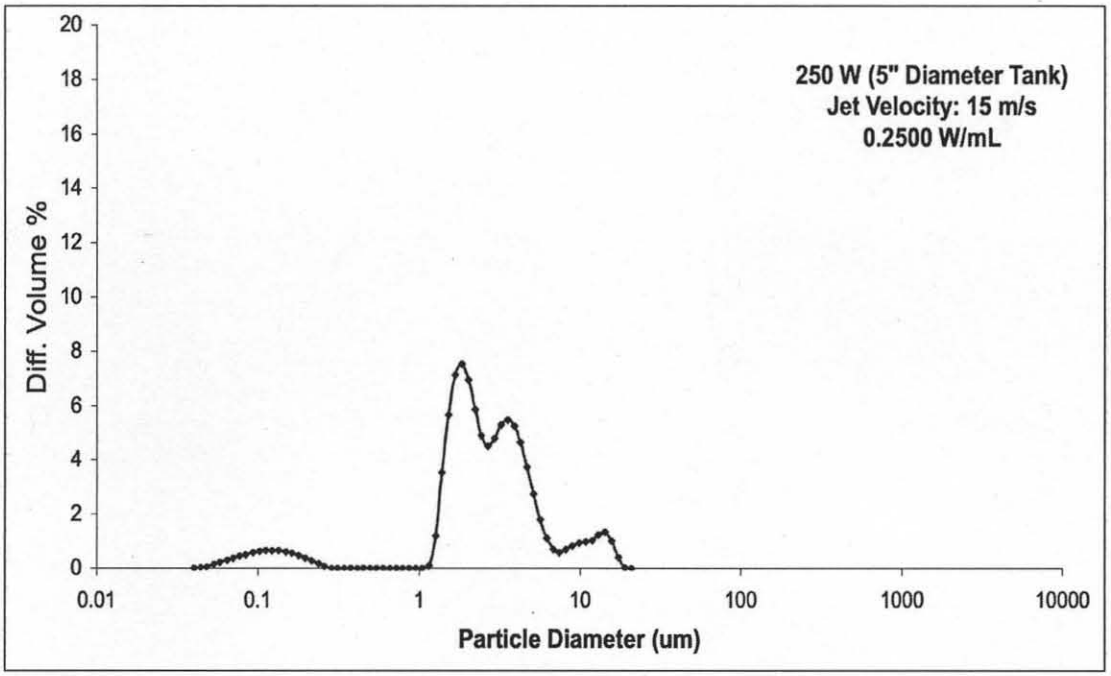

Figure 3.24. Particle size distribution of Griseofulvin crystals measured with the LS230 apparatus. Experiment 66 (04/28/08): jet velocity=15 m/s; 250 W sonication power.

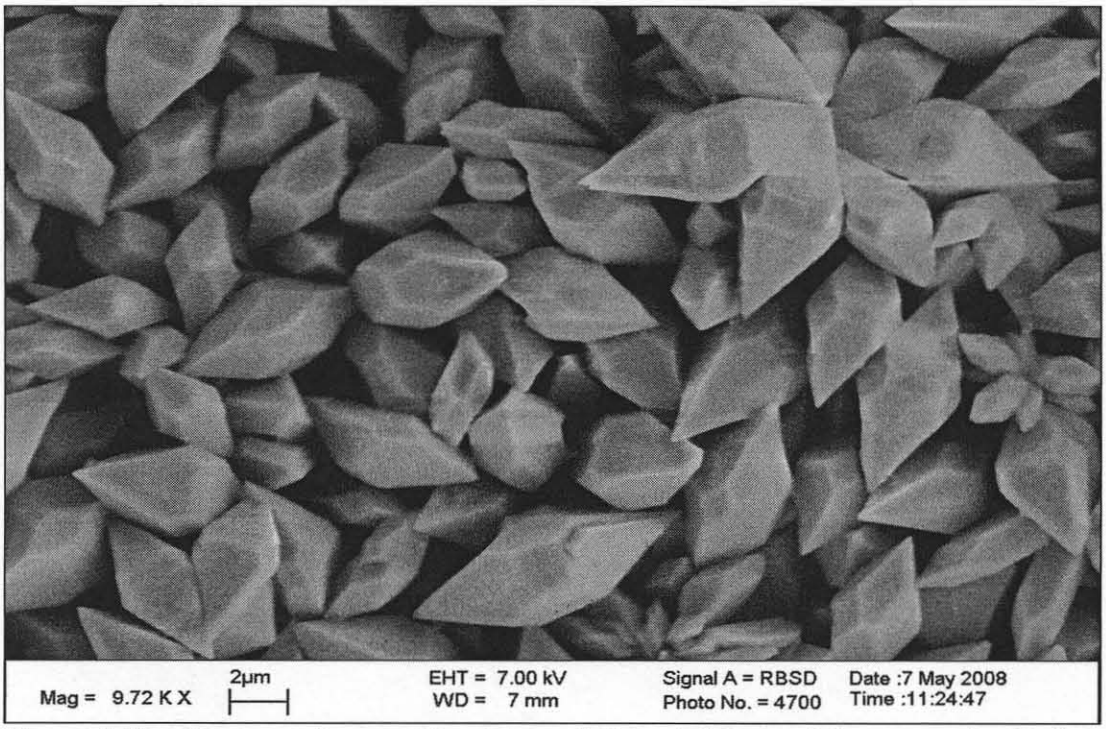

Figure 3.25. Electron micrographic picture of Griseofulvin crystals measured with the SEM apparatus. Experiment 60 (04/27/08): jet velocity=15 m/s; 250 W sonication power.

3.3 Effect of Sonication Power on Particle Size and Crystal Morphology at Different Jet Velocities

The effect of sonication power on particle size is shown in Figures 3.26 (mean particle size), 3.27 (d10 particle size) and 3.28 (d90 particle size). In each figure the impinging jet velocity was the parameter. The bars in these figures represent the standard error of replicate experiments.

A number of conclusions can be obtained from an examination of these figures. In the absence of sonication, the mean particle size was found to be, in general, very high irrespective of the jet velocity. However, the particle size was higher for the lower jet velocity than the higher jet velocity (39.83 μm vs. 28.97 μm) indicating that there was a small effect of the jet velocity. An examination of the corresponding micrographs shows that in both cases extensive agglomeration occurred, and that the particles were actually agglomerates of smaller crystals. The introduction of sonication, even at sonication powers as low as 75 W, appreciably reduced the particle sizes. Interestingly, although the mean particle size at 75 W was nearly the same irrespective of the impinging jet velocity (8.14 μm vs. 7.29 μm at the lower and higher jet velocity, respectively), the particle shape was different. A comparison of the micrographs at 75 W (Figure 3.4 vs. Figure 3.16) reveals that at 0.722 m/s the particles were made of single crystals whereas at 15 m/s the particles were agglomerates of much smaller crystals, indicating that the jet velocity had a significant impact not on the average size but the particle morphology. When the sonication power was increased to 125 W the mean particle size decreased even further (6.14 μm and 4.48 μm at the lower and higher jet velocity, respectively). However, the particle morphology was again appreciably different between the two cases (Figure 3.6 vs. 3.19), with the small jet velocity generating single crystals and the higher

jet velocity producing small agglomerates. Only when the sonication power was increased to 200 W and beyond did the crystal obtained with different jet velocities appear to be made of single crystals. However, and examination of the corresponding micrographs (Figure 3.8 vs. Figure 3.22) reveals a small difference in the crystals: those obtained at the lower jet velocity appear to be more needle-like than those obtained at the higher velocity. This difference remained even at the highest sonication power tested here (250 W). The mean crystals size at sonication powers equal to or larger than 200 W did not change appreciably with sonication power beyond their values at 125 W (e.g., 7.33 μm vs. 4.67 μm at 200 W, and 6.66 μm vs. 5.22 μm at 250 W). Therefore, it appears that an asymptotic value of the particle size is achieved which is only slightly affected by the jet velocity. It is also interesting to notice that the mean particle size for sonication powers beyond 125 W actually resulted in a small *increase* in particle size compared to the value at 125 W. This phenomenon is probably attributable to a local heating effect that would promote crystal growth.

Figure 3.27 shows the effect of sonication power and impinging jet velocity on d10, i.e., the size below which 10% of the particles are found (by volume). This figure clearly shows that minimal or no differences exist between the two curves, indicating that for a given sonication power the jet velocity has little influence on d10. In addition, once the sonication power is at or above 75 W d10 remains relatively uniform irrespective of both jet velocity and sonication power.

By contrast, Figure 3.28 show that the effect of sonication power and impinging jet velocity on d90, i.e., the size below which 90% of the particles are found (by volume), is more pronounced. At lower sonication power, this is likely to be the result of

agglomeration effects, which have a greater impact on larger particles rather than smaller particles. At higher sonication powers the d90 curves show a somewhat larger deviation depending on the jet velocity.

A comparison was made between the XRD spectra obtained under different experimental conditions. Figures 3.29 and 3.30 show the XRD data from samples obtained in experiments at the lower jet velocity and higher jet velocity, respectively. The results presented in Figure 3.29 show that very similar spectra for griseofulvin were obtained irrespective of the operating conditions used in the experiments. This indicates that the crystal habit of griseofulvin was the same irrespective of the experimental conditions. The results of that figure can be compared with those of Figure 3.30 obtained at the higher impinging jet velocity (lower four panels). This figure also shows the spectrum for unprocessed Griseofulvin as a reference (top panel), and those for pure HPMC and SDS (second and third panel). All the Griseofulvin spectra in Figures 3.29 and 3.30 appear identical to each other irrespective of the sonication power and jet velocity, indicating that the same Griseofulvin crystal structure was formed. These spectra do not overlap with the HPMC and SDS spectra, which were therefore not incorporated in the Griseofulvin particles, confirming that the crystals were just made of Griseofulvin in all cases.

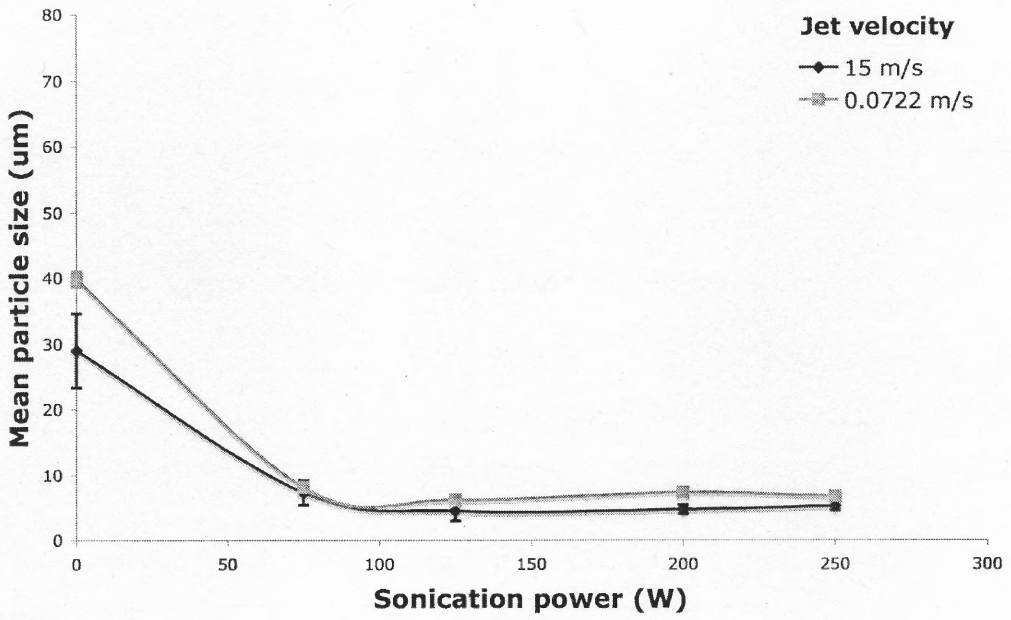

Figure 3.26. Effect of sonication power and impinging jet velocity on mean particle size

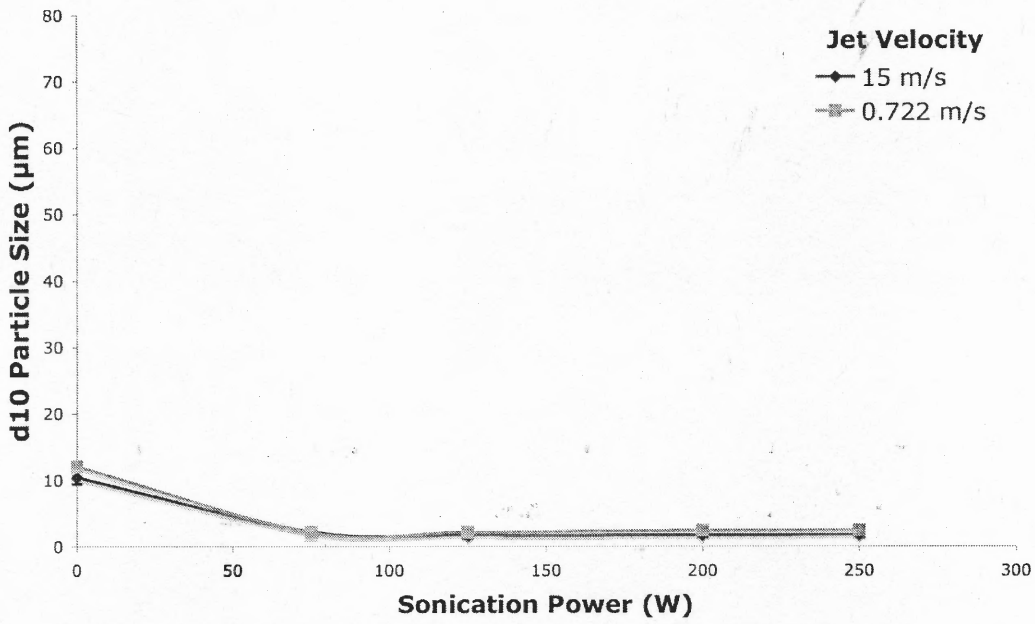

Figure 3.27. Effect of sonication power and impinging jet velocity on d10

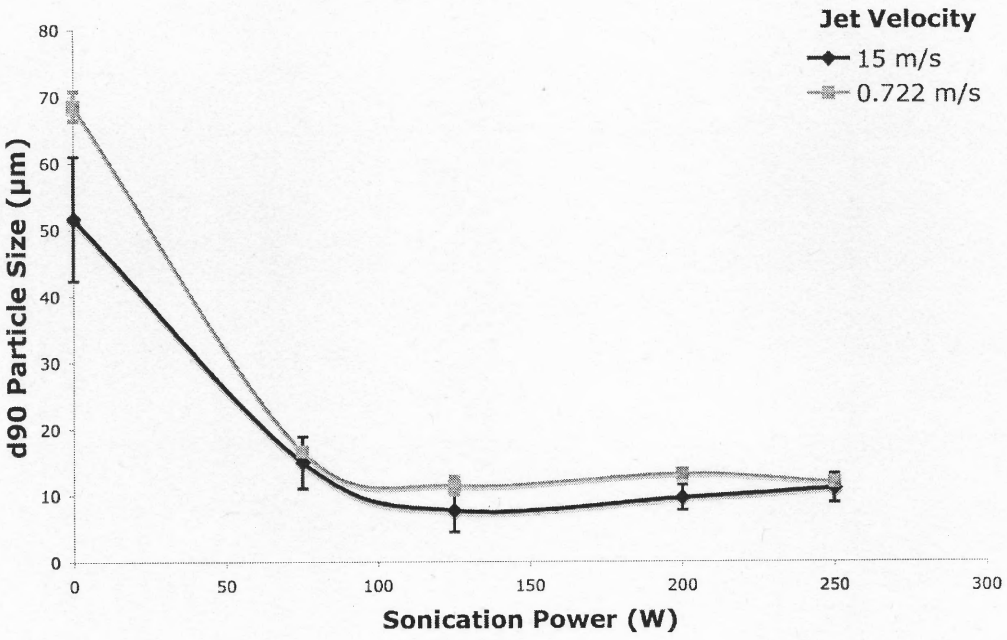

Figure 3.28. Effect of sonication power and impinging jet velocity on d90

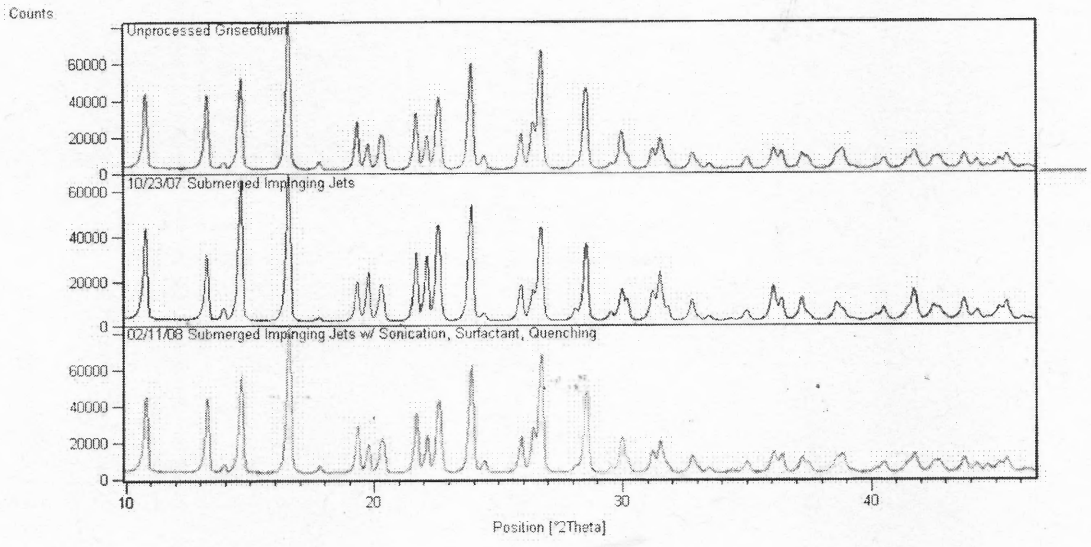

Figure 3.29. XRD Data for the lower jet velocity cases (0.722 m/s)

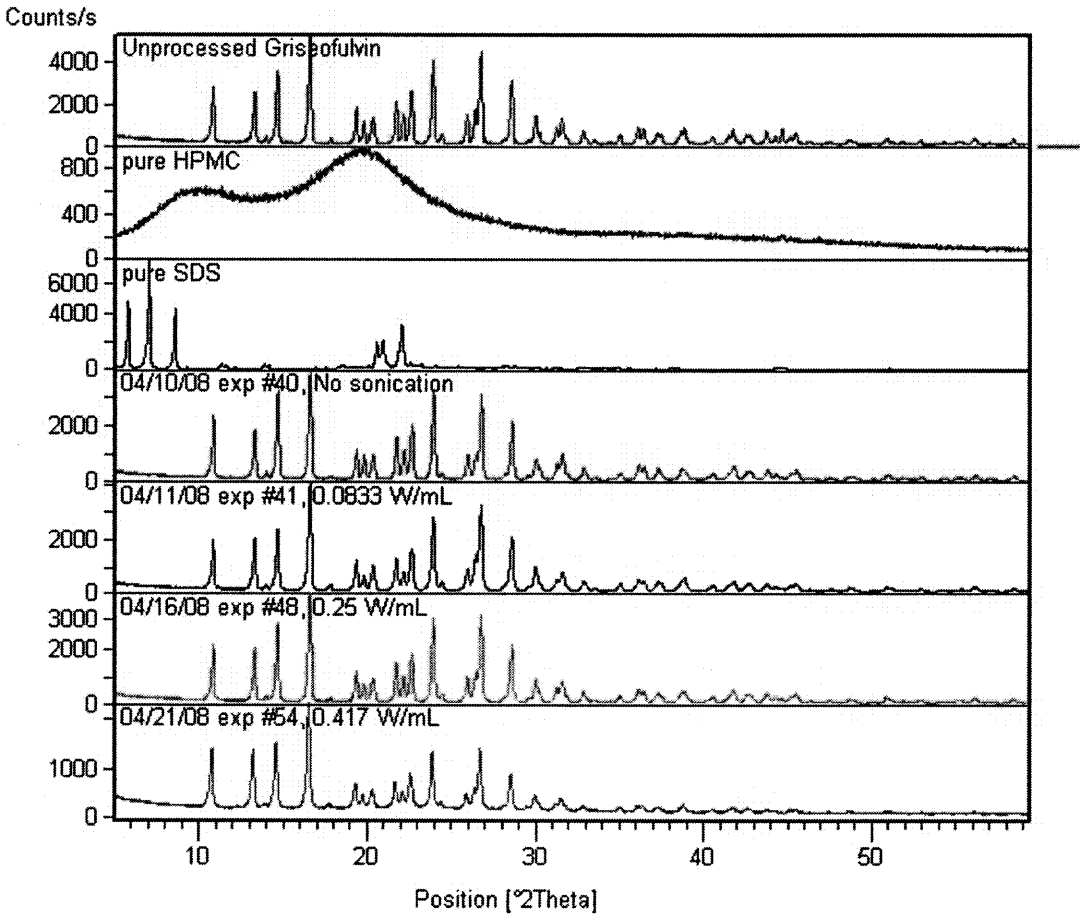

Figure 3.30. XRD Data for the higher jet velocity cases (15 m/s)

3.4 Effect of Sonication Power vs. Sonication Power per Unit Volume on Particle Size

All the results presented above demonstrate the positive effect of sonication power on decreasing the particle size until a lower particle size limit is reached which can no longer be affected by the dynamics of the system. However, one could argue that sonication power per unit volume is a more appropriate variable to use in this case rather

than sonication power. To test this hypothesis, the same particle size data shown in Figure 3.26 for the 15 m/s impinging jet velocity were plotted in Figure 3.31 as a function of sonication power, using the liquid volume in the reactor as a parameter. This figure shows that the liquid volume had a limited effect on particle size.

In Figures 3.32, 3.33 and 3.34, respectively, the mean particle size, d10 and 90 were plotted as a function of sonication power/volume. Comparing these figures with the corresponding figures having the sonication power as the independent variable (Figures 3.26, 3.27 and 3.28.) one can see that the fit is not as good when sonication power/volume is used. This point is further evidenced by the data shown in Figure 3.35, in which the particle size was plotted as a function of liquid volume in the reactor using the sonication power/volume as a parameter (for each of the two curves in this figure the sonication power was changed in order to keep the sonication power/volume constant). The fact that different particles sizes were obtained at different sonication power/volume is an additional indication that this variable is less appropriate than the sonication power to explain the data. The rationale for this conclusion is in the fact that antisolvent precipitation is a rapid process and it is likely to occur in the impinging zone only. Therefore only the power dissipated in the impinging region is likely to affect the process and hence the particle size. If the reaction is taking place at the same sonication power but in a reactor filled with a larger volume of liquid (thus decreasing the average sonication power/volume) the power delivered to the precipitation zone will not likely change and hence the particle size will not change as well, to any significant degree. One could rationalize this conclusion by assuming that the power per unit volume is indeed the key variable controlling the process, provided that the actual precipitation volume is

used in the calculation. This precipitation volume will probably remain unchanged if the reactor contains more liquids. Therefore, increasing the power but leaving the "uncontrollable" precipitation zone volume (not the total volume) unchanged will have a beneficial effect (until a limit value is reached), but decreasing the power while decreasing the total volume will not, since the precipitation volume will not be affected.

Table 3.1. Particle size based on reactor volume

Sonication power (W)	Volume (mL)	Sonication power/ Volume (W/mL)	Mean (µm)	d10 (µm)	d90 (µm)
75	300	0.2500	6.7277	2.2208	13.3929
125	300	0.4167	4.1866	1.7732	7.5065
200	300	0.6667	4.2194	1.3321	8.4194
250	300	0.8333	5.9472	1.8938	12.9880
125	500	0.2500	3.3978	1.5729	5.4930
125	750	0.1667	9.8018	2.7678	18.8575
75	900	0.0833	8.6846	2.3169	18.6838
250	1000	0.2500	3.5950	1.5160	6.4383
0	1500	0.0000	28.9723	10.3612	51.6537
125	1500	0.0833	4.2213	1.5883	6.9047
200	1500	0.1333	5.0560	2.0967	10.4954

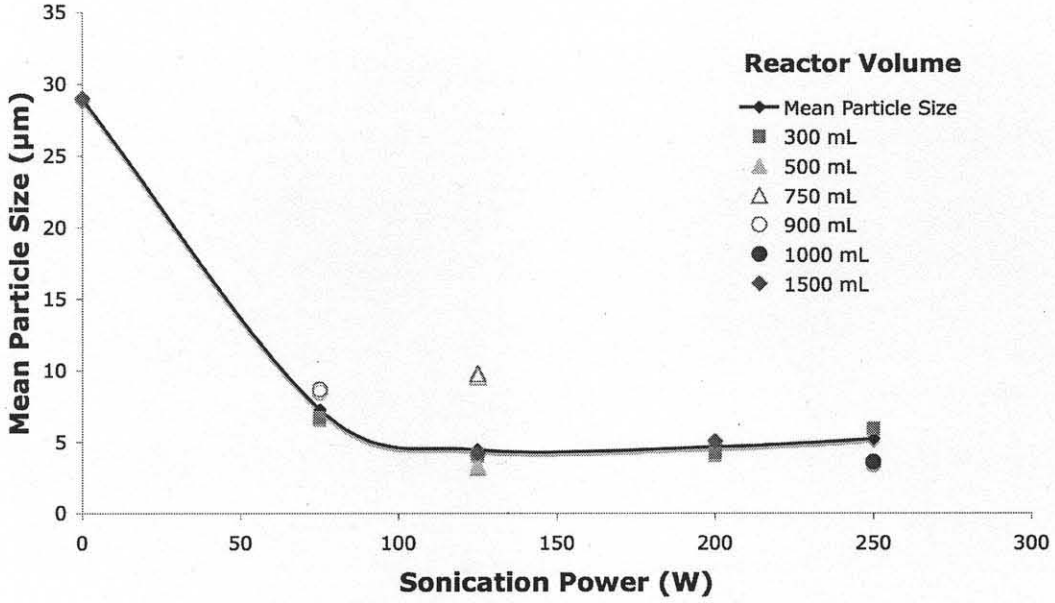

Figure 3.31. Particle size as a function of sonication power for different reactor volume

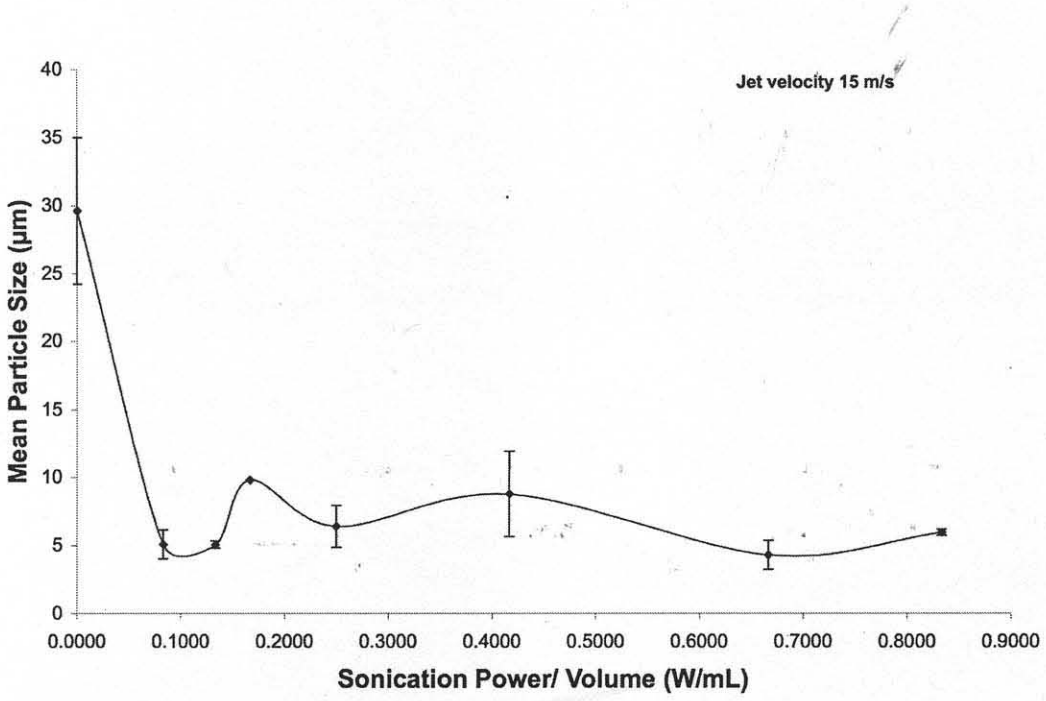

Figure 3.32. Particle size as a function of sonication power/volume (W/mL)

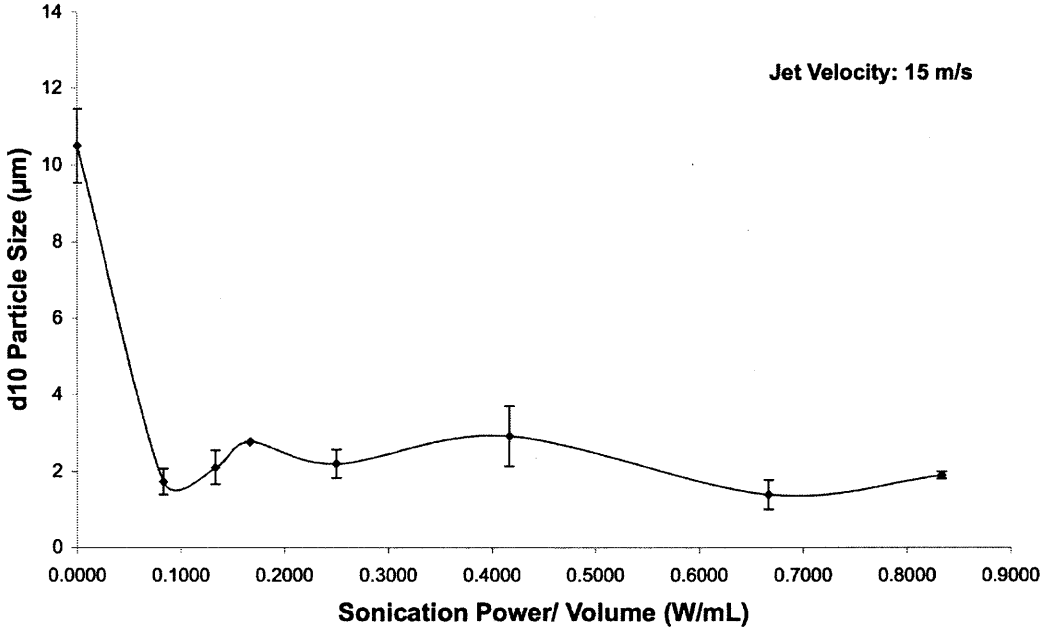

Figure 3.33. d10 as a function of sonication power/volume (W/mL)

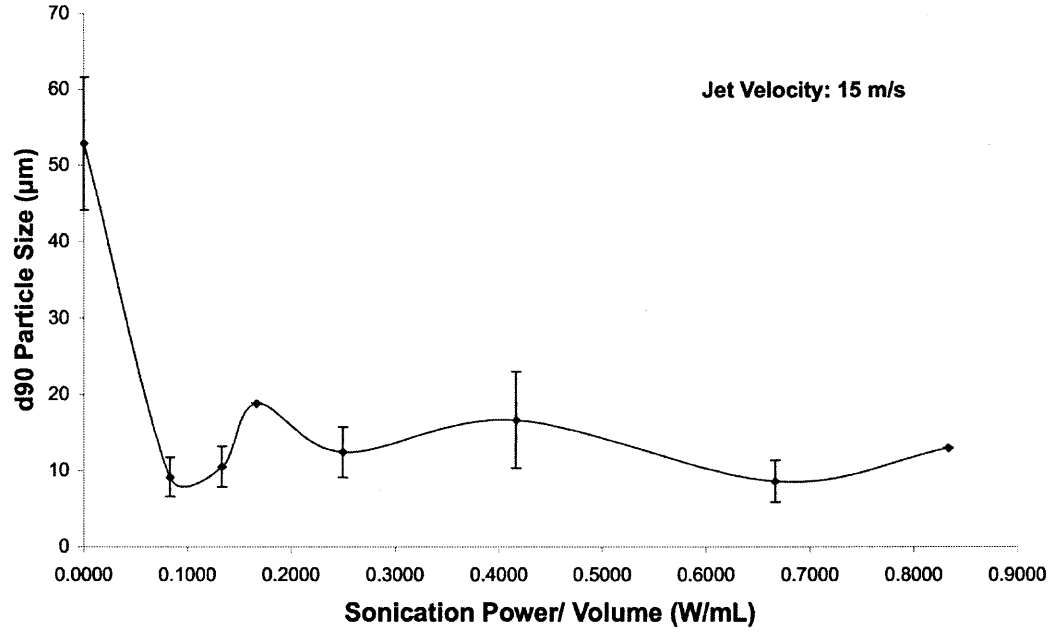

Figure 3.34. d10 as a function of sonication power/volume (W/mL)

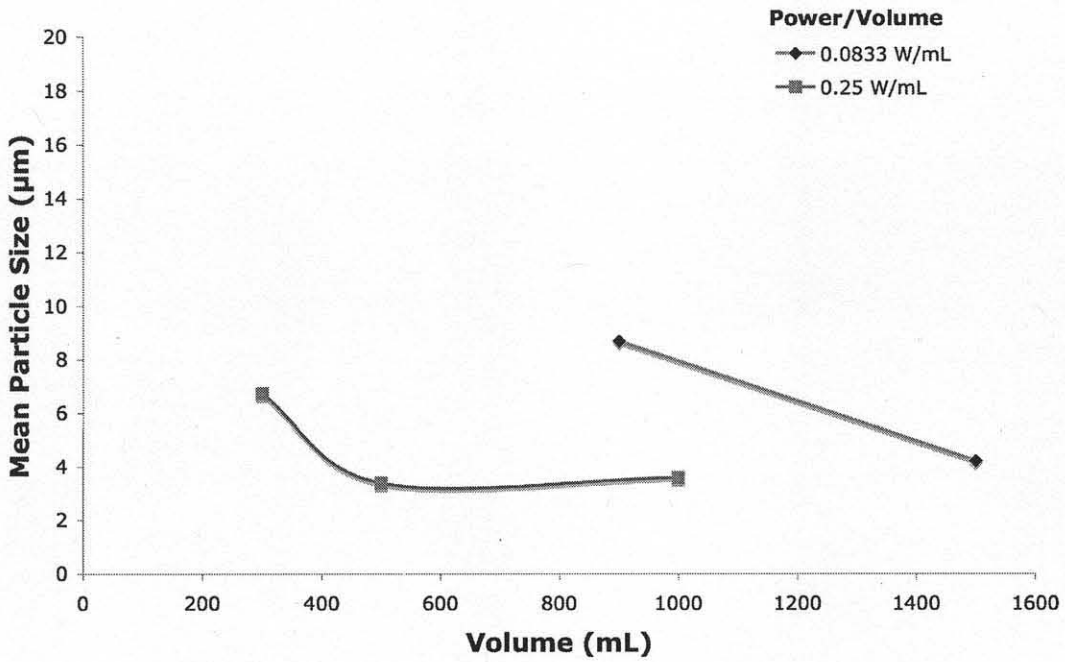

Figure 3.35. Particle size as a function of reactor volume for different sonication power/volume

CHAPTER 4

CONCLUSIONS

In this work, the effect of sonication power on the anti-solvent precipitation of Griseofulvin in an impinging jet system was experimentally determined at two impinging jet velocities. The following conclusions can be derived from the results obtained in this study:

- In the absence of sonication, the mean particle size was found to be, in general, relatively high (on the order of tens of μm) irrespective of the jet velocity. However, the particle size was larger for the lower jet velocity than the higher jet velocity, implying that that the jet velocity had a small but detectable effect on the size of the precipitated particles;
- The introduction of sonication appreciably reduced the mean particle size, even when the sonication power was as low as 75 W. Although the mean particle size at 75 W was nearly the same irrespective of the impinging jet velocity, the particle shape was different: the particles formed at the lower jet velocity were single crystals, while the higher impinging jet velocity resulted in particles formed by open agglomerates of smaller crystals;
- At a sonication power equal to 125 W, the particle morphology was also different depending on the jet velocity, with the small jet velocity generating single crystals and the higher jet velocity producing compact agglomerates of smaller crystals;
- At sonication powers of 200 W or higher, all particles were made of single crystals, irrespective of the jet velocity, although more elongated crystals were obtained at the lower impinging jet velocity;

- The mean crystals size at sonication powers equal to, or larger than, 200 W did not change appreciably with sonication power, and was only slightly smaller than the size obtained at 125 W. Such asymptotic values of the particle size were only partially affected by the jet velocity, with mean asymptotic particles sizes on the order of 3-6 μm for the higher jet velocity and 6-8 μm for the lower jet velocity.
- The crystal habit of Griseofulvin was the same irrespective of the experimental conditions;
- Antisolvent precipitation is a rapid process that is likely to take place, and be completed, in the impinging zone between the jets. Therefore, only the power dissipated in the impinging region is likely to affect the process and hence the final particle size of the precipitate. This was evidenced by the fact that the particle size results obtained here could be better correlated with sonication power rather than sonication power per unit liquid volume of the entire reactor.

APPENDIX A

RESULTS OF EXPERIMENTS WITH LOWER JET VELOCITY (0.722 m/s)

Experiment/ LS run	Sonication power (W)	Volume (mL)	Sonication power/ Volume (W/mL)	Mean	Median	d10	d90
Experiment 23/1	0	2000	0.0000	43.3700	41.7900	12.3000	76.5300
Experiment 23/2	0	2000	0.0000	43.0900	41.3500	12.3100	76.1600
Experiment 23/3	0	2000	0.0000	37.0900	37.0200	11.4500	62.6500
Experiment 23/4	0	2000	0.0000	34.7900	34.9300	11.1600	58.4400
Experiment 23/5	0	2000	0.0000	40.1400	39.7700	11.7700	69.3500
Experiment 23/6	0	2000	0.0000	39.5900	39.2000	12.0600	68.0800
Experiment 23/7	0	2000	0.0000	40.9300	40.4500	12.4500	70.2500
Experiment 23/8	0	2000	0.0000	39.6600	40.1600	12.6500	67.3100
Average	**0**	**2000**	**0.0000**	**39.8325**	**39.3338**	**12.0188**	**68.5963**
Experiment 34/1	75	300	0.2500	9.3400	7.6180	2.3550	19.1100
Experiment 34/2	75	300	0.2500	8.1460	6.9540	2.3930	15.7500
Experiment 34/3	75	300	0.2500	6.6900	5.4660	1.9340	13.6300
Experiment 34/4	75	300	0.2500	6.3190	5.3820	1.9800	12.2500
Experiment 34/5	75	300	0.2500	9.0360	7.1080	2.0070	19.0000
Experiment 34/6	75	300	0.2500	9.3160	7.2270	2.0170	19.6200
Average	**75**	**300**	**0.2500**	**8.1412**	**6.6258**	**2.1143**	**16.5600**
Experiment 32/1	125	300	0.4167	6.1570	4.9310	1.9920	11.6000
Experiment 32/2	125	300	0.4167	5.2220	4.3770	1.8140	9.9570
Experiment 32/3	125	300	0.4167	5.8460	5.0000	2.0620	10.9700
Experiment 32/4	125	300	0.4167	5.4320	4.7180	1.9310	10.2000
Experiment 32/5	125	300	0.4167	7.2270	5.9520	2.4240	13.0900
Experiment 32/6	125	300	0.4167	6.9820	5.7900	2.3770	12.6400
Average	**125**	**300**	**0.4167**	**6.1443**	**5.1280**	**2.1000**	**11.4095**
Experiment 36/1	200	300	0.6667	7.1910	6.0490	2.5060	12.5300
Experiment 36/2	200	300	0.6667	6.5270	5.8950	2.5460	11.4900
Experiment 36/3	200	300	0.6667	7.1400	6.1810	2.3140	13.0200
Experiment 36/4	200	300	0.6667	7.0280	6.1220	2.3100	12.7500
Experiment 36/5	200	300	0.6667	7.3300	6.3300	2.3710	13.2300
Experiment 36/6	200	300	0.6667	7.3040	6.2790	2.3630	13.0200
Experiment 36/7	200	300	0.6667	8.3030	6.4650	2.4110	15.1100
Experiment 36/8	200	300	0.6667	7.7990	6.3320	2.4370	13.8400
Average	**200**	**300**	**0.6667**	**7.3278**	**6.2066**	**2.4073**	**13.1238**

Experiment/ LS run	Sonication power (W)	Volume (mL)	Sonication power/ Volume (W/mL)	Mean	Median	d10	d90
Experiment 35/1	250	300	0.8333	6.6390	5.9510	2.4250	11.8900
Experiment 35/2	250	300	0.8333	6.3600	5.7630	2.3680	11.3400
Experiment 35/3	250	300	0.8333	7.0140	6.1960	2.3580	12.6600
Experiment 35/4	250	300	0.8333	6.7340	6.0290	2.3030	12.2100
Experiment 35/5	250	300	0.8333	7.2830	6.4000	2.4730	12.9300
Experiment 35/6	250	300	0.8333	6.9640	6.2180	2.4140	12.5000
Experiment 35/7	250	300	0.8333	6.5040	5.9910	2.4840	11.3600
Experiment 35/8	250	300	0.8333	5.8130	5.4310	2.4490	9.7810
Average	**250**	**300**	**0.8333**	**6.6639**	**5.9974**	**2.4093**	**11.8339**

A.1 Experimental Data for 0 W of Sonication Power

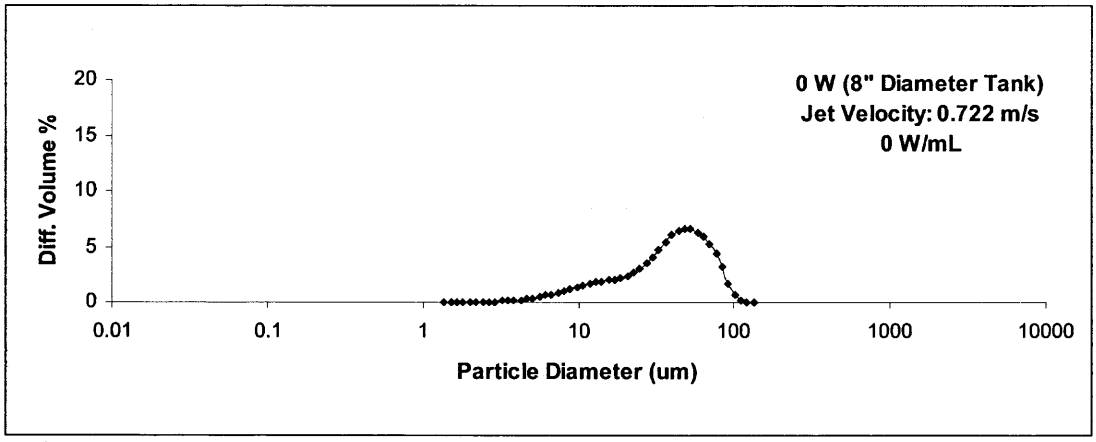

Figure A.1-1 Particle size distribution of experiment without sonication, Exp. 23, LS 1

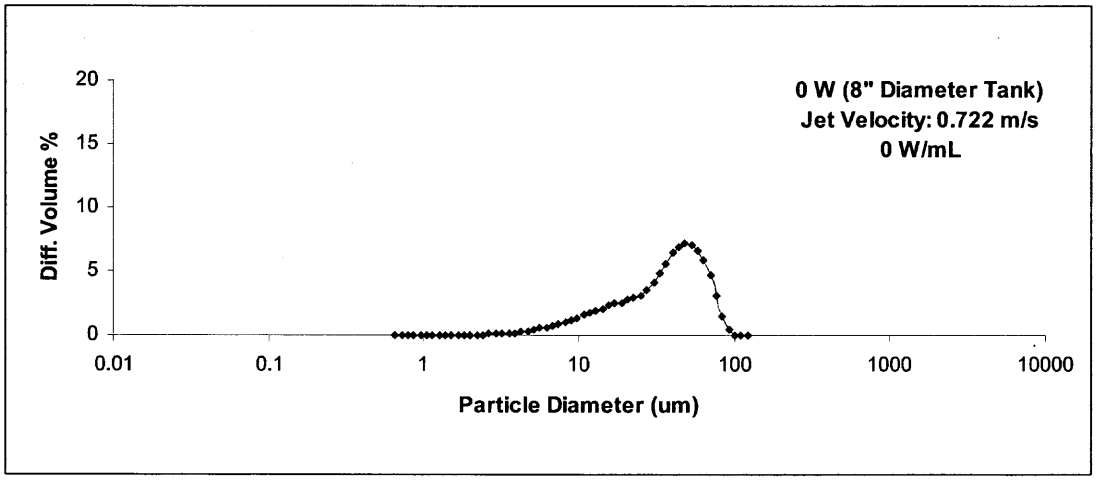

Figure A.1-2 Particle size distribution of experiment without sonication, Exp. 23, LS 5

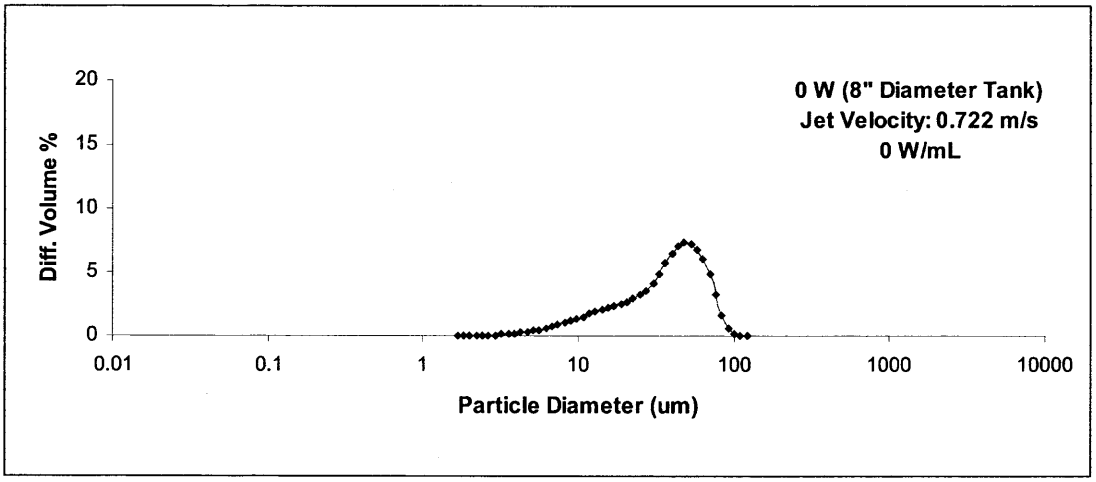

Figure A.1-3 Particle size distribution of experiment without sonication, Exp. 23, LS 7

A.2 Experimental Data for 75 W of Sonication Power

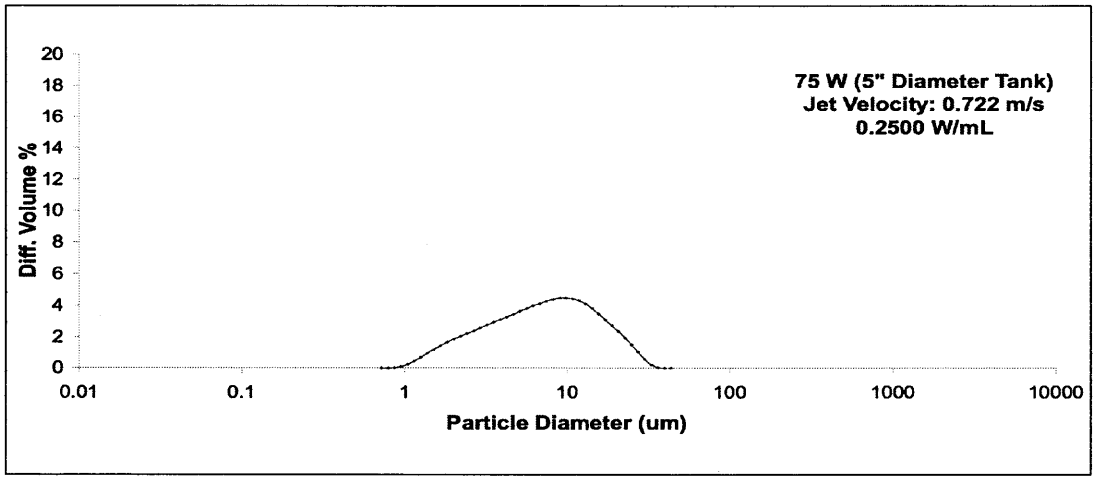

Figure A.2-1 Particle size distribution of experiment with 75W sonication, Exp. 34, LS 1

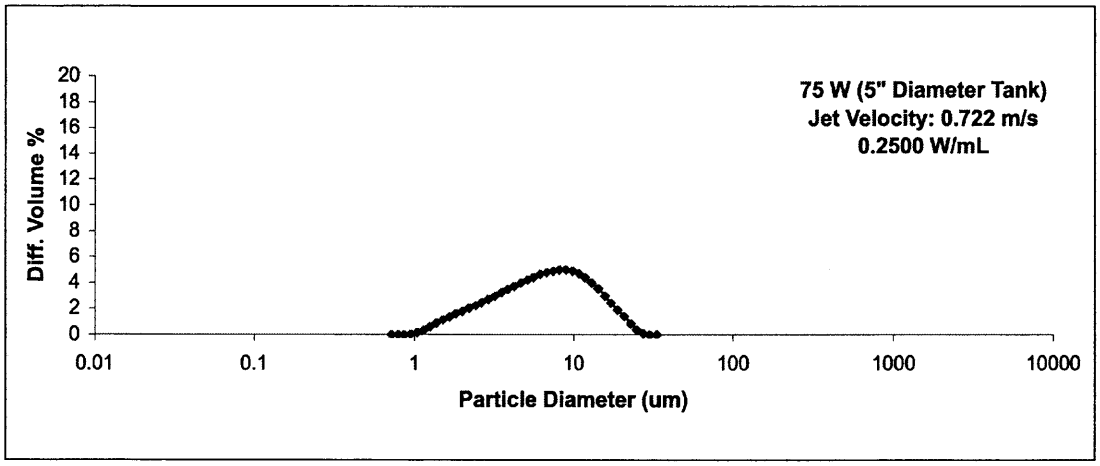

Figure A.2-2 Particle size distribution of experiment with 75W sonication, Exp. 34, LS 2

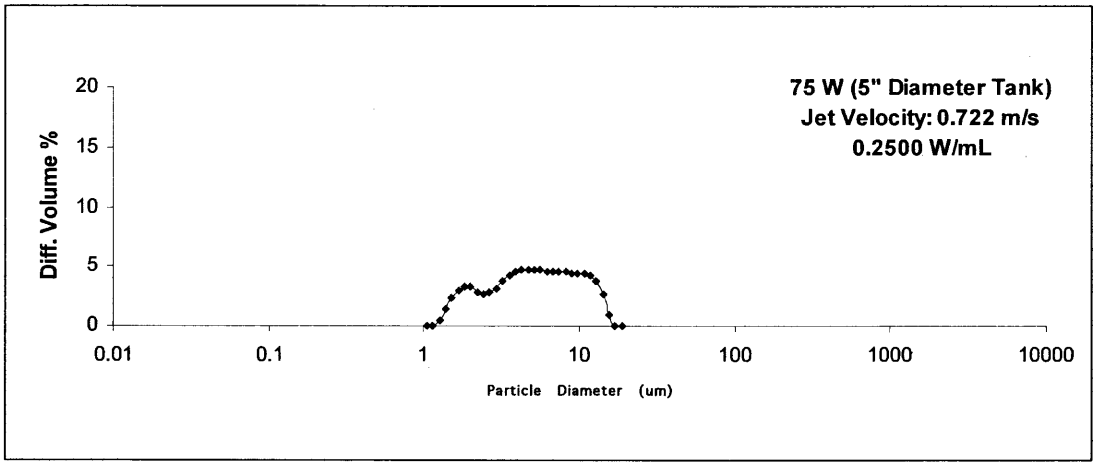

Figure A.2-3 Particle size distribution of experiment with 75W sonication, Exp. 34, LS 4

A.3 Experimental Data for 125 W of Sonication Power

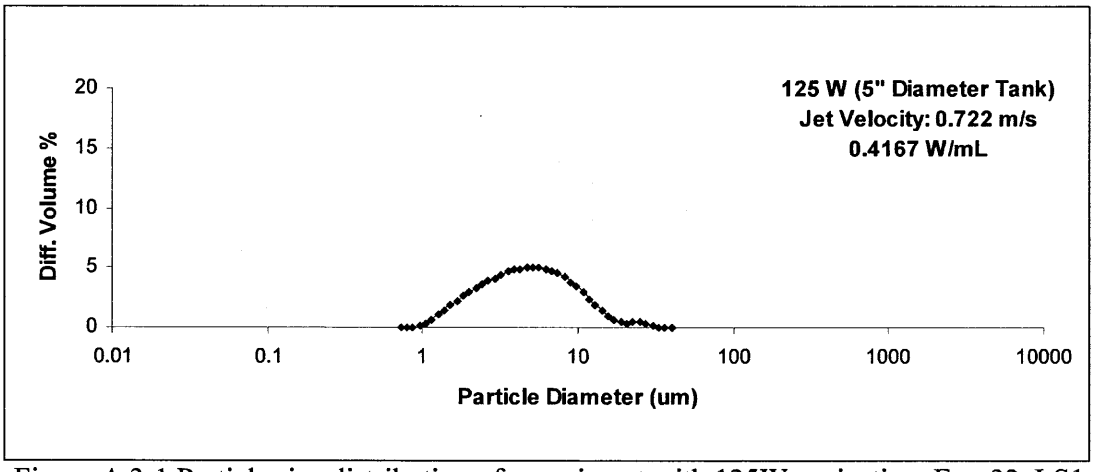

Figure A.3-1 Particle size distribution of experiment with 125W sonication, Exp 32, LS1

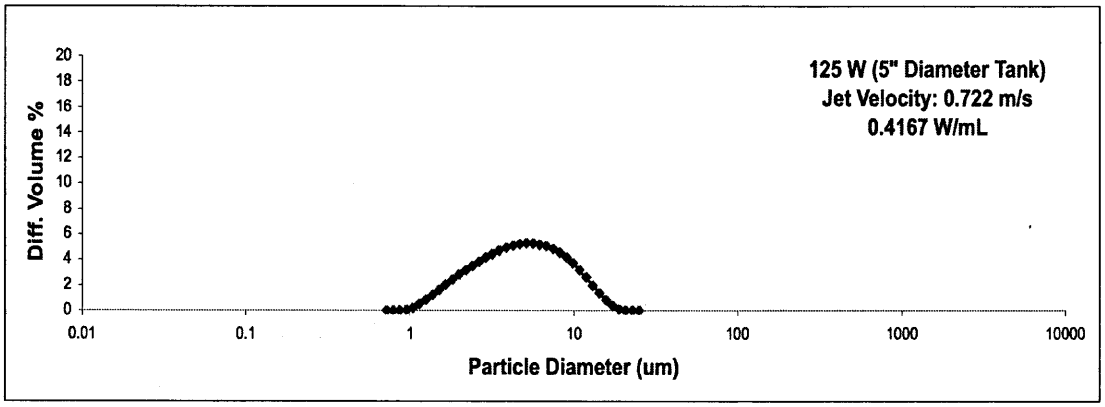

Figure A.3-2 Particle size distribution of experiment with 125W sonication, Exp 32, LS3

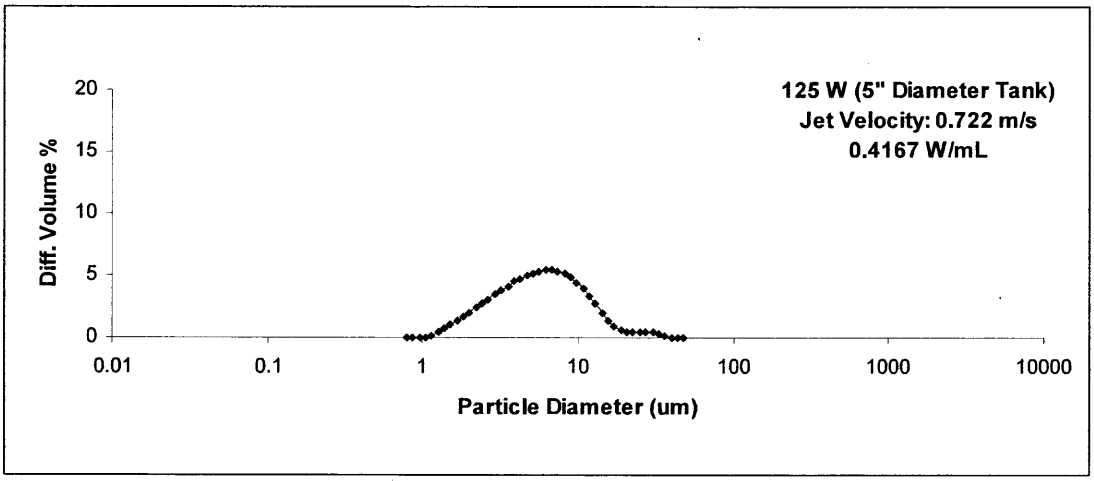

Figure A.3-3 Particle size distribution of experiment with 125W sonication, Exp 32, LS5

A.4 Experimental Data for 200 W of Sonication Power

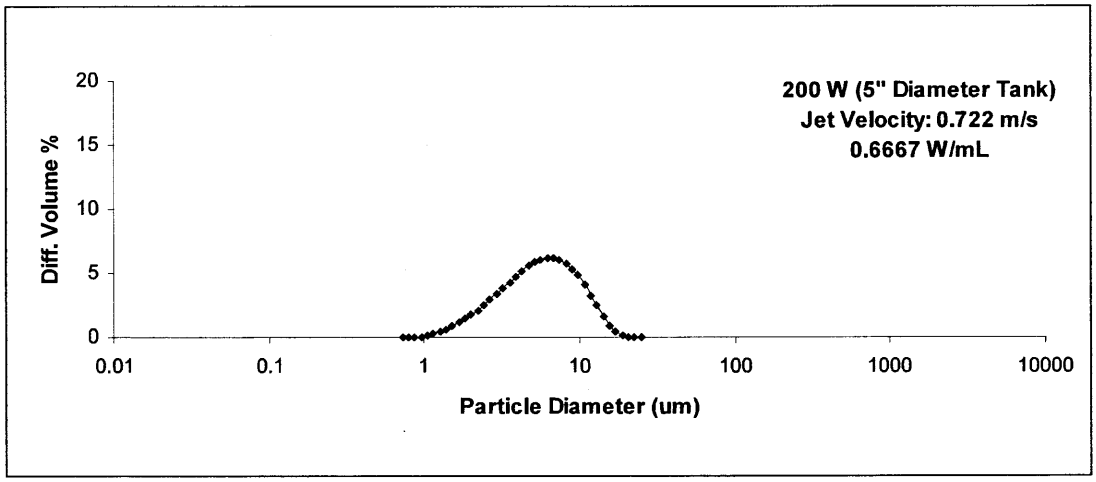

Figure A.4-1 Particle size distribution of experiment with 200W sonication, Exp 36, LS2

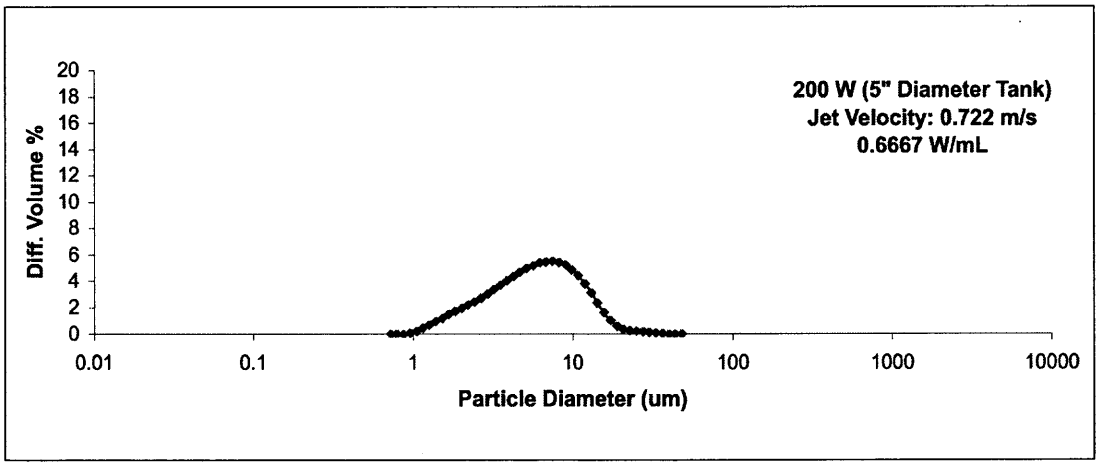

Figure A.4-2 Particle size distribution of experiment with 200W sonication, Exp 36, LS3

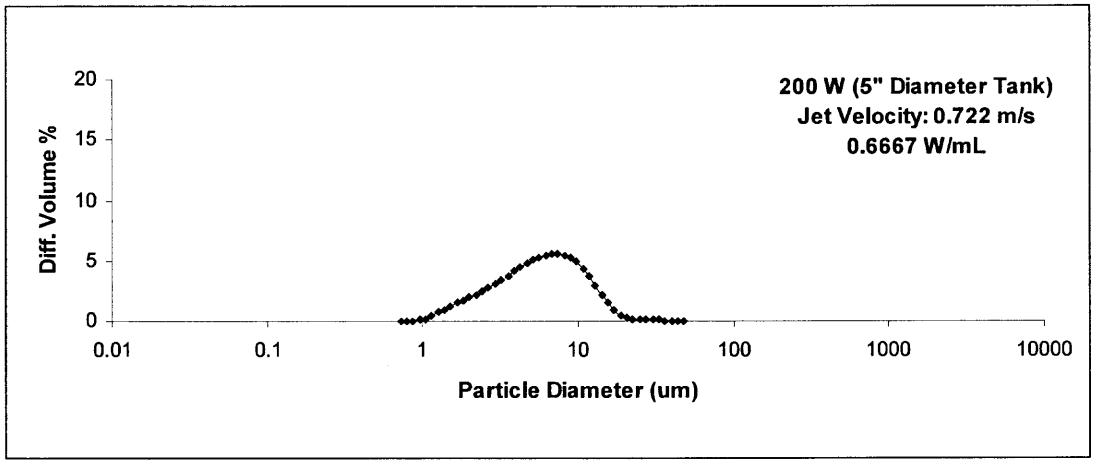

Figure A.4-3 Particle size distribution of experiment with 200W sonication, Exp 36, LS4

A.5 Experimental Data for 250 W of Sonication Power

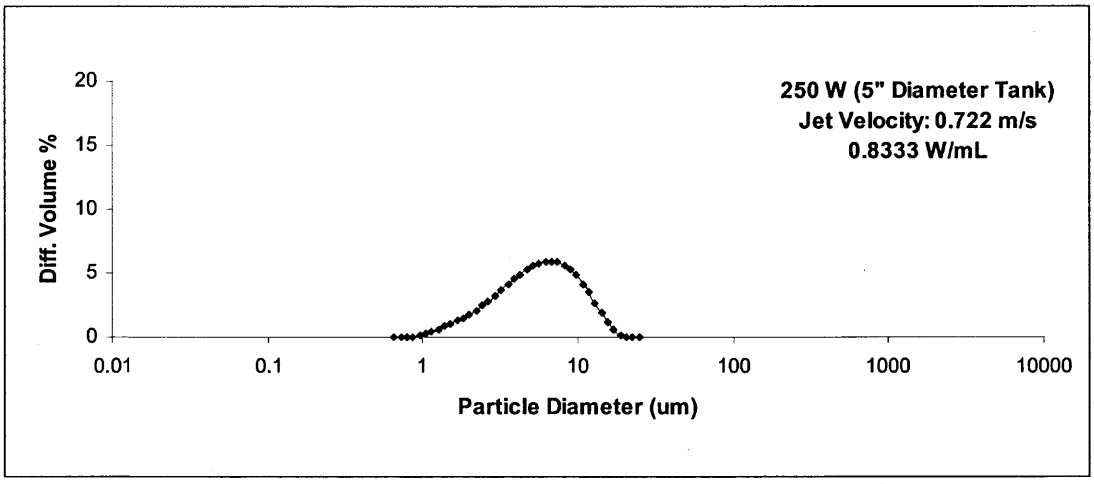

Figure A.5-1 Particle size distribution of experiment with 250W sonication, Exp 35, LS2

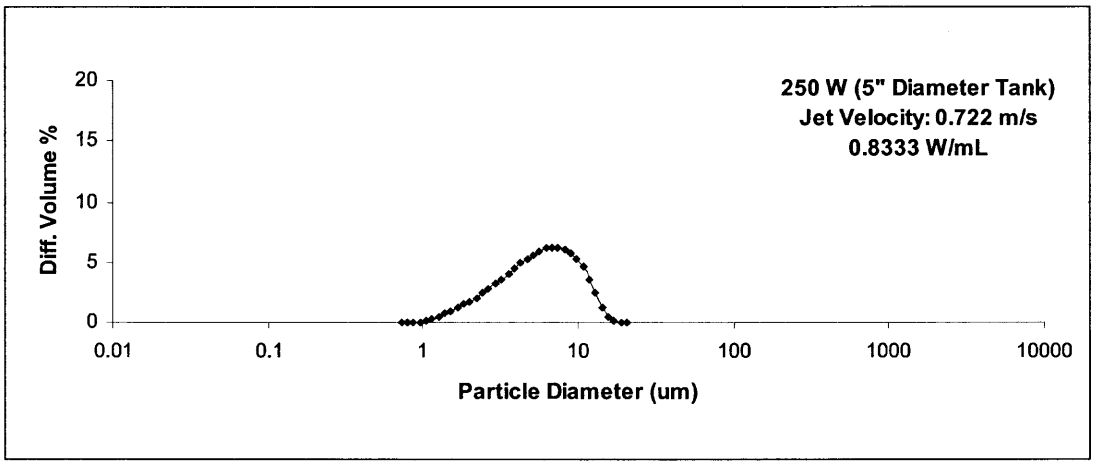

Figure A.5-2 Particle size distribution of experiment with 250W sonication, Exp 35, LS8

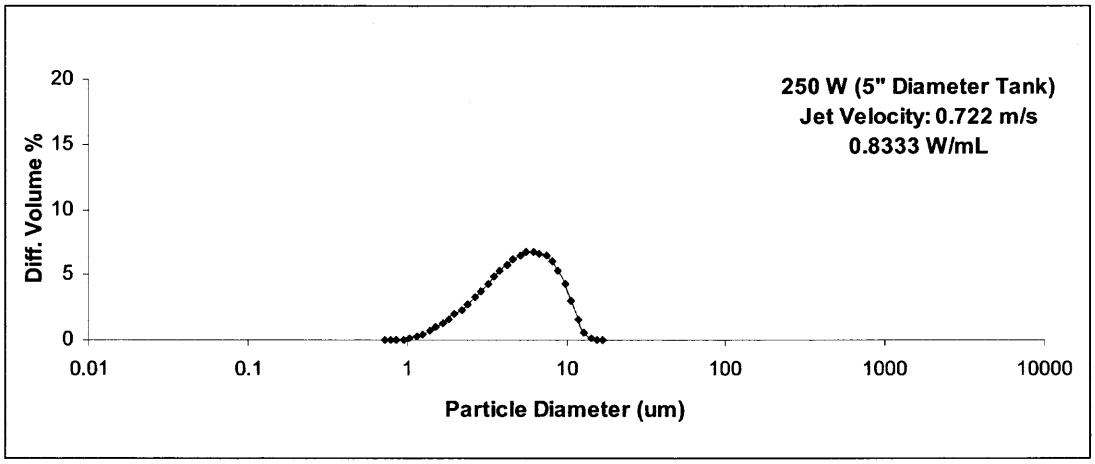

Figure A.5-3 Particle size distribution of experiment with 250W sonication, Exp 35, LS9

APPENDIX B

RESULTS OF EXPERIMENTS WITH HIGHER JET VELOCITY (15 m/s)

Experiment/ LS run	Sonication power (W)	Volume (mL)	Sonication power/ Volume (W/mL)	Mean	Median	d10	d90
Experiment 40/1	0	1500	0.0000	44.1000	42.1100	12.3400	78.7600
Experiment 40/2	0	1500	0.0000	37.9500	35.6700	10.6100	68.4400
Experiment 40/3	0	1500	0.0000	29.2000	27.2000	7.7310	53.4500
Experiment 40/4	0	1500	0.0000	28.5500	26.4000	7.4080	52.8400
Experiment 40/5	0	1500	0.0000	43.3000	46.4900	8.5070	70.2300
Experiment 40/6	0	1500	0.0000	33.4500	36.1200	9.1730	51.7700
Experiment 40/7	0	1500	0.0000	25.8400	27.8400	7.8910	39.7400
Experiment 40/8	0	1500	0.0000	52.8900	49.9600	14.0300	96.8500
Experiment 40/9	0	1500	0.0000	37.1600	37.7800	10.4000	62.1200
Experiment 40/10	0	1500	0.0000	35.7700	36.0800	9.6900	60.7600
			average	**36.8210**	**36.5650**	**9.7780**	**63.4960**
Experiment 42/1	0	1500	0.0000	18.5700	15.7500	10.0100	30.8900
Experiment 42/2	0	1500	0.0000	14.0800	11.9200	8.1330	22.0600
Experiment 42/3	0	1500	0.0000	10.8500	9.6090	6.5500	16.5000
Experiment 42/4	0	1500	0.0000	21.0900	18.0900	10.0100	37.5200
Experiment 42/5	0	1500	0.0000	18.2400	14.9800	8.0120	35.9800
Experiment 42/6	0	1500	0.0000	15.2100	12.5900	7.0920	29.4200
Experiment 42/7	0	1500	0.0000	24.9500	19.9300	12.0700	50.4500
Experiment 42/8	0	1500	0.0000	18.0700	14.3600	8.8890	35.7900
Experiment 42/9	0	1500	0.0000	22.2700	17.9800	10.4400	42.8800
Experiment 42/10	0	1500	0.0000	16.8200	14.1400	8.4020	29.8600
			average	**18.0150**	**14.9349**	**8.9608**	**33.1350**
Experiment 45/1	0	1500	0.0000	30.3300	27.1600	13.1900	52.3300
Experiment 45/2	0	1500	0.0000	27.5200	23.4000	12.5000	50.1300
Experiment 45/3	0	1500	0.0000	28.2000	25.1800	11.5100	50.3700
Experiment 45/4	0	1500	0.0000	24.6200	21.7300	11.5800	42.0800
Experiment 45/5	0	1500	0.0000	32.4300	28.2500	13.0200	61.7100
Experiment 45/6	0	1500	0.0000	26.1500	22.7400	11.1400	49.6100
Experiment 45/7	0	1500	0.0000	78.8200	84.6300	18.8000	140.3000
Experiment 45/8	0	1500	0.0000	30.5400	24.7000	11.7900	61.9000
Experiment 45/9	0	1500	0.0000	22.2500	19.4200	10.3900	38.8800
Experiment 45/10	0	1500	0.0000	19.9500	17.2700	9.5280	35.9900
			average	**32.0810**	**29.4480**	**12.3448**	**58.3300**
Average	**0 W**			**28.9723**	**26.9826**	**10.3612**	**51.6537**
Experiment 46/1	75	300	0.2500	9.4850	7.0680	2.6290	20.8000
Experiment 46/2	75	300	0.2500	8.6220	7.4070	2.9740	16.5400
			average	**9.0535**	**7.2375**	**2.8015**	**18.6700**

Experiment/ LS run	Sonication power (W)	Volume (mL)	Sonication power/ Volume (W/mL)	Mean	Median	d10	d90
Experiment 47/1	75	300	0.2500	16.6600	13.7800	4.1680	33.9800
Experiment 47/2	75	300	0.2500	15.5300	13.1900	4.0890	30.7000
Experiment 47/3	75	300	0.2500	10.9700	8.1220	3.2630	25.9900
Experiment 47/4	75	300	0.2500	7.4160	6.3330	2.2840	14.7300
Experiment 47/5	75	300	0.2500	9.2310	7.1230	2.9920	18.5900
Experiment 47/6	75	300	0.2500	7.2120	6.1310	2.6460	13.7100
			average	**11.1698**	**9.1132**	**3.2403**	**22.9500**
Experiment 55/1	75	300	0.2500	3.3950	2.8710	1.5130	6.0000
Experiment 55/2	75	300	0.2500	3.1600	2.9210	1.3660	5.6330
Experiment 55/3	75	300	0.2500	3.3500	2.7400	1.4360	6.0190
Experiment 55/4	75	300	0.2500	2.9370	2.6400	0.2480	5.3740
Experiment 55/5	75	300	0.2500	4.2750	3.7920	1.8380	7.5030
Experiment 55/6	75	300	0.2500	4.1110	3.7340	1.7840	7.2150
Experiment 55/7	75	300	0.2500	4.2520	3.8580	1.8160	7.4750
Experiment 55/8	75	300	0.2500	4.2130	3.8600	1.8390	7.2870
			average	**3.7116**	**3.3020**	**1.4800**	**6.5633**
Experiment 64/1	75	300	0.2500	5.1520	3.7940	1.9010	10.9400
Experiment 64/2	75	300	0.2500	5.2530	3.8860	1.9590	11.2600
Experiment 64/3	75	300	0.2500	4.6380	3.6050	1.8110	8.8800
Experiment 64/4	75	300	0.2500	4.6910	3.6690	1.8600	9.2320
			average	**4.9335**	**3.7385**	**1.8828**	**10.780**
Experiment 67/1	75	900	0.0833	6.8890	4.5430	1.7660	16.9900
Experiment 67/2	75	900	0.0833	6.9300	5.6810	2.0180	14.1000
Experiment 67/3	75	900	0.0833	6.9310	4.4190	1.7640	17.4600
Experiment 67/4	75	900	0.0833	6.9790	4.9380	1.8860	16.2300
			average	**6.9323**	**4.8953**	**1.8585**	**16.1950**
Experiment 70/1	75	900	0.0833	10.2900	8.2240	2.7930	20.6200
Experiment 70/2	75	900	0.0833	9.9280	7.9960	2.7440	19.8400
Experiment 70/3	75	900	0.0833	10.7700	8.3890	2.8020	22.0500
Experiment 70/4	75	900	0.0833	10.7600	8.2680	2.7620	22.1800
			average	**10.4370**	**8.2193**	**2.7753**	**21.1725**
Average	**75 W**			**7.2868**	**5.8208**	**2.2483**	**14.9046**
Experiment 39/1	125	1500	0.0833	3.5750	2.8070	1.5490	5.4530
Experiment 39/2	125	1500	0.0833	3.7140	3.2500	1.5850	5.3390
Experiment 39/3	125	1500	0.0833	2.8170	2.6290	1.3680	4.7780
Experiment 39/4	125	1500	0.0833	3.2320	3.2070	1.5200	4.8490
Experiment 39/5	125	1500	0.0833	3.4630	3.4370	1.7290	4.8860
Experiment 39/6	125	1500	0.0833	2.9840	2.6640	0.4110	5.0120
Experiment 39/7	125	1500	0.0833	3.2850	3.5020	0.2640	4.8960
Experiment 39/8	125	1500	0.0833	3.6260	3.7280	0.2540	5.0580
Experiment 39/9	125	1500	0.0833	2.8910	2.9520	0.3410	4.7000

Experiment/ LS run	Sonication power (W)	Volume (mL)	Sonication power/ Volume (W/mL)	Mean	Median	d10	d90
Experiment 39/10	125	1500	0.0833	3.1280	3.3980	0.2570	4.6970
Experiment 39/11	125	1500	0.0833	3.3440	3.6150	0.2510	4.8220
Experiment 39/12	125	1500	0.0833	3.3810	3.7040	0.2200	4.9850
			average	**3.2867**	**3.2411**	**0.8124**	**4.9563**
Experiment 41/1	125	1500	0.0833	6.7460	5.7550	2.9670	11.2200
Experiment 41/2	125	1500	0.0833	6.2080	5.4300	3.1500	10.5100
Experiment 41/3	125	1500	0.0833	6.0700	5.3310	3.2700	10.0400
Experiment 41/4	125	1500	0.0833	5.7190	5.2720	2.7910	9.3780
Experiment 41/5	125	1500	0.0833	6.2180	5.4880	2.8090	10.3900
Experiment 41/6	125	1500	0.0833	5.8410	5.0640	2.4580	10.2000
			average	**6.1337**	**5.3900**	**2.9075**	**10.2897**
Experiment 44/1	125	1500	0.0833	4.3830	3.8520	2.1250	6.9040
Experiment 44/2	125	1500	0.0833	4.5760	3.9760	2.1500	7.0300
Experiment 44/3	125	1500	0.0833	4.9110	4.4600	3.0180	7.4140
Experiment 44/4	125	1500	0.0833	4.2160	4.0660	2.1850	6.4150
Experiment 44/5	125	1500	0.0833	4.1370	4.1030	1.5460	6.3250
Experiment 44/6	125	1500	0.0833	4.8120	3.8110	1.9790	8.0400
Experiment 44/7	125	1500	0.0833	5.2530	4.1150	2.1510	8.2500
Experiment 44/8	125	1500	0.0833	5.0680	4.0710	2.0390	8.7380
			average	**4.6695**	**4.0568**	**2.1491**	**7.3895**
Experiment 54/1	125	300	0.4167	3.7640	2.5520	1.4490	8.0450
Experiment 54/2	125	300	0.4167	3.7880	2.7290	1.4650	8.3300
Experiment 54/3	125	300	0.4167	4.0360	2.8850	1.5100	9.3510
Experiment 54/4	125	300	0.4167	3.1160	2.3440	1.5170	5.0390
Experiment 54/5	125	300	0.4167	3.1870	2.4120	1.5300	5.1350
Experiment 54/6	125	300	0.4167	3.4180	2.5440	1.5600	5.6420
			average	**3.5515**	**2.5777**	**1.5052**	**6.9237**
Experiment 56/1	125	300	0.4167	5.0370	4.5080	2.1830	8.7430
Experiment 56/2	125	300	0.4167	5.0420	4.5080	2.1900	8.7470
Experiment 56/3	125	300	0.4167	4.6580	4.0410	1.8800	8.2050
Experiment 56/4	125	300	0.4167	4.7160	4.0910	1.9260	8.2300
			average	**4.8633**	**4.2870**	**2.0448**	**8.4813**
Experiment 62/1	125	300	0.4167	4.3870	3.7270	1.9230	7.3240
Experiment 62/2	125	300	0.4167	4.3350	3.7710	1.8770	7.1280
Experiment 62/3	125	300	0.4167	4.6310	3.8020	1.9320	7.7420
Experiment 62/4	125	300	0.4167	4.4980	3.8110	1.8830	7.4300
			average	**4.4753**	**3.7778**	**1.9038**	**7.406**
Experiment 63/1	125	500	0.2500	3.5170	3.3200	1.6400	5.7430
Experiment 63/2	125	500	0.2500	3.5020	3.3290	1.6810	5.6170
Experiment 63/3	125	500	0.2500	3.5000	3.3260	1.7080	5.6180
Experiment 63/4	125	500	0.2500	3.4990	3.3310	1.7760	5.5100
			average	**3.5045**	**3.3265**	**1.7013**	**5.6220**

Experiment/ LS run	Sonication power (W)	Volume (mL)	Sonication power/ Volume (W/mL)	Mean	Median	d10	d90
Experiment 65/1	125	500	0.2500	3.3490	2.3780	1.4340	5.5020
Experiment 65/2	125	500	0.2500	3.5280	2.7250	1.5540	5.6430
Experiment 65/3	125	500	0.2500	3.1470	2.5380	1.3900	5.1190
Experiment 65/4	125	500	0.2500	3.1400	2.6440	1.4000	5.1920
			average	**3.2910**	**2.5713**	**1.4445**	**5.3640**
Experiment 68/1	125	1500	0.0833	3.8270	3.2560	1.5220	6.8370
Experiment 68/2	125	1500	0.0833	3.8930	3.3280	1.5390	7.0060
Experiment 68/3	125	1500	0.0833	3.8300	3.0210	1.4880	6.9440
Experiment 68/4	125	1500	0.0833	3.8600	3.3310	1.5660	6.9670
Experiment 68/5	125	1500	0.0833	3.8420	3.0220	1.4710	7.0400
Experiment 68/6	125	1500	0.0833	3.6890	3.3450	0.3590	6.8300
Experiment 68/7	125	1500	0.0833	3.6740	2.8990	1.3940	6.9140
Experiment 68/8	125	1500	0.0833	3.3110	3.4620	0.2750	5.8920
			average	**3.7408**	**3.2080**	**1.2018**	**6.8038**
Experiment 69/1	125	750	0.1667	9.8620	8.1820	2.7600	18.9600
Experiment 69/2	125	750	0.1667	9.7970	8.1110	2.7550	18.8000
Experiment 69/3	125	750	0.1667	9.9370	8.2310	2.7790	19.1100
Experiment 69/4	125	750	0.1667	9.6110	8.0290	2.7770	18.5600
			average	**9.8018**	**8.1383**	**2.7678**	**18.8575**
Average	**125 W**			**4.4754**	**3.8870**	**1.7080**	**7.6537**
Experiment 38/1	200	1500	0.1333	6.3890	3.7020	1.6950	17.1700
Experiment 38/2	200	1500	0.1333	6.7490	4.0280	1.8160	17.3000
Experiment 38/3	200	1500	0.1333	5.6770	3.4390	1.6540	15.2000
Experiment 38/4	200	1500	0.1333	5.9230	3.6560	1.7660	15.9700
Experiment 38/5	200	1500	0.1333	4.9920	3.2980	1.6440	12.2100
Experiment 38/6	200	1500	0.1333	4.8240	3.3740	1.5890	11.3400
Experiment 38/7	200	1500	0.1333	4.8900	3.4370	1.6130	11.5400
Experiment 38/8	200	1500	0.1333	4.6740	3.2000	1.6400	10.4200
Experiment 38/9	200	1500	0.1333	4.4970	3.1980	1.4660	10.1900
Experiment 38/10	200	1500	0.1333	4.5970	3.5330	1.6570	10.3000
Experiment 38/11	200	1500	0.1333	5.2180	3.3110	1.6400	13.2900
			average	**5.3118**	**3.4705**	**1.6527**	**13.1755**
Experiment 49/1	200	300	0.6667	3.4170	2.9370	0.2170	6.6010
Experiment 49/2	200	300	0.6667	2.3850	2.1530	0.1780	5.0620
Experiment 49/3	200	300	0.6667	3.3260	2.9280	0.2470	6.3910
Experiment 49/4	200	300	0.6667	2.2040	2.1020	0.1860	4.6070
Experiment 49/5	200	300	0.6667	3.2630	3.0260	0.2680	6.1580
Experiment 49/6	200	300	0.6667	2.4860	2.3250	0.2070	4.9030
Experiment 49/7	200	300	0.6667	3.4020	2.9480	1.6080	5.9070
			average	**2.9261**	**2.6313**	**0.4159**	**5.6613**
Experiment 50/1	200	300	0.6667	3.8310	3.2260	1.7120	6.4900
Experiment 50/2	200	300	0.6667	2.4020	2.1180	1.5090	4.0700
Experiment 50/3	200	300	0.6667	3.5630	2.6950	1.6660	6.6370
Experiment 50/4	200	300	0.6667	2.8590	2.4530	1.5750	4.7750
			average	**3.1638**	**2.6230**	**1.6155**	**5.4930**

Experiment/ LS run	Sonication power (W)	Volume (mL)	Sonication power/ Volume (W/mL)	Mean	Median	d10	d90
Experiment 58/1	200	300	0.6667	7.2140	5.1160	2.2050	15.2400
Experiment 58/2	200	300	0.6667	7.4620	5.2720	2.2720	16.0200
Experiment 58/3	200	300	0.6667	7.7530	5.0880	2.1800	18.8200
Experiment 58/4	200	300	0.6667	7.7350	5.3140	2.2890	18.3300
			average	**7.5410**	**5.1975**	**2.2365**	**17.1025**
Experiment 61/1	200	300	0.6667	4.2280	3.6160	1.7650	7.5170
Experiment 61/2	200	300	0.6667	3.8840	3.3600	1.6780	6.9060
Experiment 61/3	200	300	0.6667	4.4770	3.7730	1.7940	8.0400
Experiment 61/4	200	300	0.6667	4.2770	3.5730	1.7540	7.4950
			average	**4.2165**	**3.5805**	**1.7478**	**7.4895**
Experiment 43/1	200	1500	0.1333	5.0850	4.2010	2.2070	8.5560
Experiment 43/2	200	1500	0.1333	5.1510	4.2290	2.5580	8.7080
Experiment 43/3	200	1500	0.1333	5.6090	4.3810	2.8150	10.1500
Experiment 43/4	200	1500	0.1333	4.6000	4.1130	2.2020	7.4320
Experiment 43/5	200	1500	0.1333	4.6220	4.0930	2.4870	7.3480
Experiment 43/6	200	1500	0.1333	4.8000	4.1490	2.6990	7.5360
Experiment 43/7	200	1500	0.1333	4.4190	4.0200	2.1360	7.3270
Experiment 43/8	200	1500	0.1333	4.5510	4.1090	2.4480	7.1510
Experiment 43/9	200	1500	0.1333	4.7920	4.2130	3.2900	7.2130
Experiment 43/10	200	1500	0.1333	4.5330	4.1290	2.1620	7.3190
Experiment 43/11	200	1500	0.1333	4.6400	4.1700	2.9430	7.2280
			average	**4.8002**	**4.1643**	**2.5406**	**7.8153**
Average	**200 W**			**4.6683**	**3.6099**	**1.7424**	**9.5333**
Experiment 59/1	250	300	0.8333	5.6530	4.3190	1.8270	12.1800
Experiment 59/2	250	300	0.8333	5.9990	4.4350	1.9260	12.6300
Experiment 59/3	250	300	0.8333	6.0590	4.5170	1.9660	12.6100
Experiment 59/4	250	300	0.8333	6.4760	4.8190	2.0210	13.7800
Experiment 59/5	250	300	0.8333	6.5810	5.0300	2.1470	13.6300
			average	**6.1536**	**4.6240**	**1.9774**	**12.9660**
Experiment 60/1	250	300	0.8333	6.4270	4.2710	1.8850	16.0600
Experiment 60/2	250	300	0.8333	4.8040	3.8030	1.6070	9.9720
Experiment 60/3	250	300	0.8333	6.0690	4.2380	1.9020	14.1200
Experiment 60/4	250	300	0.8333	5.4570	4.0650	1.7630	11.9100
			average	**5.6893**	**4.0943**	**1.7893**	**13.0155**
Experiment 66/1	250	1000	0.2500	3.5220	2.8670	1.5220	5.7010
Experiment 66/2	250	1000	0.2500	3.6900	3.0780	1.5830	5.9670
Experiment 66/3	250	1000	0.2500	3.6100	2.6220	1.4170	6.6720
Experiment 66/4	250	1000	0.2500	3.5580	2.9870	1.5420	7.4130
			average	**3.5950**	**2.8885**	**1.5160**	**6.4383**
Average	**250 W**			**5.2235**	**3.9270**	**1.7775**	**10.9727**

B.1 Experimental Data for 0 W of Sonication Power

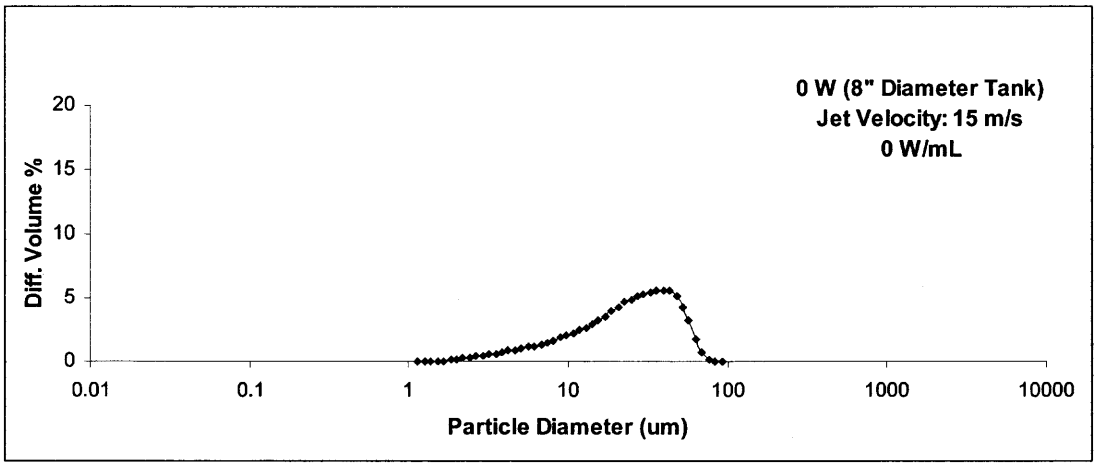

Figure B.1-1 Particle size distribution of experiment with 0W sonication, Exp 40, LS4

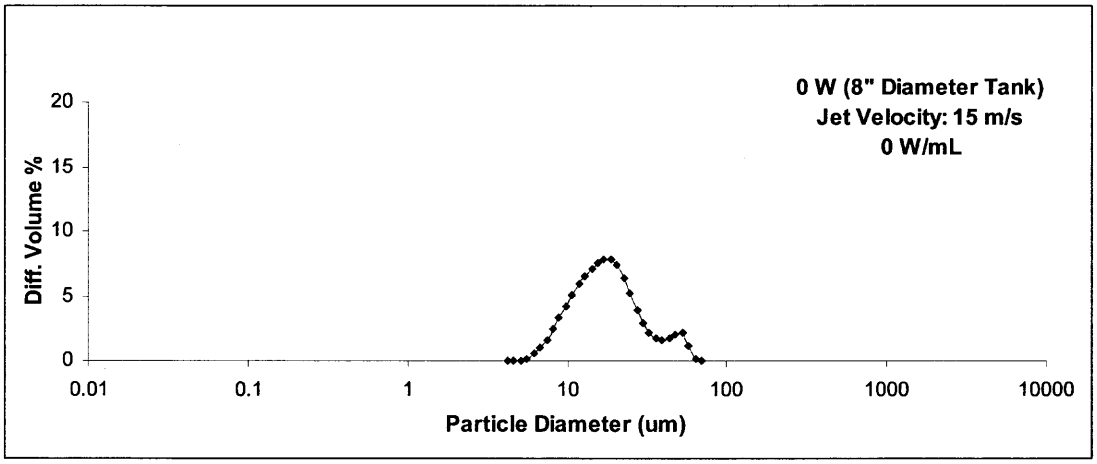

Figure B.1-2 Particle size distribution of experiment with 0W sonication, Exp 42, LS4

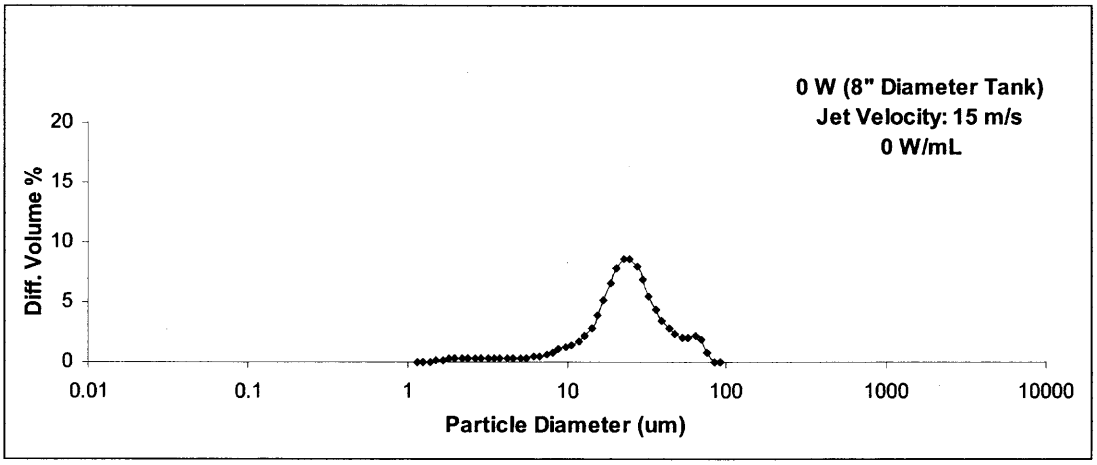

Figure B.1-3 Particle size distribution of experiment with 0W sonication, Exp 45, LS3

B.2 Experimental Data for 75 W of Sonication Power

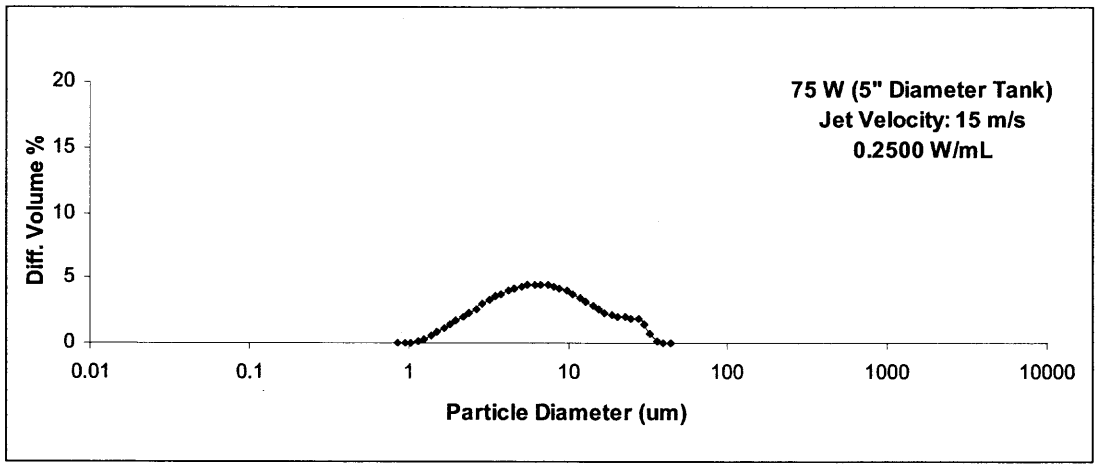

Figure B.2-1 Particle size distribution of experiment with 75W sonication, Exp 46, LS1

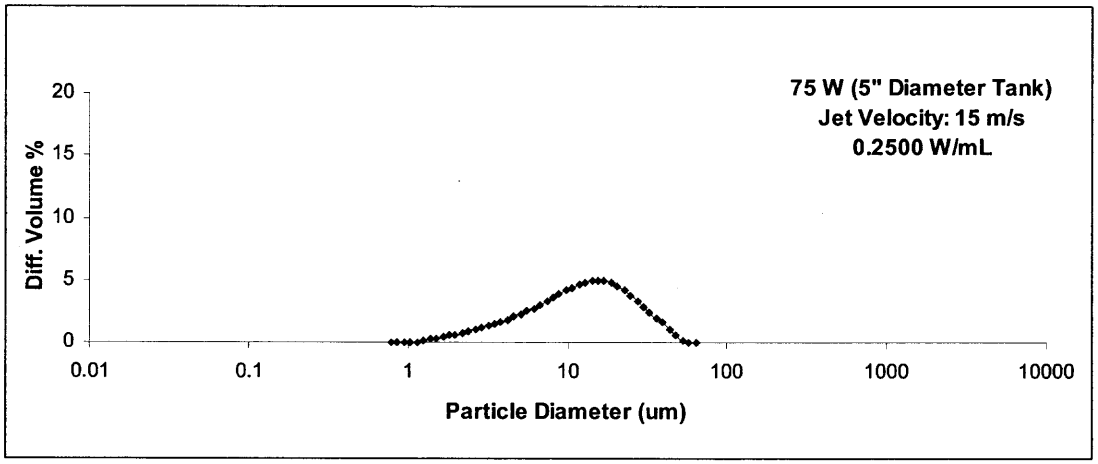

Figure B.2-2 Particle size distribution of experiment with 75W sonication, Exp 47, LS2

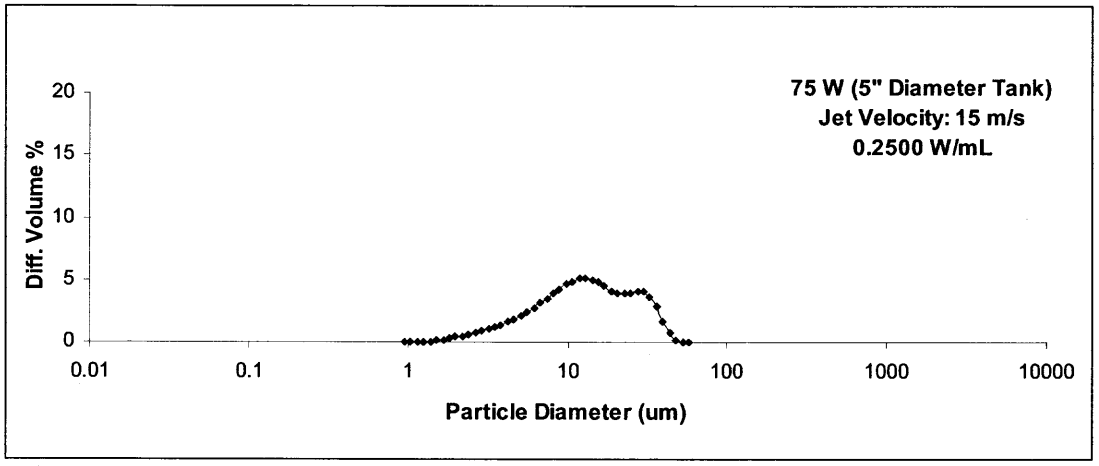

Figure B.2-3 Particle size distribution of experiment with 75W sonication, Exp 52, LS4

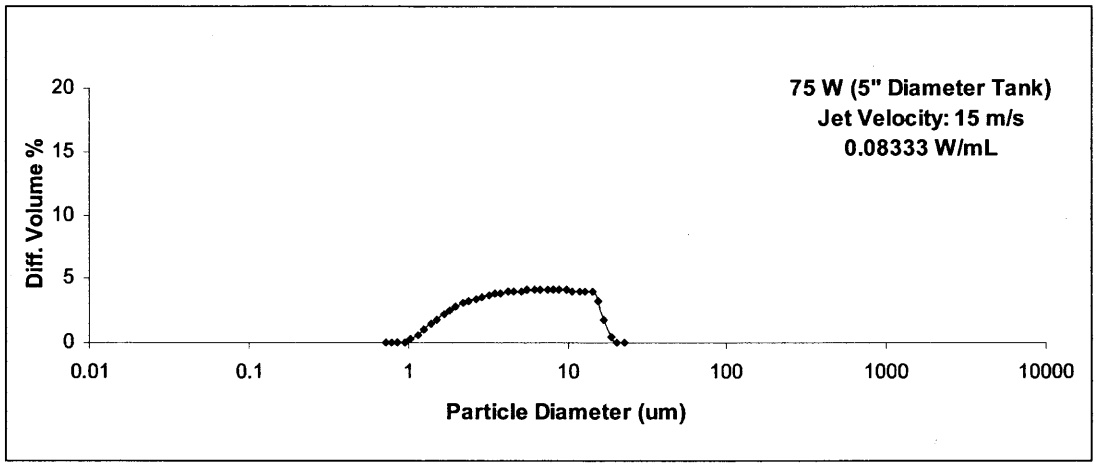

Figure B.2-4 Particle size distribution of experiment with 75W sonication, Exp 67, LS2

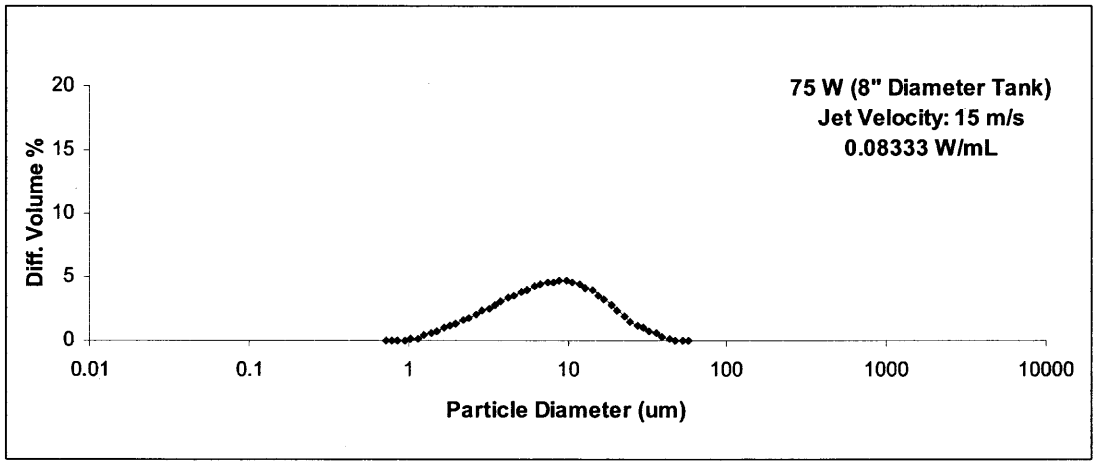

Figure B.2-5 Particle size distribution of experiment with 75W sonication, Exp 70, LS1

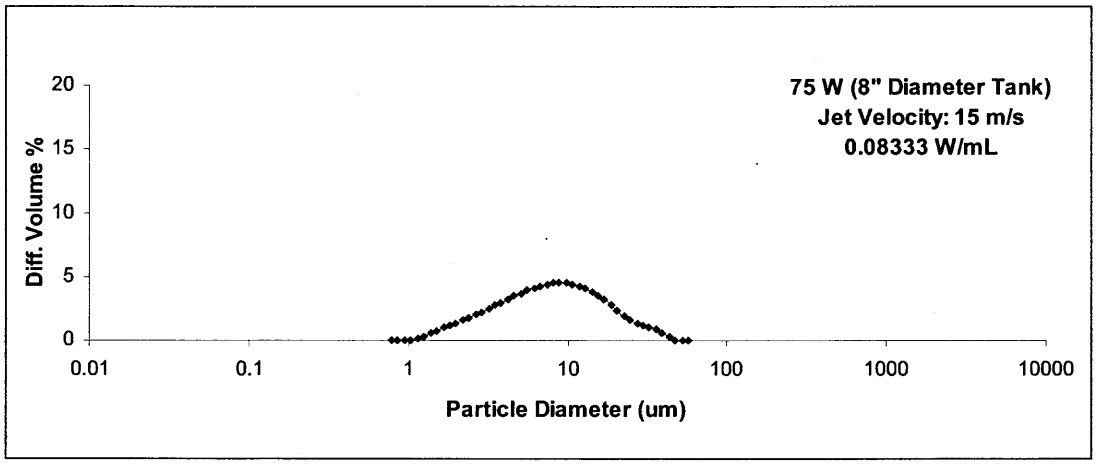

Figure B.2-6 Particle size distribution of experiment with 75W sonication, Exp 70, LS3

B.3 Experimental Data for 125 W of Sonication Power

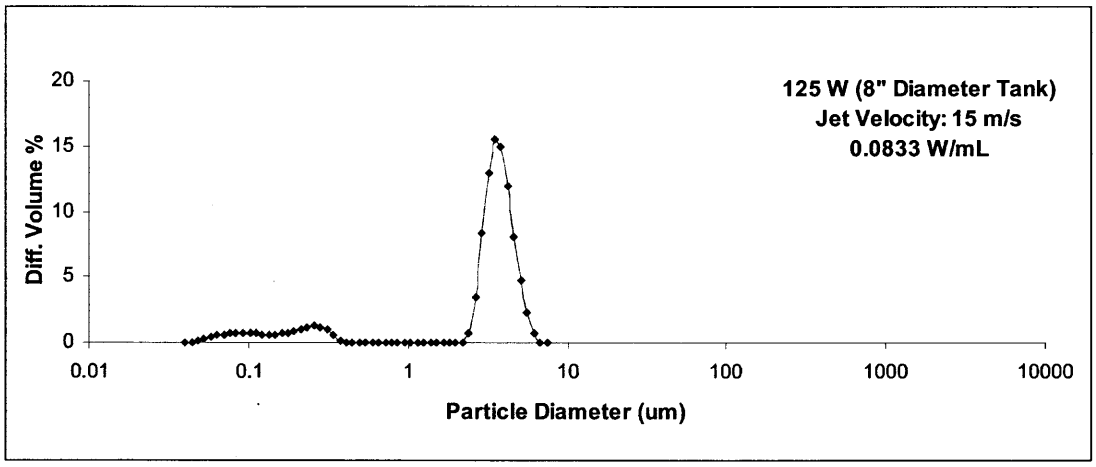

Figure B.3-1 Particle size distribution of experiment with 125W sonication, Exp 39,LS12

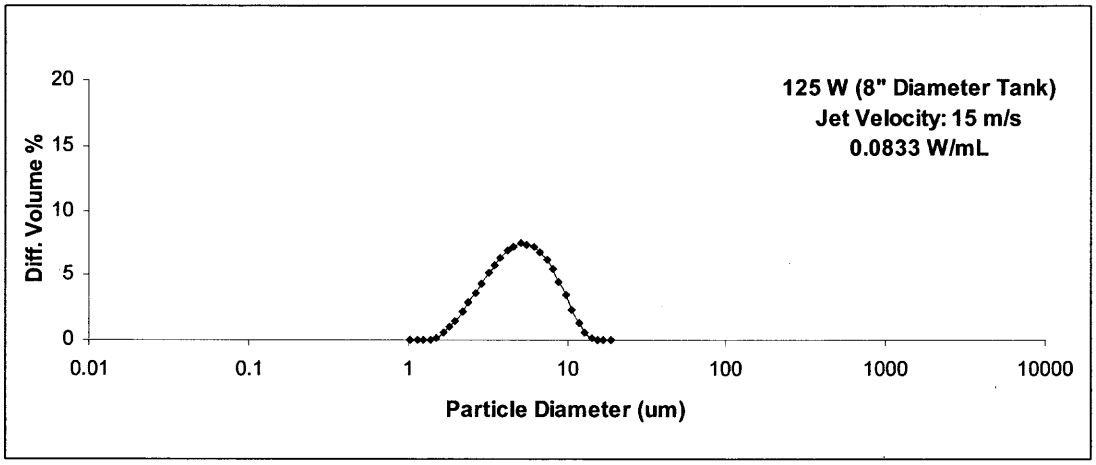

Figure B.3-2 Particle size distribution of experiment with 125W sonication, Exp 41, LS4

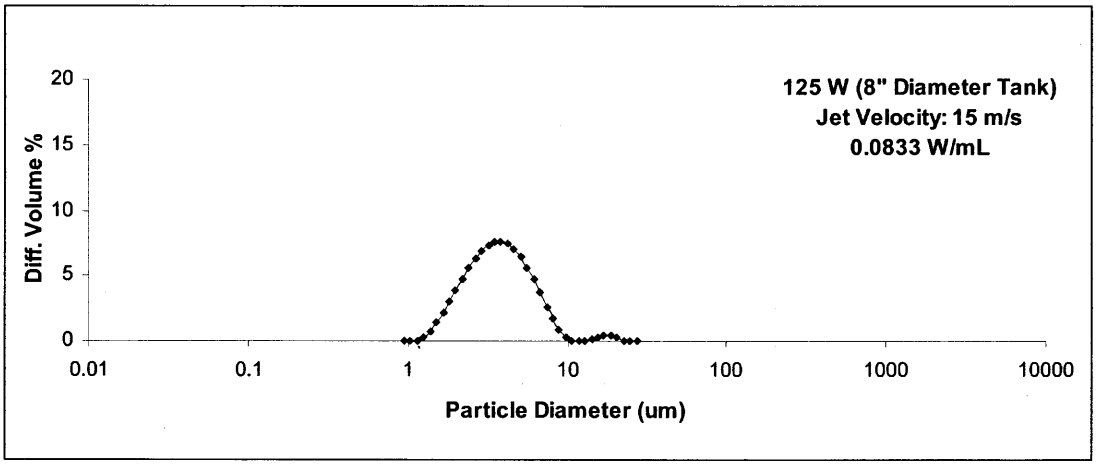

Figure B.3-3 Particle size distribution of experiment with 125W sonication, Exp 44, LS1

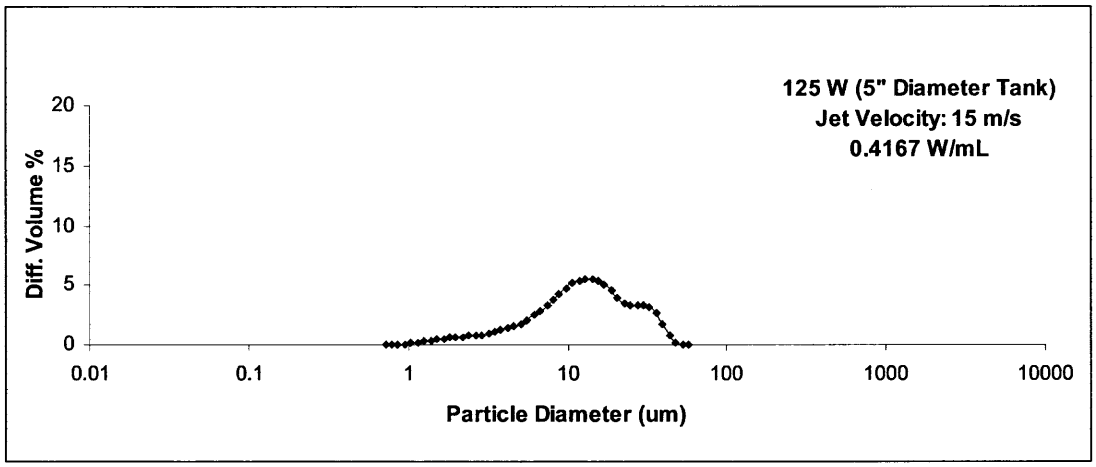

Figure B.3-4 Particle size distribution of experiment with 125W sonication, Exp 53, LS3

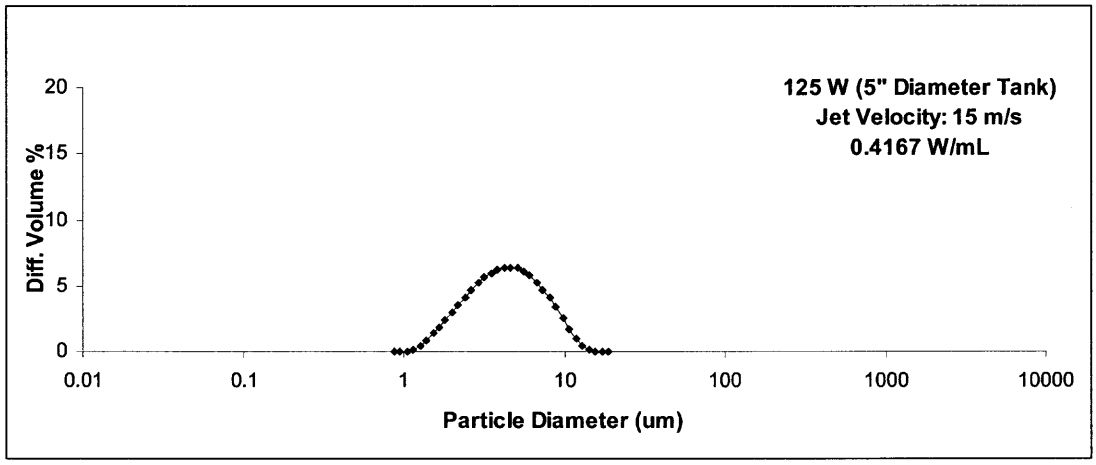

Figure B.3-5 Particle size distribution of experiment with 125W sonication, Exp 56, LS1

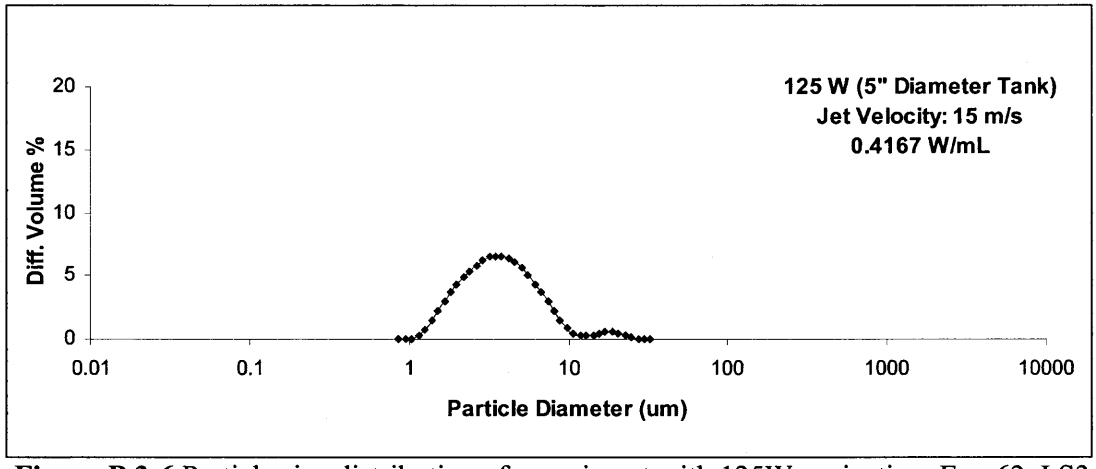

Figure B.3-6 Particle size distribution of experiment with 125W sonication, Exp 62, LS3

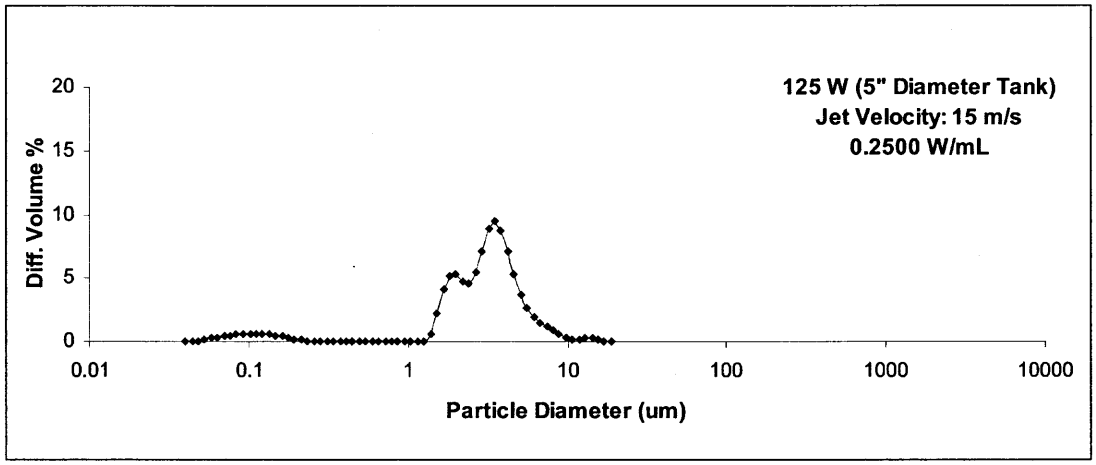

Figure B.3-7 Particle size distribution of experiment with 125W sonication, Exp 63, LS2

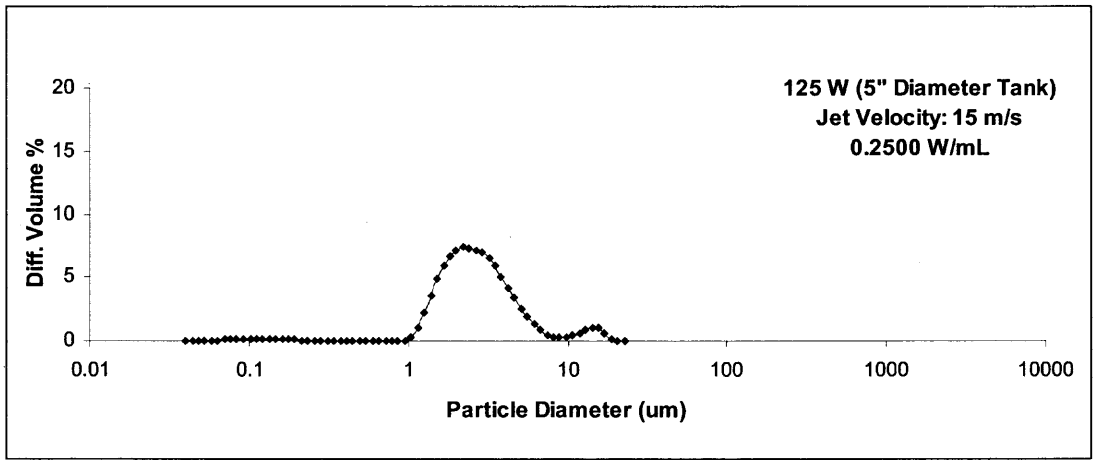

Figure B.3-8 Particle size distribution of experiment with 125W sonication, Exp 65, LS2

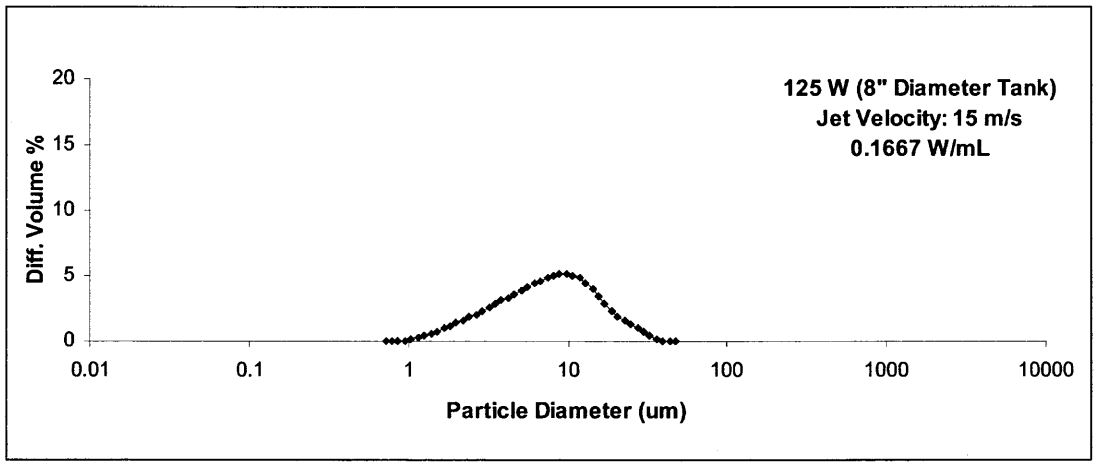

Figure B.3-9 Particle size distribution of experiment with 125W sonication, Exp 69, LS4

B.4 Experimental Data for 200 W of Sonication Power

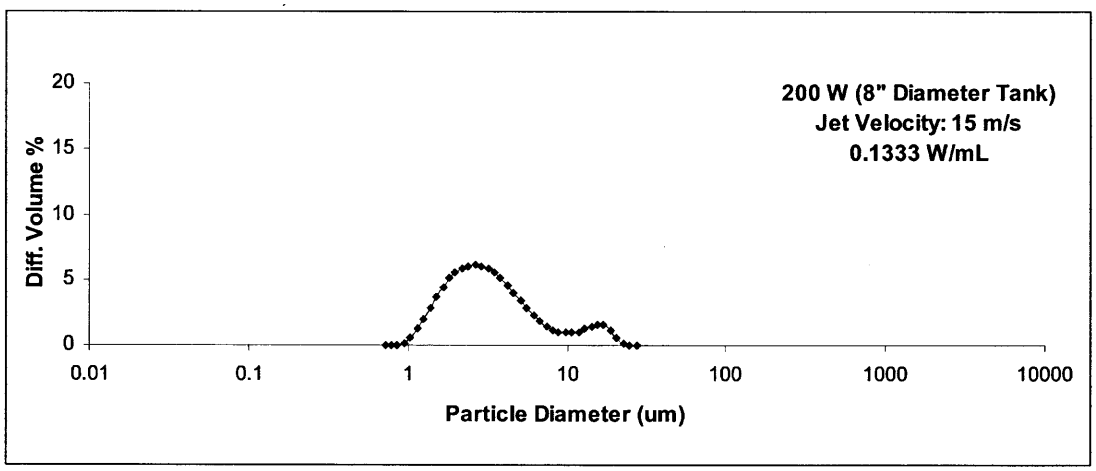

Figure B.4-1 Particle size distribution of experiment with 200W sonication, Exp 38, LS8

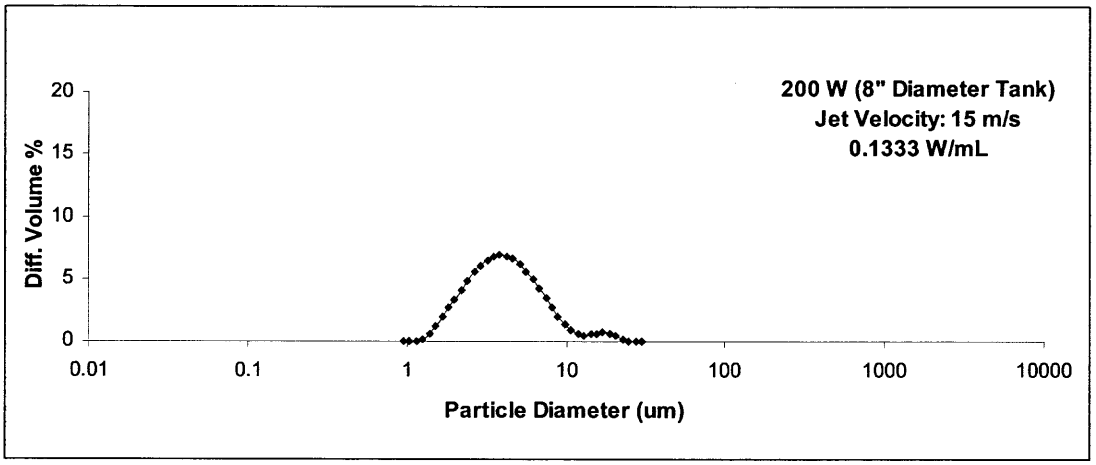

Figure B.4-2 Particle size distribution of experiment with 200W sonication, Exp 43, LS1

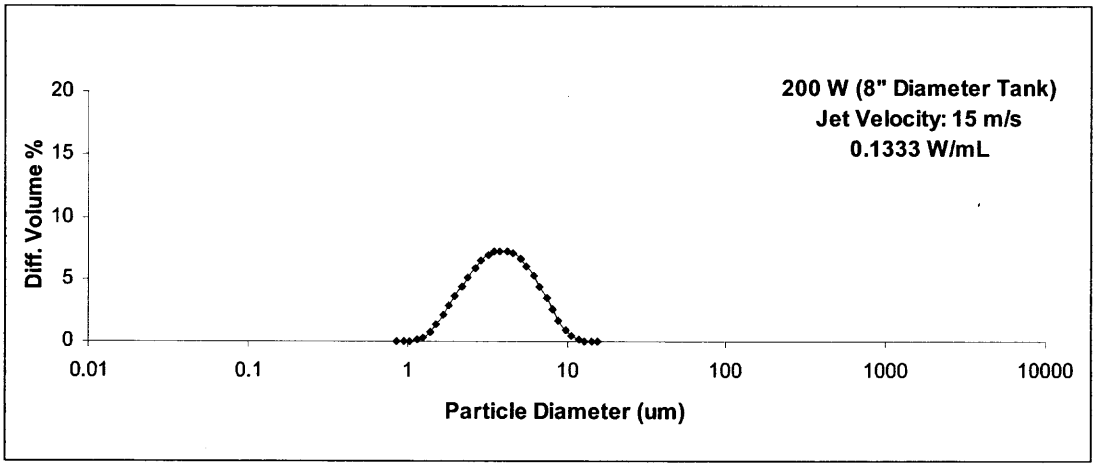

Figure B.4-3 Particle size distribution of experiment with 200W sonication, Exp 43, LS7

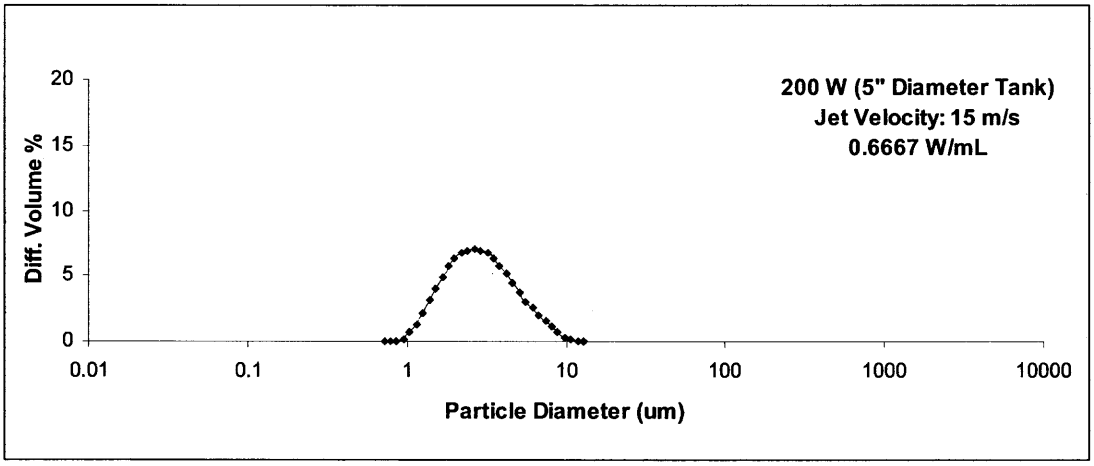

Figure B.4-4 Particle size distribution of experiment with 200W sonication, Exp 49, LS8

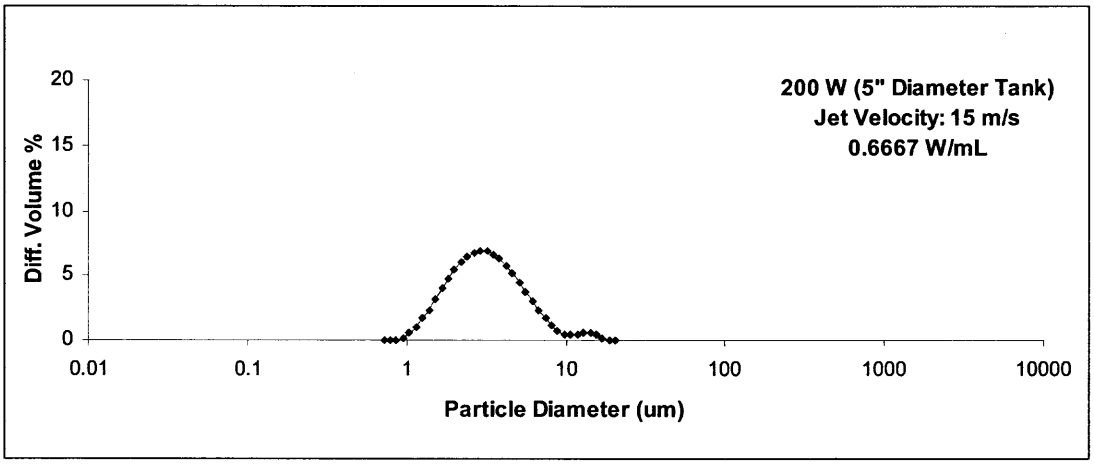

Figure B.4-5 Particle size distribution of experiment with 200W sonication, Exp 50, LS2

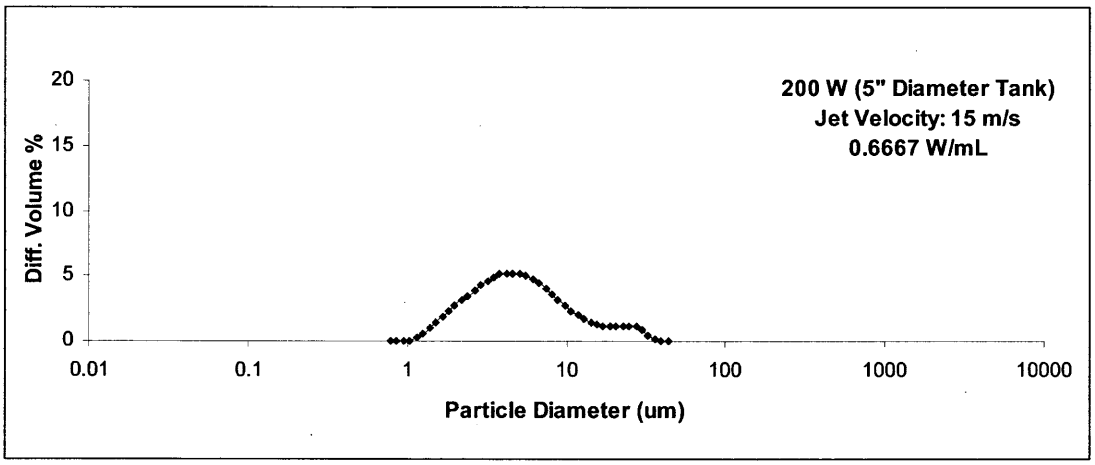

Figure B.4-6 Particle size distribution of experiment with 200W sonication, Exp 58, LS1

B.5 Experimental Data for 250 W of Sonication Power

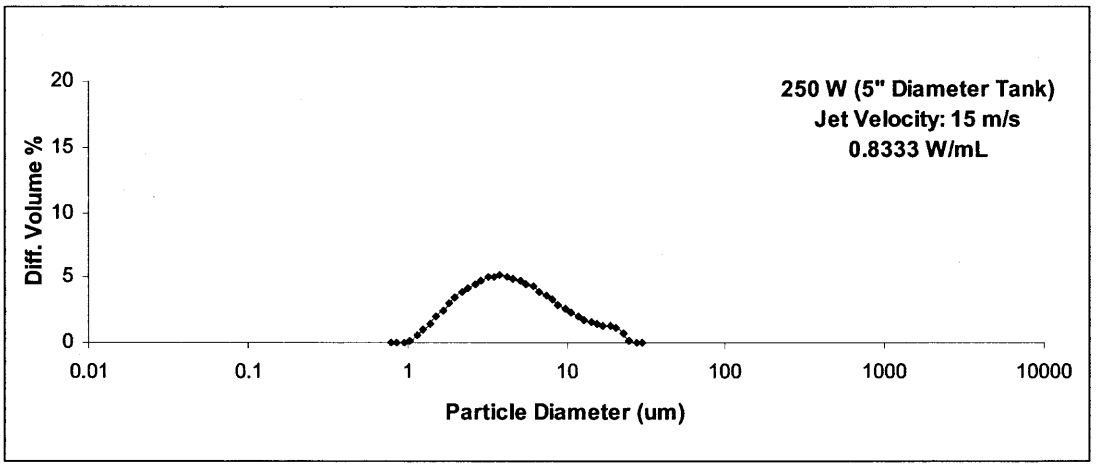

Figure B.5-1 Particle size distribution of experiment with 250W sonication, Exp 59, LS3

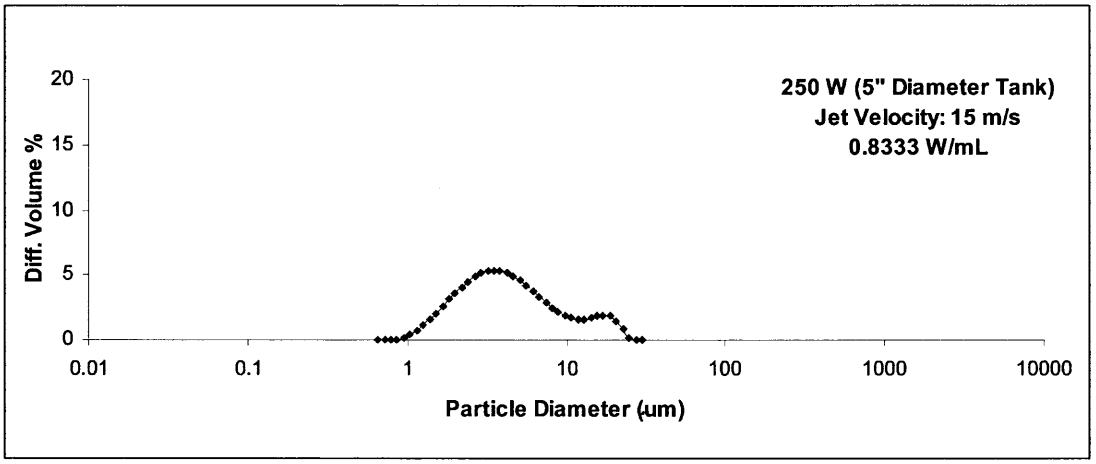

Figure B.5-2 Particle size distribution of experiment with 250W sonication, Exp 60, LS3

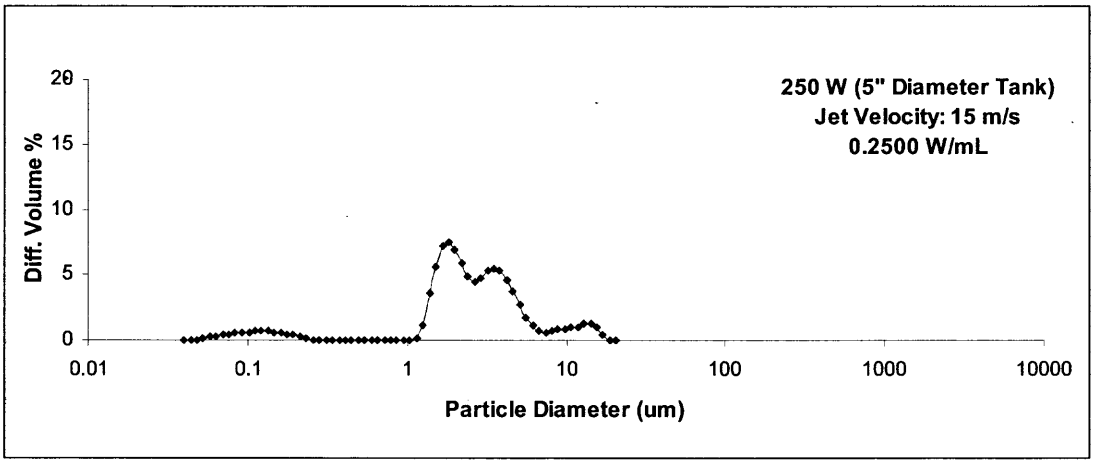

Figure B.5-3 Particle size distribution of experiment with 250W sonication, Exp 66, LS3

REFERENCES

1. Roberts C. J. and Debenedetti, P.G. (2002). Engineering pharmaceutical stability with amorphous solids. *AIChE J.* **48**(6): 1140-1144.

2. Midler, M., Paul, E.L., Whittington, E.F., Futran, M., Liu, P.D., Hsu, J., Pan, S.H. (1994). Crystallization method to improve crystal structure and size. US Patent 5314506. May 24, 1994.

3. Myerson, A.S. (2001). *Handbook of Industrial Crystallization*, 2nd Edition, Butterworth-Heinemann.

4. Luque de Castro, M.D. and Priego-Capote, F. (2007). Ultrasound-assisted crystallization (Sonocrystallization). *Ultrasonics Sonochemistry.* **14**(6): 717-724.

5. Lindrud, M.D., Kim, S., and Wei, C. (2001) Sonic Impinging Jet Crystallization Apparatus and Process. US Patent 6302958. Oct. 16, 2001.

6. Johnson, B.K., and Prud'homme, R.K. (2003) Chemical Processing and Micromixing in Confined Impinging Jets. *AIChE J.* **49**: 2264-2282.

7. http://ycees.njit.edu/labs/analysis3.htm (accessed on May 21, 2008)